NASA CR-66216

DEVELOPMENT AND TESTING OF ADVANCED SHAPED CHARGE METEORITIC SIMULATORS

PART II - CALIBRATION OF FLIGHT GUNS

by: R. L. Woodall and E. L. Clark

Prepared under Contract No. NAS 1-5212 by
THE FIRESTONE TIRE & RUBBER COMPANY
Defense Research Division
Akron, Ohio

for

NATIONAL AERONAUTICS AND SPACE ADMINISTRATION

NASA CR-66216

DEVELOPMENT AND TESTING OF ADVANCED SHAPED CHARGE METEORITIC SIMULATORS

PART II - CALIBRATION OF FLIGHT GUNS

by: R. L. Woodall and E. L. Clark

Prepared under Contract No. NAS 1-5212 by
THE FIRESTONE TIRE & RUBBER COMPANY
Defense Research Division
Akron, Ohio

for

NATIONAL AERONAUTICS AND SPACE ADMINISTRATION

ABSTRACT

This calibration study was conducted to obtain statistical data on the mass, shape, and velocity of two types of shaped charge meteor simulator guns. Flash radiographs of the meteor pellets were taken in low ambient pressure environment to simulate re-entry conditions, so that pellet characteristics could be measured. The methods of radiographic analysis are described. One type of gun was found to produce nickel pellets with an average velocity 9.54 km/sec and average mass 0.88 gram. The other type of gun was found to produce iron pellets with average velocity 8.56 km/sec and average mass 0.82 gram.

TABLE OF CONTENTS

TABLES

FIGURES

APPENDICES

SUMMARY

This calibration study was conducted to obtain statistical data on the mass, velocity, shape, and orientation of artificial meteors launched by shaped charge guns. Tests were conducted on two types of guns. One of the guns used a 40 degree hyperbolic liner manufactured of type 200 nickel while the other gun used a 30 degree conic liner manufactured of Ingot Iron. Three basic tests were made of each liner type: (1) a statistical survey of mass, velocity, and orientation of the pellet when fired in vacuum (the Modified Flight Test); (2) effect of spin at a rate of 25 rps (the Spin Test); (3) test actual flight assemblies for comparison (the Full Flight Test). In addition to those tests, two other tests were made to evaluate the 40° hyperbolic liner: (1) Body Confinement Test, (2) Initial Pellet Mass Test.

Test data indicated that the velocity and mass of the pellets could be predicted within fairly narrow limits and that the 40 Degree Hyperbolic pellet was not affected by spinning at 25 rps, however, the mass of the 30 Degree Ingot Iron pellets was decreased by spinning.

The Modified Flight Tests (statistical surveys) yielded the following average values with the indicated 95 per cent confidence intervals on the average values: the 40° Hyperbolic liners produced nickel pellets with an average velocity of 9.54 ± 0.06 km/sec, and average mass of 0.84 ± 0.11 gram; the 30° Conic liners produced Ingot Iron pellets with an average velocity of 8.56 ± 0.01 km/sec, and average mass of 0.77 ± 0.05 gram. The Full Flight Tests yielded the following values with the indicated 95 per cent confidence intervals on the average values: the 40° Hyperbolic liners produced nickel pellets with an average velocity of 9.66 ± 0.06 km/sec, and average mass of 1.09 ± 0.30 gram; the 30° Conic liners produced Ingot Iron pellets with an average velocity of 8.58 ± 0.06 km/sec, and an average mass of 0.95 ± 0.13 gram.

INTRODUCTION

Background

To evaluate key coefficients in the physical theory of meteors, it is necessary to carry out flight simulations with artificial meteors of known mass, shape, density, and velocity (ref. 1).

NASA is engaged in a program to provide the required information by firing launch vehicles out of the atmosphere to carry accelerators aloft. At the proper point in the trajectory of the vehicle, the artificial meteor is accelerated to the range of meteor re-entry velocities and is observed during re-entry.

The main purpose of these experiments is to obtain the value of the luminous efficiency of a meteor-like body of known mass and composition moving at a known speed. The value of the luminous efficiency, or the per cent of kinetic energy converted into visible light, is computed from the observed photographic data of the visible re-entry trail (ref. 2).

This program is being conducted by the Langley Research Center at Hampton, Virginia. The actual launch tests are conducted at the NASA Wallops Station using a "Trailblazer," multistage, solid propellant vehicle.

Purpose of Calibration Study

This calibration study was conducted for the Langley Research Center to obtain statistical data on the mass, velocity, shape, orientation in space, and tumbling rate of artificial meteors launched by two types of shaped charge guns.

One of the two guns calibrated was of a new design developed under NASA contract NAS 1-5212 by the Firestone Tire & Rubber Company, Defense Research Division, of Akron, Ohio. This gun was manufactured from type 200 nickel and was referred to as the "forty degree Hyperbolic" liner. A newly developed inhibiting technique was used with this liner to produce a single compact pellet.

The other gun calibrated was a modification of a design developed by the Ballistic Research Laboratories of Aberdeen Proving Grounds, Aberdeen, Maryland. This gun was manufactured from Ingot Iron and was referred to as the "thirty degree Conic" liner. A plastic inhibitor was used with this liner to produce a single, compact pellet.

Test Plan

The NASA test plan required Firestone to conduct three basic tests of each liner type: a modified flight assembly test to obtain statistical data of the pellet characteristics, a test to determine the effect of spin at the rate of 25 rps, and tests using the actual flight test assembly to determine whether it yielded the same results as the modified flight test assembly. Since the forty degree Hyperbolic liner was developed as a bare charge, i.e., without a body, a test of the effect of body confinement was included in the test plan. In an attempt to determine the mass of the hyperbolic liner pellet portion that fragmented and broke away from the main pellet in flight, a program to determine the initial mass of the pellet was added to the test plan. It was also planned that Firestone would supply three flight test assemblies of both the nickel and the iron guns to NASA for launch flight firing.

Tables IA and IB outline the planned test schedule. The complete calibration program required 47 test shots. However, it was necessary to fire several instrumentation shots in some of the programs due to instrumentation difficulties. Most of the instrumentation shots were fired in the spin test programs.

DESCRIPTION OF TEST ITEMS

Forty Degree Hyperbolic Test Assemblies Design

General. - Figures 1 and 2 show the details of the 40° Hyperbolic liner that was used in this calibration. The groove in the liner caused the pellet to be cut free from the balance of the jet; therefore, the groove produced an inhibiting effect on the jet. The liner register and bottom surfaces were cemented with rubber-base adhesive to an aluminum adapter plate and loaded in a loading fixture. Three loading fixtures were used to load the liners. All three loading fixtures were manufactured to drawing DRC-11-2040 (Figure 3) and assigned a serial number. The serial numbers used were 5, 6, and 7.

Body confinement and initial pellet mass test assembly. - Since the 40° Hyperbolic liner was developed as a bare charge, i.e., without a body, a test of the effect of body confinement was included in the test plan. Figure 4 shows the test assembly used for the Body Confinement Tests in Program 839, and was also used in Program 856 to determine the initial mass of the pellet. All of the aluminum components used in the 40° Hyperbolic test assemblies were made of 6061-T6 aluminum alloy. A twisted pair of wires that acted as an

initiation time (t_o) sensor was inserted into the base plug of this assembly similar to the sensor shown in Fig. 5. The twisted pair of wires shorted when the ionization front of the explosion reached that location. The shorting of the twisted pair of wires started the operation of electronic equipment in the blockhouse. The base plug, body, and liner-adaptor plate-charge were assembled using slip fit of components for securement. The slip fit of the components was adequate since these two tests were conducted with the gun stationary and well supported.

Modified flight test assembly. - The assembly used for the Modified Flight Test is shown in Fig. 5. This assembly was designed to simulate the Full Flight assembly but be less expensive to manufacture. The retainer ring threaded onto the body and pressed against the adapter plate and therefore held the liner and charge in the body. The twisted pair of wires that acted as an initiation time sensor was located well off center so that it would not interfere with the detonators.

Spin test assembly. - The assembly used for the Spin Test is shown in Fig. 6. An arc-firing detonator (Dupont X 98AA) was used, in place of the DD8 HO detonator shown in the alternate detonator arrangement, with an M18 stab detonator for the first three successful shots of the program (program round numbers 850-9, 850-10, 850-11). The arc-firing detonator exhibited a short reproducible firing time, therefore, the firing pulse could be used directly as a source of the initiation time.

The M36A1 and M18 detonator arrangement shown was used for the last two successful shots of the program (program round numbers 850-13 and 850-14). The change in detonator type was made because of instrumentation difficulties encountered when using the arc-firing detonator. The M36A1 detonator did not exhibit a short reproducible firing time, therefore, a different method of obtaining an initiation time source was used. A twisted pair of wires was located at a distance of one inch from the spinning body of the assembly. The twisted pair was mounted to a support stand so that the wires started at a point one inch below the top of the charge. When the charge exploded, the body of the assembly was forced against the twisted pair of wires causing them to short. The shorting of the twisted pair served as an initiation time sensor.

The test assembly was hung vertically on a piece of stiff steel wire inserted into the end of the spin adapter and held with a set screw. This wire provided a spin axis for the test assembly.

Full flight test assembly. - Figure 7 shows the assembly used for the Full Flight Test. The body of this assembly was slotted on one side, five inches from the liner end of the body, so that a twisted pair of wires could be taped against the explosive filler

to act as an initiation time sensor. The slot was approximately .020 inch wide and .050 inch long. This assembly used a DD8 HO delay detonator with a M18 stab detonator for initiation. Three pieces of this assembly, less the sensor slot were supplied to NASA for Flight Test by NASA using rocket launch. Table II shows a listing of the component weights of the full flight assembly of Fig. 7.

THIRTY DEGREE CONIC TEST ASSEMBLIES DESIGN

General. - Figure 8 shows the details of the 30° conic liner that was used in this calibration. An Ingot Iron cover was cemented to the end of the spit back tube of the liner with rubber base adhesive. The metal cap was .005 inch thick and .531 inch in diameter. Two loading fixtures were used to load the liners. Both loading fixtures were manufactured to drawing DRB-N-57 (Figure 9) and assigned a serial number. The serial numbers used were 16 and 17. Figure 10 shows the details of the plastic inhibitor used in the 30° conic liner test assemblies.

Modified flight test assembly. - The assembly used for the Modified Flight Test is shown in Fig. 11. This assembly was designed to simulate the full flight assembly but be less expensive to manufacture. The "Assembly Notes" shown on Fig. 11 describe the procedures used to cement the components together. Similar to the 40° Hyperbolic Modified Flight Test assembly, the twisted pair of wires that acted as an initiation time sensor was located well off center so that it would not interfere with the detonators.

Spin test assembly. - The assembly used for the Spin Test is shown in Fig. 12. Due to instrumentation difficulties, an M36A1 detonator was substituted for the X98AA arc-firing detonator. Figure 6 shows a similar arrangement for using the M36A1 detonator for a spin test.

Two types of initiation time sensors were used in this program. The first successful shot (program round number 858-17) used a shorting screen with a one inch diameter hole in it, located 2-1/2 inches in front of the round. The shorting screen consisted of a thin sheet of plastic, a few thousandths of an inch thick, with aluminum foil covering the top and bottom surfaces. The foil sheets were attached to wires and behaved much like a twisted pair of wires for supplying an initiation time source. The balance of the successful shots fired in this program (program round numbers 858-22, 858-23, 858-24, and 858-25) used a twisted pair of wires standing beside the spinning round as an initiation time sensor. This was the same initiation time sensor as was used for the last two shots of the 40°

Hyperbolic Spin Test (program round numbers 850-13 and 850-14).

The test assembly was hung vertically on a piece of stiff steel wire inserted into the end of the spin adapter and held with a set screw. This wire provided a spin axis for the test assembly.

Full flight test assembly. - Figure 13 shows the assembly used for the Full Flight Test. The body of the assembly was slotted on one side, 6 inches from the liner end of the body, so that a twisted pair of wires could be taped against the explosive filler to act as an initiation time sensor. The slot was approximately .020 inch wide and .050 inch long. The assembly used a DD8 HO delay detonator with an M18 stab detonator for initiation. Two pieces of this assembly, less the initiation time sensor slot, were supplied to NASA for Flight Test by NASA using rocket launch. Table III shows a listing of the component weights of the full flight assembly of Fig. 13. One piece of an assembly similar to that of Fig. 13, but with the base plug body section one inch longer, also less the initiation time sensor, was supplied to NASA for Flight Test by NASA using rocket launch. Table IV shows a listing of the component weights of the long full flight assembly.

HARDWARE MANUFACTURE AND QUALITY CONTROL

Liner Material Control

This calibration program was intended to provide reliable information on the performance of the meteor simulator designs tested so that the NASA Flight Test data analysis would have a statistically reliable basis. Since minute impurities in the liner composition could affect the re-entry trace, the liner material was carefully controlled. This involved the purchase of certified material, documentation of in-process heat-treatment, and chemical and spectrographic analysis.

Test pieces were subject to the same thermal treatment as the liner material and their mechanical properties were determined. Appendix A shows a summary of the material inspection and quality control data. Materials were assigned a lot number when received and are identified by that lot number in Appendix A.

Inspection of Parts

All test hardware components were 100% inspected for compliance with the drawings. The gun performance is most sensitive to asymmetries and dimensions of the liner. Since the liner was by

far the most difficult part to manufacture to the close tolerances specified, most of the metal parts quality control effort was expended on the manufacture and inspection of the liners. The plastic inhibitor used in the 30° Conic liner assembly was held within close tolerance because the solidity and size of the pellet produced by the gun was dependent upon the dimensions of the inhibitor.

Appendix B shows the inspection data summary for the liners tested. Most of the dimensions were held to the tolerances. In those instances where the parts were not within tolerance, they were accepted if the deviation was small and if experience indicated that no observable effect on performance was likely. In addition to the inspection measurements shown in Appendix B, precision plaster casts were made of the inside of the 40° Hyperbolic liners. The precision plaster casts were viewed on a ten power magnification shadowgraph and compared to a tracing of the intended hyperbolic contour (10:1 scale) drawn on Mylar plastic.

Appendix C shows the inspection data summary for the 30° Conic liner plastic inhibitors used.

Inspection Data of Loaded Assemblies

Appendix D shows the loaded assembly inspection data summary. The 40° Hyperbolic liners were cemented to aluminum adapter plates prior to loading. The concentricity and perpendicularity of the liner central axis to the adapter plate register surfaces were measured prior to loading the liners. Appendix D shows the average eccentricity was 1.28 mil with standard deviation .719 mil and theaverage perpendicularity was 1.58 mil with standard deviation .813 mil. These values were total indicator readings (TIR).

Three loading fixtures were used to load the 40° Hyperbolic liners. All three loading fixtures were manufactured to DRC-11-2040-1 (Fig. 3) and assigned serial numbers. The serial numbers used were 5, 6, and 7. These loading fixtures provided approximately 2.8 inches of explosive above the liner. The weights of the 65/35 octol explosive charges were found to have an average value of 1.240 pounds with a standard deviation of .004 pound. The concentricities of the liners to the loading fixtures were measured after loading. The average eccentricity of liner-to-loading fixtures was 3.5 mils with a standard deviation of 1.4 mil.

Two loading fixtures were used to load the 30° Conic liners.

Both loading fixtures were manufactured to DRB-N-57 (Fig. 9) and assigned serial numbers. The serial numbers assigned were 16 and 17. These loading fixtures provided approximately 1.8 inch of explosive above the liner. The weights of the composition B explosive charges were found to have an average value of 1.98 pounds with standard deviation of .005 pound. The concentricity of the outside of the bare charges (after removal from the loading fixtures) to the liners were measured. The average eccentricity was found to be 2.7 mils with a standard deviation of 1.1 mil. These values were total indicator readings (TIR).

The position of the plastic inhibitors in the liners was measured after cementing. The measurements were taken with a depth micrometer at 90° angular spacings. The reading was given a positive (+) sign if the inhibitor extended from the liner base and negative (-) sign if the inhibitor was recessed into the liner base. The average values obtained were +.2 mil, +.2 mil, -.2 mil, -.3 mil with standard deviations of 2.2 mil, 2.2 mil, 2.3 mil and 2.3 mil respectively.

TEST FACILITIES AND PROCEDURES

General

All explosive loading and firing were done at the Defense Research Division facility at the Ravenna Army Ammunition Plant, Ravenna, Ohio. The Spin Test shots of programs 850 and 858 were fired at the Large Chamber. The Initial Pellet Mass Test shots of program 856 were fired at the Open Test Site. The balance of the test shots, i.e., programs 839, 847, 851, 853, and 859, were fired at the NASA Test Site.

NASA Test Site

Figures 14A and 14B show the radiographic set-up of the NASA Test Site. This two station, orthogonal X-ray system used a Field Emission four channel flash X-ray system, model 730-4-231. This is a 105KV system having a pulse width of 30 nanoseconds for mimimum blur at high object velocities. The radiographic set-up was arranged such that the first pair of radiographs of the pellet in flight were taken at a distance of approximately 33.75 inches from the meteor gun. The second pair of radiographs were taken at a distance of approximately 96.75 inches from the meteor gun. The four conic calibration standard pieces shown in Fig. 14B were manufactured to DRA-N-25, shown in Fig. 15. The film density of the pellet could be compared to that of the conic calibration standard and the pellet density then determined.

The meteor guns were fired through a 2 inch diameter aperture hole into a 9 foot long aluminum tube, 6 inch diameter x 1/8 inch wall. The aluminum tube acted as a protective shield for the X-ray pulsers and X-ray films. This system was constructed such that the meteor guns could be fired and the pellet observed in a low pressure environment. Appendix E provides a more detailed description of the NASA Test Site.

Large Chamber

The Large Chamber facility was capable of being used as a spin test facility. The meteor gun was suspended on a piece of 3/64 inch diameter steel wire from the spin mechanism. The gun was fired through a 2-1/2 inch diameter aperture hole at a distance of 6 inches from the aperture plate.

This facility was equipped with three Field Emission Model 233 X-ray Pulsers powered by a Model 214 High Voltage Power Supply. This is a 300 KV system having a pulse width of 100 nanoseconds. The radiographs were taken in two planes spaced 120 degrees apart. The first and second radiographs of the pellet in flight were taken at distances of approximately 40 and 50 inches from the meteor gun respectively. The third radiograph was taken at a distance of approximately 70 inches from the meteor gun. Appendix E provides a more detailed description of the Large Chamber facility.

Open Test Site

The Open Test Site facility has the capability of taking close-up radiographs of meteor guns during or after firing. The gun was supported by a sheet of thin cardboard with a 1-3/4 inch diameter hole in it. The gun was located in front of a blast-proof film cassette. The film was approximately 9 inches from the pellet flight path.

The facility was equipped with two Field Emission Model 233 X-ray Pulsers powered by a model 214 High Voltage Power Supply. This is a 300 KV system having a pulse width of 100 nanoseconds. The pulsers were located one above the other in one common plane. The first radiograph of the pellet was taken at a distance of approximately 2-1/2 inches from the end of the meteor gun. The second radiograph of the pellet was taken at a distance of approximately 10-1/2 inches from the end of the meteor gun. Appendix E provides a more detailed description of the Open Test Site.

DISCUSSION OF DATA AND RESULTS

Data Analysis Methods

General. - The geometry of the X-ray systems and the radiographic film images of the pellets provided dimensional data for describing the pellets. The NASA Test Site afforded three-dimensional information about the pellets with its orthogonal, two-station X-ray system. Therefore, the data from this facility has allowed a three-dimensional analysis. The Large Chamber and the Open Test Site afforded two dimensional information about the pellets because the X-ray pulsers were arranged in linear arrays. For this reason the Large Chamber and Open Test Site could not be used to measure pellet spatial properties as accurately as the NASA Test Site. A six power eye-piece with reticle was used to measure pellet image dimensions, and a drafting ruler was used to measure pellet image location. An experimental study of the measurement error encountered in the analysis of film pellet images, with respect to pellet length, diameter, and mass, was conducted. Appendix H describes the experiment and presents the results. The data sample obtained in the experiment was insufficient to permit any definite conclusion to be made. The study indicated the following: the pellet length might have been measured about 5% too short, the pellet diameter might have been measured about 3% too small, and the computed pellet mass might have been about 6% too low.

Spatial Data. - Since the pellet could tumble in flight, the center of the pellet, which is an estimate of the pellet center of mass, was referred to as the location of the pellet. This definition of pellet location was made because it was least affected by the pellet orientation. The pellet velocity was determined by calculating the distance traveled from the first to the last radiographic station and dividing by the measured time interval between the firing of the associated X-ray pulsers.

The NASA Test Site data was analysed with the aid of an IBM 1620 digital computer. Two independent computer programs were devised for analysis of the NASA Test Site spatial data. One program used intersecting planes, vectors, and matrices while the other program used lines, trigonometry, and least-square nearest approach of lines. The latter method was chosen as the program to be used because, of the two programs, it was the least affected by pellet orientation. The method of analysis used by the computer is described in Appendix F. The computer program calculated the following: the geometric magnification factor of the pellet for each of the four films, the pellet velocity, orientation angles (spherical coordinates) of the pellet in station 1 and station 2, and length of the pellet in station 1 and station 2.

Mass data. - The pellet mass was determined by measuring the film image and computing the volume assuming the pellet form was approximated by conic frustums. This volume was then corrected for magnification effects. The volume thus obtained was taken to be the pellet volume for computations of pellet mass for the Large Chamber and Open Test Site. But, since the NASA Test Site afforded three dimensional data, the volume described above was corrected for orientation of the pellet, i.e., image foreshortening, in all NASA Test Site mass calculations. The mass reported for each station of the NASA Test Site was the average value of the two masses obtained at each station, i.e., film 1 and 2 for station 1, and film 3 and 4 for station 2. The mass calculations were performed by an IBM 1620 digital computer. A description of the method of mass analysis used by the computer is presented in Appendix G.

Radiographs

General. - The radiographs presented in Figures 16 through 23 provide representative views of each pellet reported in this calibration study. The radiograph shown for each round was selected as the best view in the set of radiographs obtained for that round.

Forty Degree Hyperbolic. - The radiographs presented in Figures 16, 17, and 19 show the debris that accompanied the low ambient pressure shots of the 40° Hyperbolic nickel guns. The radiographs presented in Fig. 18 show the atmospheric ambient pressure spin test shots. It can be seen that the amount of debris that accompanied the atmospheric ambient pressure test shots was much less than for

the low ambient pressure test shots. Figure 20 presents the two io-radiographs taken at the Open Test Site of round 856-2, of the Initial Pellet Mass Test. The two views shown, station 1 and station 2, are of the same pellet as it left the liner and proceeded along its flight path. The initial mass of the pellet was computed for the station 1 radiograph.

Thirty Degree Conic. - The radiographs presented in Figure 21 and Figure 23 show the debris that accompanied the 30° Conic Ingot Iron pellet when fired in a low ambient pressure environment. Figure 22 presents radiographs of the 30° Conic Spin Test (-25 rps). The pellet mass and size are much lower in the Spin Test shots and the debris visible is much less than for the low ambient pressuretest shots. The pellet character for the 30° Conic Spin Test shots was observed to be inconsistent and generally poor.

Test Data

General. - Tables V and VII present the pellet mass and dimension data of each shot for the 40° Hyperbolic nickel and 30° Conic Ingot Iron test assemblies respectively. Tables VI and VIII present the pellet velocity and orientation data of each shot for the 40° Hyperbolic nickel and 30° Conic Ingot Iron test assemblies respectively. Table IX presents the velocity data summary for both types of guns. Table X presents the mass and dimensions data summary for both types of guns.

The purpose of these tests was: to accumulate statistically significant mass and velocity data, to determine the effects of spinning at -25 rps, to determine the effects of body confinement on the Hyperbolic gun, and to estimate the mass of the debris particles that accompany the pellet from the Hyperbolic gun. Most of the sample sizes were kept to a minimum. It was therefore difficult to report statistically meaningful data for most of the tests. But, the sample sizes of the two Modified Flight Tests were made large enough to provide reliable data on that type of assembly.

Tables IX and X list the sample size, sample mean, sample spread, and the standard deviation of the velocities and masses respectively. But, since the population mean was not known for the mass and velocity data, it was desirable to know how nearly the sample mean represented the population mean. Therefore, the 95% Confidence Interval for the mean was computed for the sets of data. The population mean has a 95% probability of falling within the Confidence Interval limits. For instance, on line 2 of Table IX, the sample mean velocity is 9.536 km/sec for 11 nickel pellets fired from the 40° Hyperbolic gun design. The 95% Confidence Interval is 0.0557 km/sec. This states that there is a 95% probability that the population mean falls within the range 9.536 $\pm$ .0557 km/sec, i.e., between 9.480 km/sec and 9.592 km/sec.

The same technique was applied to the sample standard deviation to establish the reliability of the reported value. In the standard deviation tabulations, the 95% Confidence Intervals presented are actual values instead of the plus or minus value given for the mean. This tabulation states that, for the 11 nickel pellets above, there is 95% probability that the standard deviation of the population will fall between 0.0562 km/sec and 0.1397 km/sec.

Velocity and orientation. - Tables VI and VIII present the pellet velocity and orientation data for each round in this calibration study. Table IX presents the statistical summary of the velocity data. The pellet orientation is reported in spherical coordinates where the pellet was traveling in the positive Z direction. The angle Gamma corresponds to the angle Phi commonly used in spherical coordinates. The orientation angles were not reported in the summary tables since the values appear to be random. An approximation of the tumbling rate is presented in Tables VI and VIII. Due to limitations of the X-ray system geometry and methods of computation, the values shown were calculated by assuming that the pellet did not tumble more than $\frac{1}{2}$ revolution from Station 1 to Station 2. The tumbling rate was not reported in the summary tables because of the approximation character of the values computed.

The average velocities of the 40° Hyperbolic nickel gun programs were as follows: Body Confinement Test, 9.46 km/sec; Modified Flight Test, 9.54 km/sec; Full Flight Test, 9.66 km/sec; Spin Test (-25rps), 9.49 km/sec. In comparing the Body Confinement Test average velocity with previous bare charge tests, with the same liner and charge configuration, no velocity effect due to body confinement was apparent. The Modified Flight Test average velocity differed from the Full Flight Test average velocity by -0.12 km/sec. This was an unexpectedly large difference. Unfortunately, the small sample size of the Full Flight Test prohibits a satisfactory statistical treatment of this difference of average values. Therefore, no definite statement of significance of differences of the mean can be made. The Spin Test average velocity differed from the Modified Flight Test average velocity by only 0.05 km/sec.

The average velocities of the 30° Conic Ingot Iron gun programs were as follows: Modified Flight Test, 8.56 km/sec; Full Flight Test, 8.58 km/sec; Spin Test (-25rps), 8.39 km/sec. The Modified Flight Test average velocity was 0.02 km/sec less than that of the Full Flight Test. Unfortunately, the small sample size of the Full Flight Test prohibits a satisfactory statistical treatment of this difference of average values. Therefore, no definite statement of significance of difference of the mean can be made. The Spin Test (-25rps) average velocity was 0.18 km/sec less than that of the Modified Flight Test. The velocities obtained for the Spin Test Shots had a much larger maximum spread than the Modified Flight Test. This large maximum spread was believed to have been caused by the

character of the pellet observed in the 30° Conic Spin Test. The Spin Test pellet was of poor quality, i.e., breaking up, in some of the Spin Test shots and therefore hampered a precise determination of the pellet location.

Mass and dimension data. - Tables V and VII present the pellet mass and dimensions data for each round in this calibration study. Table X presents the statistical summary of the mass data. The data is presented as Station 1 data and Station 2 data as well as the combined Station 1 + 2, i.e., the average value for that round.

The average mass values for the rounds of the 40° Hyperbolic nickel gun programs were as follows: Body Confinement Test, 0.84 gram; Modified Flight Test, 0.84 gram; Full Flight Test, 1.09 gram; Spin Test (-25rps), 1.32 gram. The Body Confinement Test average mass differed from the Modified Flight Test by less than 0.01 grams. The Modified Flight Test average mass differed from the Full Flight Test by 0.26 gram. Unfortunately, the small sample size of the Full Flight Test prohibits a satisfactory statistical treatment of this difference of average values. Therefore, no definite statement of significance of difference of the mean can be made. The Spin Test (-25rps) differed from the Modified Flight Test by 0.48 gram. The large difference between the average mass of the Spin Test shots and the Modified Flight Test shots could be explained by the ambient pressure difference between the two test programs. It was observed that the type of inhibiting used on the Hyperbolic liner in this calibration study, introduced a shock into the rear of the pellet. In the atmospheric shots, the pellet appeared stable and did not suffer appreciable damage due to the inhibition-induced shock. But, when the gun was fired in a low pressure environment, the pellet suffered a progressive fragmentation of the rear of the pellet. This fragmentation progressed about 0.1 inch along the length of the pellet and therefore reduced the mass of the pellet. The air apparently acted as a compressive force on the sides of the pellet, and therefore retarded the fragmentation tendency.

Assuming that the bulk of the particles that were found to surround the 40° Hyperbolic nickel pellet in this calibration study were formed by the fragmentation of the rear of the pellet, a program was included to determine the initial mass of the pellet, i.e., before fragmentation. The mass of the pellet was found for the pellet about 2.5 inches out of the gun. The initial pellet mass was found to be about 1.68 gram. This value was found for one shot, therefore the value of the initial mass obtained can only be stated as an approximate value. The mass of the particles surrounding the low ambient pressure shots was therefore estimated to be about 0.84 gram for the Modified Flight Test, and 0.59 grams for the Full Flight Test.

Another experimental determination of the debris surrounding

the 40° Hyperbolic nickel pellet was undertaken. This determination was based only on measuring the film images of the debris. Appendix I presents the method of analysis and the results.

The average mass values for the rounds of the 30° Conic Ingot Iron gun programs were as follows: Modified Flight Test, 0.77 gram; Full Flight Test, 0.95 gram; Spin Test (-25rps), 0.49 gram. The Modified Flight Test average mass differed from the Full Flight Test by 0.18 gram. Unfortunately, the small sample size of the Full Flight Test prohibits a satisfactory statistical treatment of this difference of average values. Therefore, no definite statement of significance of difference of the mean can be made. The Spin Test average mass differed from the Modified Flight Test by 0.29 gram. The large difference between the average mass of the Spin Test and the Modified Flight Test could be explained by the pellet character. The Spin Test pellet was of poor quality, i.e., breaking up, in some of the Spin Test shots. The maximum spread of the masses of the Spin Test was 0.35 gram, which is over three times as large as that of the 11 Modified Flight Test shots.

Combined mass and velocity data. - If all of the low ambient pressure test shots of each type of liner were assumed to be from common populations, the corresponding velocity and mass data could be combined. This assumption could not be based on statistical tests, as was discussed in the preceeding sections of this report. Figures 24 and 25 present graphic displays of the velocity and combined station 1 and 2 mass data of the low ambient pressure tests of Tables V and VI, and Tables VII and VIII respectively. The figures display the pellet mass vs the pellet velocity. The circle plot represents the over-all average value for all of the low ambient pressure test shots shown on each graph. The rectangle inclosing the over-all average value represents the included 95 per cent confidence interval on the over-all average value. That is, there is a probability of .95 that the average value of the total population (an infinitely large number of shots) would lie within the rectangle. The over-all average value shown in Fig. 24 (40° Hyperbolic liner) was: velocity, 9.54 km/sec, with 95 per cent confidence interval $\pm$ 0.05 km/sec, and standard deviation 0.09 km/sec; mass, 0.88 gram, with 95 per cent confidence interval $\pm$ 0.04 gram, and standard deviation 0.17 gram. The over-all average value shown in Fig. 25 (30° Conic Liner) was: velocity, 8.565 km/sec, with 95 per cent confidence interval $\pm$ 0.015 km/sec, and standard deviation 0.02 km/sec; mass 0.82 gram, with 95 per cent confidence interval $\pm$ 0.06 gram, and standard deviation 0.10 gram.

CONCLUSIONS

(1) The Modified Flight Tests provided statistically significant data describing the pellets produced by the two types of guns. The Full Flight Test data was expected to correlate well

with the Modified Flight Test data and therefore determine the Full Flight Test pellet characteristics. Unfortunately, for both the 40° Hyperbolic and the 30° Conic assemblies, the Full Flight Test assemblies produced slightly higher velocity and larger mass, than the Modified Flight Test assemblies. The small sample size of the Full Flight Tests prohibited a satisfactory statistical treatment of the differences. Possibly there was no significant difference between the Full Flight Test pellets and the Modified Flight Test pellets, but this conclusion could not be based on statistical tests.

(2) If the low ambient pressure test data for the 40° Hyperbolic nickel liners are assumed to belong to one common population, the following average values with the indicated 95 per cent confidence intervals result: average velocity, 9.54 $\pm$ 0.05 km/sec; average mass, 0.88 $\pm$ 0.04 gram. If the low ambient pressure test data for the 30° Conic Ingot Iron liners are assumed to belong to one common population, the following average values with the indicated 95 per cent confidence intervals result: average velocity, 8.565 $\pm$ 0.015 km/sec; average mass, 0.82 $\pm$ 0.06 gram.

(3) The 40° Hyperbolic nickel pellets appeared to be more solid than the 30° Conic Ingot Iron pellets. The nickel pellets displayed a strong tendency to split lengthwise from the rear. This splitting tendency was probably the effect of a shock induced into the pellet by the inhibiting mechanism used. A different type of inhibitor might reduce the inhibitor induced shock and therefore reduce the splitting tendency.

(4) An estimation of the debris surrounding the 40° Hyperbolic nickel pellets fired in low ambient pressure environment indicated that the mass of the debris could be as large as the mass of the pellet.

(5) The 40° Hyperbolic nickel pellets appeared to be unaffected by the presence of an aluminum body. That is, the Body Confinement Test yielded the same basic pellet as previous shots fired without a body.

RECOMMENDATIONS

After reviewing the results of this calibration study, the following recommendations were made:

(1) Since the differences between the Modified Flight Test pellets and the Full Flight Test pellets were not satisfactorily resolved, all shots fired in future calibration studies should be of the Full Flight Test design. This would remove any doubt that the statistical results and predictions were true for the Full Flight Test assembly supplied to NASA for rocket launched Flight Testing.

(2) Future Spin Test firing should be done in a low ambient pressure environment. This would remove any atmospheric pressure affects on the pellets so that a true test of spin affects could be obtained.

APPENDIX A

LINER MATERIAL CHARACTERISTICS

Material Record

Type Material: Type 200 Nickel, cold drawn, 2-1/8 inch diameter bars.

Firestone Lot No.: 57, and 57A*

End Use: Hyperbolic liners, Firestone DRB-23-2295

Thermal Treatment: Pieces were rough machined, heated to 1500° F in a neutral salt bath, held for 30 minutes at temperature, and air cooled.

Mechanical Properties:

Yield Strength	26,500 psi
Tensile Strength	73,000 psi
Elongation in 2 inches	49%
Reduction in Area	58%
Rockwell Hardness	B 51

These properties were obtained on a test piece after annealing.

Spectrographic Analysis:

Nickel	Major
Carbon	0.080%
Manganese	0.15
Phosphorous	0.0025
Sulfur	0.004
Silicon	0.025
Iron	0.022

Spectrographic analysis showed no other trace metals greater than 0.01%.

*Lots 57 and 57A were certified to be of the same heat number and composition.

APPENDIX A

Material Record

Type Material: Ingot Iron, cold drawn, Armco Magnetic, 3-1/2 inch diameter bars.

Firestone Lot No.: 60

End Use: Conical liners, Firestone DRB-N-54

Thermal Treatment: None

Mechanical Properties:

Yield Strength	48,600 psi
Tensile Strength	52,500 psi
Elongation in 2 inches	25%
Reduction in Area	65%
Rockwell Hardness	B 69

Chemical Analysis:

Carbon	0.03%
Manganese	0.04
Phosphorous	0.012
Sulfur	0.023
Silicon	0.003
Nickel	0.02
Chromium	0.01
Molybdenum	0.02
Copper	0.10

Spectrographic Analysis:

Iron	Major
Carbon	0.038%
Manganese	0.021
Phosphorous	0.0065
Sulfur	0.014
Chromium	0.025

Spectrographic analysis showed no other trace metals greater than 0.01%

Appendix B
LINER INSPECTION
40 Degree, .030 Wall Nickel Hyperbolic DRB-23-2295

LINE	LINER SERIAL NUMBER	WEIGHT (GRAMS) BEFORE GROOVING	WEIGHT (GRAMS) AFTER GROOVING	OVER-ALL HEIGHT	REGISTER DIAMETER SIZE	REGISTER DIAMETER TIR	DATUM DIAMETER LOCATION SPACING	DATUM DIAMETER LOCATION LOWER DATUM	APEX THICK-NESS	WALL THICKNESS .030 SPEC.	WALL THICKNESS .0447 SPEC.	WALL THICKNESS .0715 SPEC.	WALL THICKNESS VARIATION UPPER DATUM (PLUS)	WALL THICKNESS VARIATION LOWER DATUM (PLUS	40° ANGLE	PERP. 1 OF BASE	GROOVE LOCA-TION	GROOVE DEPTH (NOTE 2)	LINE
1	281	60.88	-----	2.402	1.979	.0010	1.501	.296	.330	.0295	.0442	.0694	.0016	.0014	OK	.0008	322	.0215	1
2	284	60.44	-----	2.402	1.978	.0010	1.501	.298	.312	.0295	.0434	.0700	.0011	.0012	"	.0010	319	.0210	2
3	295	60.02	-----	2.404	1.978	.0010	1.502	.299	.324	.0290	.0435	.0694	.0008	.0008	"	.0015	320	.0220	3
4	286	60.42	-----	2.403	1.978	.0018	1.503	.297	.311	.0296	.0443	.0700	.0005	.0006	"	.0012	319	.0205	4
5	298	60.12	-----	2.404	1.978	.0010	1.504	.302	.308	.0293	.0428	.0693	.0024	.0012	"	.0010	325	.0220	5
6	291	60.99	-----	2.405	1.978	.0020	1.505	.299	.314	.0304	.0440	.0687	.0020	.0009	"	.0008	323	.0215	6
7	293	61.20	-----	2.401	1.978	.0015	1.500	.297	.324	.0294	.0439	.0697	.0023	.0017	"	.0005	322	.0210	7
8	294	60.50	-----	2.404	1.978	.0020	1.501	.298	.325	.0294	.0439	.0698	.0005	.0007	"	.0015	322	.0195	8
9	295	60.27	-----	2.402	1.979	.0020	1.501	.299	.304	.0294	.0439	.0692	.0013	.0011	"	.0005	324	.0180	9
10	297	59.80	-----	2.403	1.977	.0010	1.503	.297	.306	.0293	.0437	.0686	.0011	.0007	"	.0015	318	.0210	10
11	349	60.49	-----	2.406	1.979	.0008	1.502	.300	.334	.0304	.0445	.0707	.0002	.0001	"	.0006	316	.0200	11
12	351	59.94	-----	2.405	1.978	.0007	1.503	.300	.326	.0302	.0438	.0705	.0004	.0004	"	.0008	.318	.0220	12
13	352	59.76	-----	2.404	1.979	.0004	1.502	.298	.327	.0303	.0436	.0705	.0002	.0002	"	.0008	.317	0210	13
14	353	60.24	-----	2.405	1.980	.0006	1.501	.301	.321	.0304	.0440	.0712	.0002	.0002	"	.0006	.318	.0215	14
15	354	59.24	-----	2.405	1.979	.0009	1.505	.299	.320	.0302	.0433	.0696	.0005	.0002	"	.0008	317	.0205	15
16	379	59.57	59.27	2.404	1.980	.0026	1.499	.300	.337	.0294	.0430	.0685	.0006	.0005	"	.0018	.318	.0215	16
17	380	59.73	59.39	2.405	1.980	.0008	1.501	.300	.318	.0297	.0437	.0683	.0002	.0001	"	.0003	318	.0215	17
18	382	58.87	-----	2.404	1.980	.0005	1.502	.300	.308	.0291	.0430	.0679	.0001	.0002	"	.0006	318	.0224	18
19	383	59.59	-----	2.403	1.980	.0007	1.502	.300	.316	.0298	.0432	.0680	.0003	.0001	"	.0003	.317	.0225	19
20	384	59.34	59.05	2.403	1.979	.0004	1.502	.300	.327	.0294	.0431	.0676	.0004	.0001	"	.0003	.320	.0220	20
21	385	59.21	-----	2.403	1.979	.0007	1.501	.299	.304	.0296	.0431	.0679	.0001	.0002	"	.0004	.320	.0224	21
22	386	60.11	59.85	2.405	1.980	.0007	1.501	.300	.322	.0299	.0442	.0692	.0001	.0001	"	.0004	.320	.0205	22
23	388	60.02	59.67	2.403	1.980	.0006	1.500	.300	.321	.0300	.0438	.0687	.0002	.0001	"	.0007	.319	.0220	23
24	389	59.12	58.85	2.405	1.978	.0007	1.500	.300	.337	.0290	.0432	.0683	.0001	.0001	"	.0006	.320	.0215	24
25	390	58.86	58.61	2.404	1.979	.0007	1.502	.300	.332	.0290	.0429	.0678	.0002	.0002	"	.0011	.320	.0225	25
26	391	59.44	59.12	2.404	1.979	.0004	1.502	.300	.316	.0296	.0436	.0684	.0001	.0001	"	.0005	.320	.0215	26
27	392	59.29	59.00	2.401	1.979	.0007	1.501	.300	.320	.0294	.0433	.0683	.0001	.0002	"	.0006	320	.0220	27
28	393	59.16	-----	2.406	1.979	.0007	1.502	.300	.310	.0295	.0433	.0681	.0001	.0001	"	.0005	.315	.0224	28
29	394	59.58	59.25	2.406	1.980	.0004	1.502	.300	.321	.0297	.0435	.0681	.0003	.0001	"	.0009	.320	.0215	29
DRAWING SPECIFICATIONS				2.404Ref.	1.980-.002	.001Max.	1.500±.002	.300+.003	.324Ref.	.030±.002	.0447±.002	.0715±.002	.002Max.	.002Max.	40°±0°5	.002Max.	.312+.010	.0213+.003	
AVERAGE		59.869	59.206	2.4038	1.9789	.00098	1.5018	.2993	.3198	.02963	.04358	.06902	.00062	.00047	-----	.00079	.3195	02137	
STD. DEV.		.624770	369088	.001390	.000859	.000574	.001379	.001333	.009502	.000430	.000450	.000965	.000684	.000468	-----	.000398	002308	.001016	

Note: 1. All dimensions are in inches.
2. Drawing specifies .020 - .003 perpendicular to the outside surface of the liner. This converts to .0213 perpendicular to the axis.
3. Liners 281 through 297 were manufactured from Nickel 200, Lot 57; Liners 349 through 394 were from Lot 57A. Both lots were from the same heat.

Appendix B
INSPECTION DATA SUMMARY
30° Ingot Iron (0.105-in. Wall) Liner

LINER	LINER SERIAL NUMBER	WEIGHT (GR.)	HEIGHT (IN.)	RING INNER DIAMETER (IN.)	DATUM DIAMETER SPACING (IN.)	WALL THICKNESS		WALL THICKNESS VARIATION		SPIT BACK DIAMETER		CONCENTRICITY T.I.R. (SPIT BACK)		FLANGE PERPEN-DICULAR-ITY (IN.)	LINER
						DATUM A (IN.)	DATUM B (IN.)	DATUM A (IN.)	DATUM B (IN.)	O. D. (IN.)	I. D. (IN.)	O. D. (IN.)	I.D. (IN.)		
1	414	342	4.910	2.9538	3.420	.1052	.1053	.0003	.0004	.5589	.3495	.0018	.0012	.0008	1
2	415	339	4.910	2.9546	3.418	.1045	.1048	.0002	.0001	.5617	.3495	.0011	.0013	.0008	2
3	416	339	4.911	2.9541	3.418	.1047	.1047	.0002	.0002	.5617	.3495	.0015	.0012	.0005	3
4	418	339	4.909	2.9537	3.420	.1047	.1047	.0002	.0003	.5603	.3495	.0014	.0015	.0007	4
5	419	340	4.910	2.9535	3.420	.1044	.1050	.0003	.0002	.5602	.3500	.0020	.0007	.0008	5
6	420	340	4.912	2.9540	3.420	.1047	.1051	.0004	.0002	.5603	.3495	.0024	.0010	.0008	6
7	421	338	4.910	2.9536	3.420	.1049	.1048	.0002	.0001	.5606	.3490	.0005	.0009	.0004	7
8	422	337	4.911	2.9535	3.420	.1037	.1045	.0007	.0004	.5605	.3495	.0020	.0012	.0005	8
9	423	339	4.909	2.9535	3.419	.1047	.1045	.0003	.0005	.5605	.3495	.0014	.0014	.0002	9
10	424	338	4.909	2.9538	3.420	.1044	.1047	.0002	.0003	.5596	.3495	.0020	.0015	.0008	10
11	425	338	4.909	2.9542	3.419	.1043	.1044	.0004	.0004	.5598	.3500	.0020	.0008	.0006	11
12	426	339	4.908	2.9538	3.421	.1049	.1054	.0002	.0002	.5607	.3490	.0020	.0018	.0008	12
13	427	340	4.912	2.9536	3.419	.1051	.1049	.0005	.0006	.5606	.3495	.0013	.0015	.0008	13
14	428	340	4.911	2.9534	3.420	.1048	.1050	.0002	.0003	.5604	.3500	.0017	.0015	.0004	14
15	430	340	4.911	2.9536	3.418	.1043	.1049	.0001	.0006	.5598	.3490	.0012	.0017	.0007	15
16	441	340	4.908	2.9534	3.416	.1047	.1049	.0007	.0004	.5610	.3505	.0018	.0010	.0010	16
17	442	339	4.911	2.9535	3.416	.1049	.1051	.0006	.0007	.5614	.3498	.0020	.0021	.0008	17
18	443	340	4.910	2.9534	3.418	.1049	.1050	.0005	.0004	.5569	.3495	.0020	.0024	.0009	18
19	444	343	4.910	2.9531	3.419	.1048	.1054	.0002	.0008	.5611	.3493	.0046	.0004	.0012	19
20	446	337	4.910	2.9536	3.419	.1044	.1042	.0010	.0011	.5605	.3502	.0012	.0009	.0007	20
21	448	340	4.911	2.9541	3.418	.1046	.1046	.0009	.0012	.5609	.3500	.0036	.0030	.0010	21
22	449	341	4.906	2.9537	3.416	.1053	.1041	.0005	.0009	.5612	.3499	.0022	.0030	.0009	22
23	450	339	4.901	2.9541	3.419	.1041	.1052	.0005	.0004	.5605	.3515	.0032	.0056	.0014	23
DRAWING SPEC.			4.910±.002	2.954±.0005	3.418±.002	.1050±.0005	.1050±.0005	.0010Max.	.0010Max.	.5600±.0005	.3500±.0005	.001TIR	.001TIR	.001Max.	
AVERAGE		339.4	4.9095	2.9537	3.4188	.10465	.10483	.00040	.00046	.56040	.34970	.00195	.00163	.00076	
STD. DEV.		1.408612	.002313	.000335	.001402	.000362	.000349	.000243	.000300	.001005	.000546	.000875	.001088	.000262	

Appendix C
INSPECTION DATA SUMMARY
Inhibitor for 30 Degree Ingot Iron Liner

LINE	INHIBITOR SERIAL NUMBER	WEIGHT (gr.)	HEIGHT h (in.)	HEIGHT H (in.)	d (in.)	D (in.)	ANGLE α Deg.	ANGLE α Min.	ANGLE β Deg.	ANGLE β Min.	LINE
1	5B	136.8	1.419	2.121	.500	2.779	15	3	47	11	1
2	6B	137.2	1.419	2.126	.500	2.781	15	3	47	10	2
3	7B	137.0	1.421	2.126	.502	2.781	15	1	47	6	3
4	8B	137.4	1.421	2.133	.500	2.780	15	2	47	13	4
5	9B	136.6	1.419	2.123	.500	2.779	15	4	47	9	5
6	10B	136.6	1.419	2.123	.501	2.778	15	4	47	10	6
7	11B	136.6	1.417	2.119	.499	2.779	15	3	47	7	7
8	12B	137.1	1.420	2.122	.500	2.780	15	2	47	9	8
9	13B	136.4	1.414	2.120	.504	2.778	15	2	47	10	9
10	15B	137.1	1.416	2.122	.501	2.781	15	4	47	6	10
11	16B	136.9	1.416	2.122	.500	2.781	15	4	47	6	11
12	17B	137.0	1.418	2.123	.501	2.780	15	4	47	6	12
13	18B	136.6	1.417	2.123	.500	2.779	15	4	47	6	13
14	19B	137.1	1.416	2.123	.501	2.780	15	4	47	6	14
15	20B	136.3	1.414	2.119	.499	2.778	15	4	47	6	15
16	21B	136.9	1.416	2.124	.501	2.780	15	4	47	6	16
17	22B	137.0	1.418	2.124	.500	2.781	15	4	47	6	17
18	23B	137.2	1.417	2.123	.500	2.781	15	4	47	6	18
19	24B	137.0	1.417	2.122	.500	2.780	15	4	47	6	19
20	26B	137.1	1.418	2.124	.500	2.781	15	4	47	6	20
21	27B	136.6	1.417	2.124	.500	2.780	15	4	47	6	21
22	28B	137.1	1.420	2.127	.501	2.780	15	4	47	6	22
23	29B	136.7	1.417	2.121	.501	2.779	15	4	47	5	23
DRAWING SPECIFICATIONS			1.417 ± .010	2.125 ± .010	.500 ± .010	2.779 ± .001	15° ± 30'		47° 05' ± 30'		
AVERAGE:		136.88	1.4176	2.1232	.5005	2.7798	15°	3.5'	47°	7.3'	
STD. DEV.:		.283888	.001921	.002938	.001038	.001029	.897955'		2.162380'		

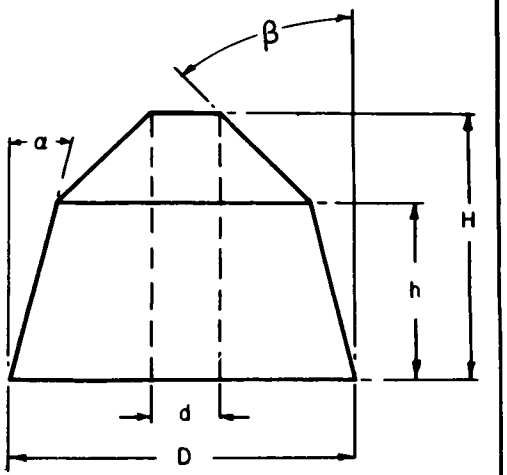

Note 1.: Refer to the attached sketch for the explanation of symbolism used in this table.

Appendix D
LOADED ASSEMBLY INSPECTION SUMMARY
Nickel Hyperbolic Liner

LINE	TYPE TEST	PROGRAM ROUND NUMBER	LINER SERIAL NUMBER	LINER-ADAPTER PLATE ASSEMBLY CONC. (IN.) (T.I.R.) (NOTE 1)	LINER-ADAPTER PLATE ASSEMBLY PERP. (IN.) (T.I.R.) (NOTE 1)	LOADING FIXTURE SERIAL NUMBER	CONC. OF LINER TO LOAD. FIX. AFTER LOADING (IN.) (T.I.R.) (NOTE 2)	OCTOL EXPLOSIVE FILLER WEIGHT (LB.)	LINE
1	Body Confinement Test	839-1	288	.0015	.0020	6	.004	1.24	1
2	" " "	839-2	281	.0020	.0015	5	.003	1.24	2
3	" " "	839-4	285	.0015	.0005	5	.003	1.24	3
4	" " "	839-7	286	.0028	.0020	5	.003	1.23	4
5	" " "	839-8	284	.0020	.0020	7	.002	1.23	5
6	Modified Flight Test	847-1	291	.0007	.0016	5	.003	1.24	6
7	" " "	847-2	293	.0014	.0009	5	.002	1.24	7
8	" " "	847-4	294	.0012	.0031	7	.004	1.24	8
9	" " "	847-5	295	.0013	.0015	6	.004	1.24	9
10	" " "	847-6	297	.0021	.0007	5	.001	1.24	10
11	" " "	847-7	349	.0035	.0012	5	.004	1.24	11
12	" " "	847-8	351	.0008	.0036	6	.002	1.24	12
13	" " "	847-9	352	.0010	.0011	6	.005	1.24	13
14	" " "	847-10	353	.0005	.0033	7	.005	1.24	14
15	" " "	847-11	354	.0018	.0010	5	.001	1.24	15
16	" " "	847-12	394	.0011	.0023	5	.003	1.24	16
17	Spin Test (25 rps)	850-9	390	.0009	.0007	6	.007	1.24	17
18	" " "	850-10	384	.0005	.0014	7	.004	1.24	18
19	" " "	850-11	386	.0005	.0020	5	.004	1.24	19
20	" " "	850-13	379	.0018	.0028	5	.005	1.24	20
21	" " "	850-14	382	.0008	.0010	6	.004	1.24	21
22	Full Flight Test	851-2	380	.0004	.0007	6	.005	1.24	22
23	" " "	851-3	389	.0007	.0012	7	.002	1.24	23
24	" " "	851-4	392	.0015	.0012	6	.005	1.25	24
25	Initial Pellet Mass Test	856-1	383	.0008	.0017	7	.003	1.24	25
26	" " " "	856-2	385	.0007	.0011	5	.004	1.23	26
27	Full Flight Shipped to NASA	-----	388	.0010	.0018	7	.004	1.25	27
28	" " " " "	-----	391	.0009	.0013	5	.001	1.24	28
29	" " " " "	-----	393	.0015	.0007	5	.004	1.24	29
AVERAGE OF ABOVE COLUMNS OF DATA:				.00128	.00158	--	.0035	1.240	
STANDARD DEVIATION OF ABOVE COLUMNS OF DATA:				.000719	.000813	--	.001404	.004211	

Note 1: The concentricity of the assembly was measured by mounting the assembly to a precision mandrel and indicating the outside surface of the adapter plate. The perpendicularity was measured while the liner was on the mandrel by indicating the surface of the adapter plate that supported the liner with respect to the loading fixture, that is, for Programs 839 and 856, the upper surface was indicated while all other programs used the lower surface.

Note 2: The concentricity of the loading fixture to the liner after loading was measured by placing the loading fixture on precision rollers and indicating the inside of the liner at the depth of 1.50 inches into the lower adapter plate assembly.

Appendix D
LOADED ASSEMBLY INSPECTION SUMMARY
Ingot Iron Conic Liner

LINE	TYPE TEST	PROGRAM ROUND NUMBER	LINER SERIAL NUMBER	LOADING FIXTURE SERIAL NUMBER	CONC. OF LINER TO CHARGE (IN.) (T.I.R.) (NOTE 1)	COMP. B EXPLOSIVE FILLER WEIGHT (LB.)	INHIBITOR SERIAL NUMBER	INHIBITOR POSITION IN LINER (IN.) (NOTE 2)	LINE
1	Modified Flight Test	853-1	414	16	.001	1.98	5B	- .001, - .003, - .003, - .002	1
2	" " "	853-2	418	17	.002	1.98	6B	.000, .000, .000, .000	2
3	" " "	853-3	420	16	.003	1.98	7B	- .001, - .001, - .002, - .002	3
4	" " "	853-4	422	16	.003	1.98	8B	+ .004, + .004, + .004, + .004	4
5	" " "	853-5	424	16	.002	1.98	9B	.000, - .001, - .001, - .002	5
6	" " "	853-6	423	17	.003	1.98	10B	- .001, - .002, - .003, - .002	6
7	" " "	853-7	426	17	.005	1.98	11B	- .001, - .002, - .003, - .002	7
8	" " "	853-8	427	16	.003	1.98	12B	- .001, .000, - .003, - .002	8
9	" " "	853-9	443	17	.002	1.98	20B	- .001, - .001, - .001, - .001	9
10	" " "	853-10	442	16	.003	1.98	16B	+ .001, + .001, .000, .000	10
11	" " "	853-11	430	16	.005	1.98	13B	- .005, - .003, - .003, - .005	11
12	" " "	853-12	441	17	.003	1.98	15B	+ .005, + .005, + .003, + .001	12
13	Spin Test (25 rps.)	858-17	446	17	.003	1.98	18B	- .001, .000, .000, .000	13
14	" " "	858-22	444	16	.003	1.98	17B	+ .001, + .002, .000, .000	14
15	" " "	858-23	448	16	.002	1.99	19B	+ .002, + .002, + .002, + .002	15
16	" " "	858-24	449	17	.005	1.98	28B	+ .003, + .003, + .004, + .004	16
17	" " "	858-25	450	16	.002	1.99	29B	- .002, - .002, - .002, - .003	17
18	Full Flight Test	859-1	421	17	.002	1.99	24B	+ .002, + .002, + .003, + .003	18
19	" " "	859-2	425	16	.002	1.99	21B	.000, .000, .000, .000	19
20	" " "	859-3	428	17	.002	1.99	27B	- .002, - .002, - .002, - .002	20
21	Full Flight Shipment	-----	415	16	.002	1.99	22B	+ .001, + .001, + .001, + .001	21
22	To NASA	-----	416	17	.002	1.99	23B	+ .002, + .002, + .002, + .002	22
23	" "	-----	419	17	.003	1.99	26B	- .001, - .001, - .001, - .001	23
	Average of above columns of data:				.0027	1.983	---	+ .0002, + .0002, - .0002, - .0003	24
	Standard Deviation of above columns of data:				.001053	.004869	---	.002187, .002187, .002315, .002265	

Note 1: The bare charge, of Composition B explosive, was placed on precision rollers and the concentricity of the liner to the charge was indicated at a location, inside the liner, three inches from the base of the liner.

Note 2: The position of the inhibitor in the liner was measured between the liner base and inhibitor base. "+" indicated that the inhibitor base was outside of the liner; "-" indicated that the inhibitor base was inside of the inhibitor. The four measurements were taken at 90 degree angular spacings.

Appendix E

TEST FACILITIES

NASA Test Site

General.-Figures E-1 and E-2 present views of the NASA Test Site facility. This facility consisted of a metal chamber with a six inch thick steel blast shield at one end. The meteor gun was mounted horizontally in an adjustable gun holder to the outside of the six-inch thick blast shield by means of a series of steel plates. A 2 inch I.D. aperture fitting was mounted in the center of these plates. The external chamber assembly, including the meteor gun, was encased in a 7-inch diameter, .064-inch wall, aluminum vacuum housing. This vacuum housing was bolted to the largest of the steel plates and sealed to it by means of an "O" ring. A $2\frac{1}{2}$-inch I.D. steel tube connected the plate outside the chamber to the inside vacuum tank mounting. A pipe from a vacuum pump (Kinney, Model KC-15) was welded to the vacuum tank mounting. A 9-foot long, 6-inch O.D. x 1/8-inch wall, 6061-T6 aluminum alloy, vacuum tank was bolted to the tank mounting and sealed by a 12-inch diameter "O" ring flange.

An adjustable steel rack was used to support the tank and support and align the four Field Emission Corporation Model 231 X-ray pulsers. The Model 231 X-ray pulsers discharged a 105 KV pulse for 30 nanoseconds. The X-ray pulsers were arranged in orthogonal pairs on both sides of the tank. As shown in Fig. E-2, the X-ray pulsers were mounted at an angle of 45° from a horizontal plane through the tank axis. One thermocouple vacuum gage, Kinney Model KTG-1, was connected to the vacuum tank and another to the vacuum pump for pressure measurement. The cassette holders for each station (orthogonal pair of X-ray pulsers) were bracketed together at right angles and mounted on top of the tank so that the film planes were perpendicular to the corresponding pulser axes. Eastman Kodak "Royal Blue Medical Film" was used in the cassettes with DuPont Industrial Intensifying Screens. A pair of Lucite plastic sheets were bracketed at right angles and hung on the underside of the vacuum tank directly below the cassettes. Conic Calibration Standards (Fig. 15) were mounted on these plastic sheets. The material of the Conic Calibration Standard used was the same as the meteor simulator being tested.

A Beckman, Model 7270, digital readout counter, set at $x10^{-7}$sec, was used to measure the time from the shorting of the "twisted pair" to the discharge of the X-ray pulsers. A single trace oscilloscope, Tektronix Model 545, with a Polaroid camera attached was used as a backup system for time measurements.

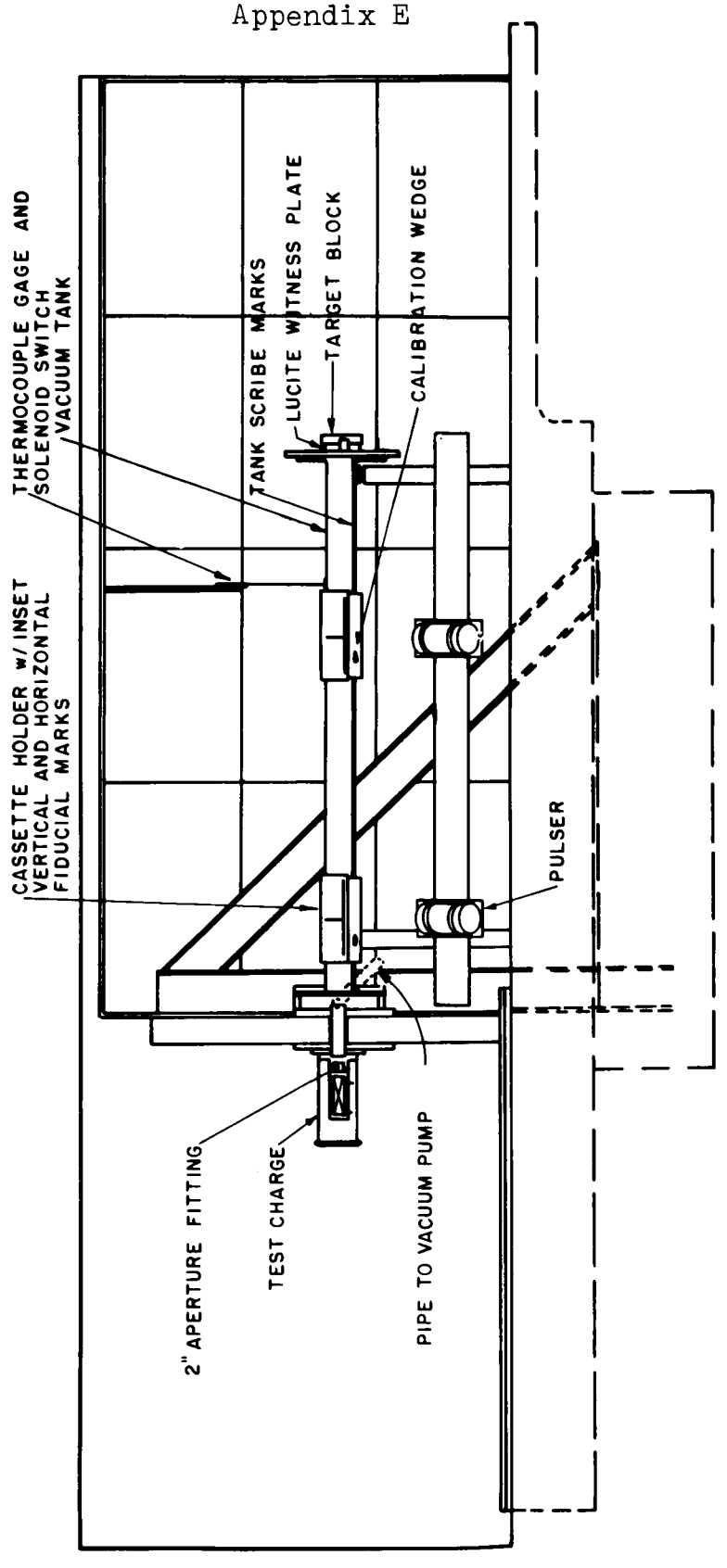

Fig. E-1. Side Schematic View of NASA Test Site.

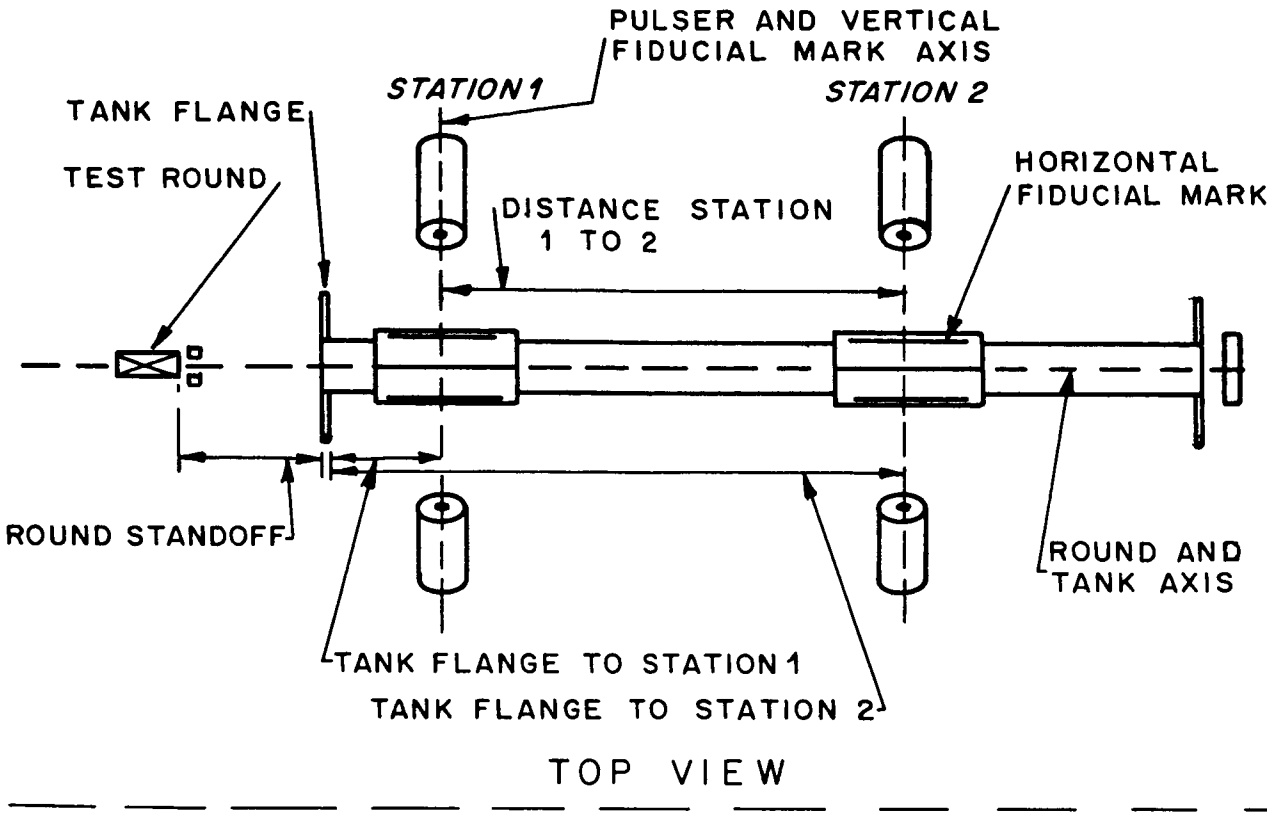

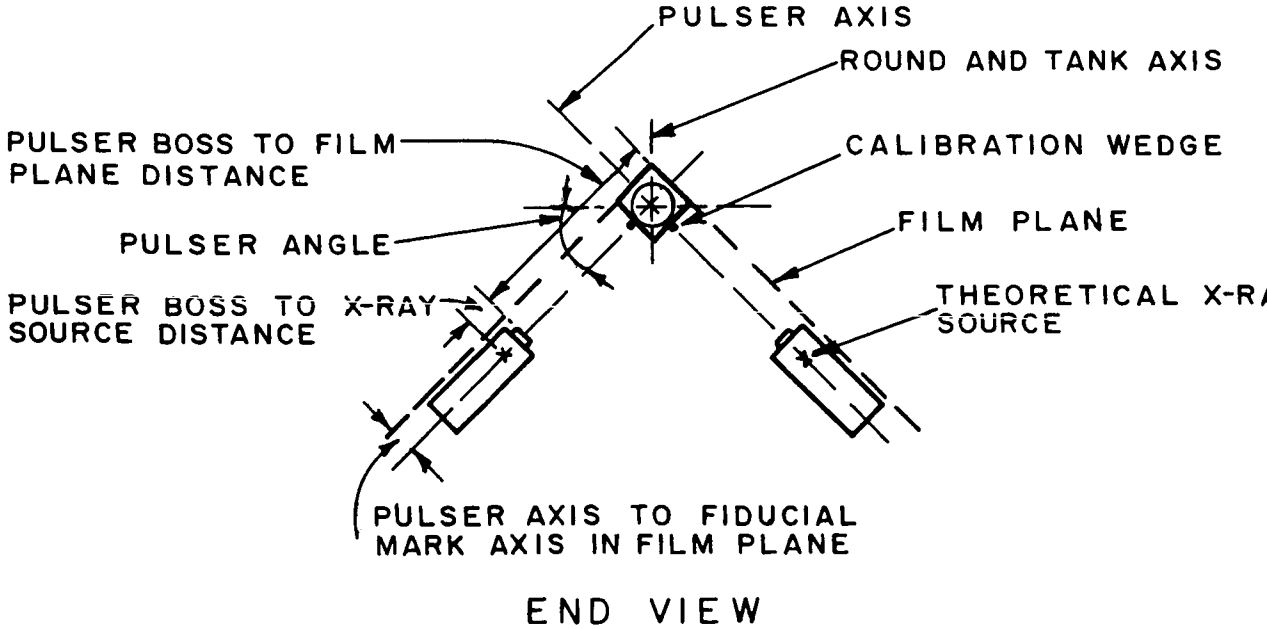

Fig. E-2. Top and End Schematic View of NASA Test Site.

Measurement procedure. - The NASA Test Site, as shown in Fig. E-2, was constructed with two separate orthogonal stations which were arranged along the horizontal axis of the vacuum tank. All spatial measurements were therefore made in relation to this tank axis to reduce error. The information necessary for proper system alignment included: X-ray beam axis to tank axis relation; X-ray beam axis to vertical fiducial mark relation; and X-ray source to film distance. A basic requirement was that at each station the two X-ray beams intersect the tank axis such that one plane was formed and that the plane was normal to the tank axis. The vertical fiducial marks were located so that they lay within the X-ray beam plane. Additional information necessary for pellet velocity computations included: the distance between station one and station two; the time interval between the X-ray pulser discharges at station one and station two; and the pellet spatial position in the reference frame of each station. Finally, a pressure reading was necessary to determine the vacuum level. The following paragraphs discuss the methods used to obtain the necessary measurements.

Because of irregularity, slope, and lack of plumb, the building housing the vacuum apparatus was not used as a reference for alignment of the equipment. Measurements between the X-ray pulsers, vacuum tank, and cassette holders were made relative to each other. The X-ray pulsers were first aligned such that the distance between the pairs of pulsers at each station was constant and each pulser of a pair was the same distance from the vacuum tank flange. Once aligned, the pulsers were set at a 45° angle to a plumb line passing through the tank axis by using a leveling device. The pulsers were then located at approximately the same distance from the tank. The vertical fiducial marks of the cassettes were located in the plane of the pulsers, at each station, by placing the cassette holder over a scribe mark on the top of the vacuum tank and placing the cassette fiducial marks the same distance from the vacuum tank flange as the pulsers of that station. The distance between the pulser boss and the cassette holder was measured using an extended machinist's square balanced on the back of the cassette holder. A straight edge was placed flat across the pulser boss and was used to indicate the machinist's square for the measurement. The measurements described above were checked throughout the program for variation. The data taken made it possible to locate the effective X-ray source, vacuum tank axis, and film fiducial marks in space.

The measurement of the time interval between the X-ray pulser discharges at the two stations was made by two independant methods. One method used a twisted pair of no. 28 enameled wire placed in direct contact with the explosive filler. When the twisted pair was shorted by the detonation of the round, a pair of delay amplifiers (Field Emission Corp., Model 154) and a pair of digital read-out counters (Beckman Model 7270) were started. One amplifier and one counter were connected to the pair of pulsers at each station through pulser triggering step-up transformers. When the pulsers were trig-

gered by the delay amplifiers the counters stopped. The time interval was then obtained by subtracting the trigger time at station one from the trigger time at station two. This system was the more accurate of the two methods used to measure the time interval and was used when ever possible in velocity computations.

The second method used a single trace oscilloscope (Tektronix, Model 545) with a Polaroid camera attached. The sweep rate of the oscilloscope was set at 20 μsec/cm. The oscilloscope was connected to the output of the delay amplifier for station one. The delay amplifier triggered the oscilloscope sweep and the pulser triggering step-up transformer simultaneously. The vertical input of the oscilloscope was attached to an antenna hung near the pulsers of both stations. The time interval was determined by measuring the distance between pulser discharge hash marks on the film and correcting for the reduction factor developed in the camera optical system.

In comparing the two time measurement systems it was found that the oscilloscope measured time interval was less than the counter measured time interval by 2.8 to 3.2μsec. This was due to error in the calibration of the sweep rate of the oscilloscope. Therefore, a correction factor was added to all oscilloscope readings, used in calculating velocities, to compensate this error.

The vacuum level, i.e., ambient pressure of the enclosed vacuum system, was measured with thermocouple vacuum gages (Kinney KTG-1). Readings were taken at both the tank and the pump. The pump reading appeared to be approximately twenty microns lower than the tank reading. The ambient pressure reading was corrected for ambient temperature since the thermocouple gage was not accurate above seventy degrees Fahrenheit.

The task of measuring the pellet image on the film required care, accuracy, and a certain amount of personal judgment on the part of the observer. One problem encountered involved the determination of the pellet central axis. If the pellet axis was nearly perpendicular to one of the two film planes of the station, it was difficult to determine the central axis of the pellet image on the film. If the pellet was bent, the axis had to be approximated. Other problems involved the location of the pellet end points of the film image. Since the pellet was usually not exactly parallel to the film, the end points lay somewhere within the pellet image. Splitting, peeling, and fragmenting of the pellet also made determination of the pellet tip and tail difficult.

Before any measurements were made, the pair of orthogonal films for each station were viewed and the general character of the pellet examined. An effort was made to determine the spatial orientation, shape, and peeling and fragmenting effects. The film to be measured was then placed on an illuminated viewing screen.

Appendix E

A transparent plastic sheet with an axis graduated in tenths of an inch was used to help in locating pellet central axis. The plastic sheet was then removed and the end points were chosen and marked lightly in pencil. Peeling or fragmenting material which seemed unstable was not considered as part of the pellet. The plastic sheet with an axis was then again positioned under the film and aligned with reference to the end points. Measurements of the distance to the horizontal and vertical fiducial marks were made for each end point using a clear plastic draftsman's ruler that was accurate to 0.02 inch.

Since the pellet diameter was squared in the calculation of the pellet volume, measurement of the pellet diameter required special measuring techniques. A reticle, accurate to 0.005 inch, and an eyepiece were used to measure the diameters and lengths of the pellet images. The plastic sheet with a graduated axis was used as a guide for measuring pellet image diameters at intervals of 0.1 inch. The diameters were measured to the middle of the penumbra-like band at the edge of the pellet image.

An IBM 1620 computer was used to perform the calculations necessary to analyze the pellet image data and produce the pellet descriptive information, i.e., mass, velocity, orientation in space, length, and tumbling rate.

Large Chamber

General. -Figures E-3 and E-4 present three views of the Large Chamber. This test facility had an open-roofed, pyramid-shaped, firing chamber at ground level and a two room basement, directly below, housing the X-ray pulsers and film cassettes. Pellets were fired from the firing chamber, through a 2-1/2-inch aperture hole on the floor of the chamber, down into the basement where radiographs of the pellet could be taken. The floor of the chamber had a 3-inch hole through its 6-inch thick steel plate.

This facility was used to spin test the meteor simulators in programs 850 and 858. The gun was supported to the spin mechanism by a piece of 3/64 inch stiff steel wire. The wire was guyed so that the gun was aligned over the aperture hole while spinning. The length of the steel wire was adjusted so that the liner in the gun was 6 inches above the aperture plate. The angular velocity of the gun was monitored on an oscilloscope so that the gun could be fired when the desired angular velocity, in this case -25rps, was obtained.

The radiographic equipment consisted of three Field Emission Corporation, Model 233 X-ray pulsers which produced a 300KV discharge for 100 nanoseconds. The X-ray pulsers were arranged to

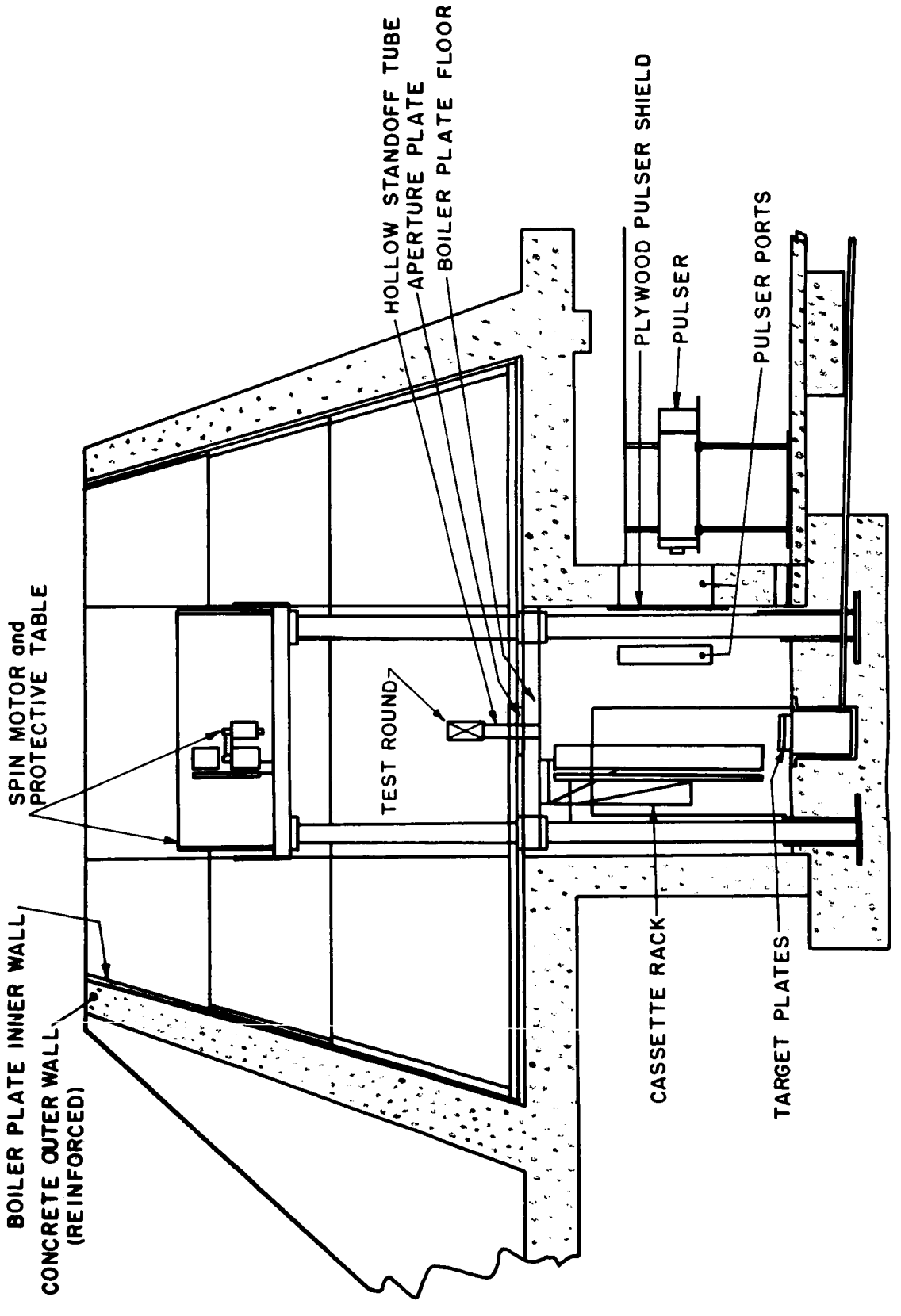

Fig. E-3. Schematic Side View of Large Test Site.

Appendix E

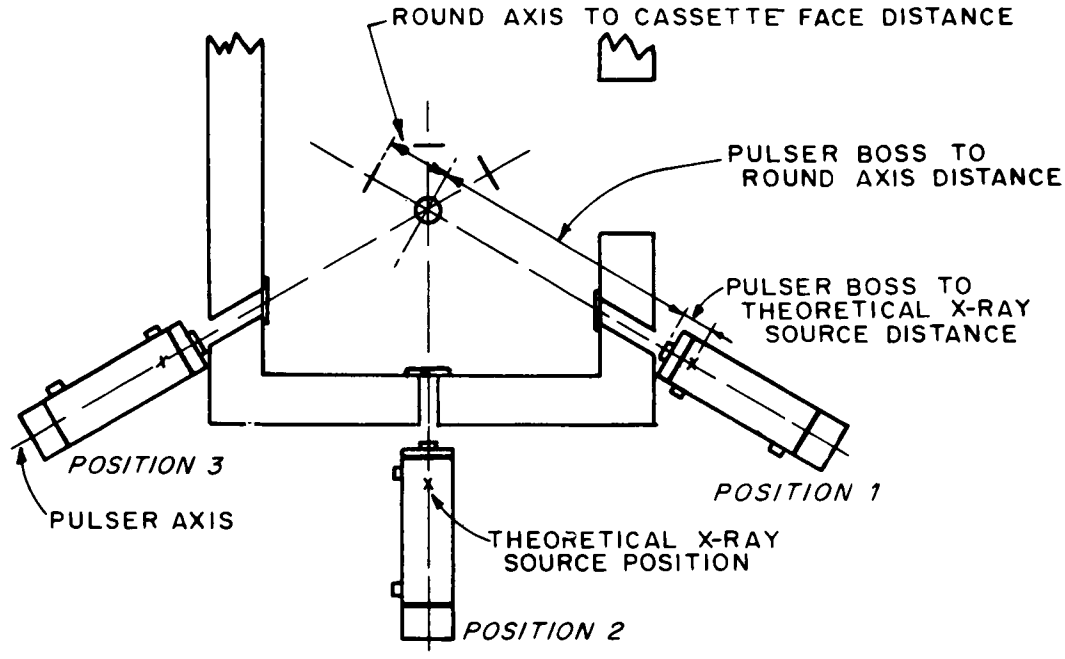

TOP VIEW

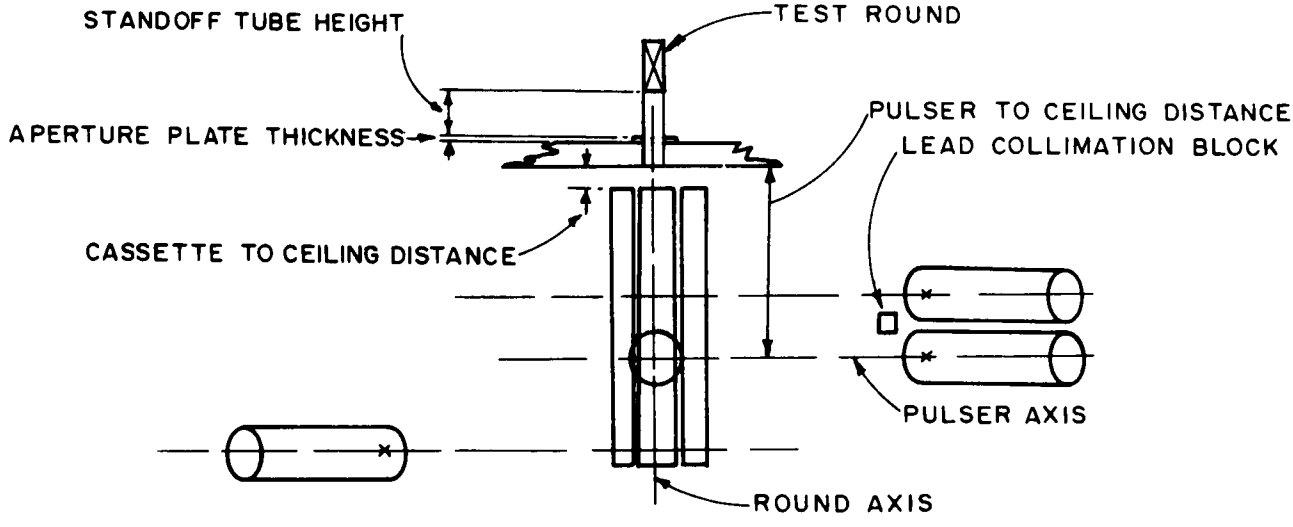

END VIEW

Fig. E-4. Schematic Top and End View of Large Test Site.

view the pellet in two planes with 120° angular spacing. The system used three delay amplifiers, Field Emission Corporation, Model 154. One X-ray pulser was attached to each delay amplifier. The delay amplifiers were started by an electrical impulse at the time of the explosion. Three methods of producing an electrical impulse were used.

(1) Shorting Screen: A shorting screen consists of a thin plastic sheet with metal foil laminated on both sides. Wire leads were attached to the metal foil sheets. When any portion of the explosion reached the shorting screen, the metal sheets were shorted. In these tests a 1-inch diameter hole was cut in the shorting screen, to allow the pellet to pass through, and the shorting screen was placed 2-1/2 inches in front of the gun.

(2) Repeatable detonation time detonators: High voltage detonators, DupontX98AA, produce a repeatable detonation time when fired at approximately 3 KV. In some of the Spin Test shots, these arc-firing detonators were used. Then, the electrical impulse used to start the delay amplifiers was the initial detonation impulse.

(3) Twisted pair of wires: A twisted pair of no. 28 enameled wires were located at about 1-inch from the spinning round and supported to a wooden stand. When the round was detonated, the twisted pair of wires shorted at the time that the shock wave or debris reached them. This system proveded a very satisfactory initiation time sensor.

The same electrical impulse that started the delay amplifiers also started three Beckman Model 7270 digital readout counters, set at $x10^{-7}$ multiplier. The counters were stopped when the delay amplifiers triggered the X-ray pulser discharges. A back up time measuring system was also used. The back up system consisted of a Tektronix Model 555 dual trace oscilloscope, with a Polaroid camera attached. The oscilloscope vertical input was attached to an antenna hung near the X-ray pulsers. When the delay amplifiers started, the oscilloscope began its sweep. When the X-ray pulsers discharged, the oscilloscope trace recorded the wave form created by the X-ray pulser discharge.

The angular velocity of the gun in the Spin Tests was measured with an oscilloscope (Dumont Model 304-H). The vertical input was attached to a magnetic pickup coil mounted in close proximity to a magnet mounted on the spin drive axis that supported the meteor simulator gun. The horizontal input was attached to a sine wave generator which produced a 25 cps signal. This set up produced Lissajou figures on the oscilloscope when the round was spinning. When the gun was spun at 25 rps, the Lissajou figure formed was a circle.

Eastman Kodak "Royal Blue Medical Film" and DuPont Industrial

Intensifying Screens were used in the film cassettes.

Measurement procedure. - Since this facility did not afford two simultaneous views of the pellet, but instead, three independent views, the pellet could not be analyzed three dimensionally. The pellet flight path was assumed to be down the center of the X-ray system. Measurements of locations of fiducial marks were made with reference to the ceiling of the basement. Information required for the alignment of the systems included: pulser to film relationship, pulser to round axis relationship, pulser to ceiling distance, and the distance from the X-ray source to the film. Additional information needed for computing the pellet velocity included: the vertical distance between X-ray pulsers, the vertical distance between fiducial marks, the time interval between X-ray pulser discharges, and the vertical distance from the pellet image to the fiducial mark on the film.

System alignment measurements were made using a tape measure and plumb line. Time intervals between X-ray pulser discharges were measured with oscilloscope and counters as at the NASA Test Site. The film measuring procedures used for this facility were identical to those used for the NASA Test Site. The mass and velocity data obtained from the Large Chamber testing did not include the three-dimensional corrections used for the NASA Test Site; therefore, the mass and velocity values obtained for the Spin Test shots should be considered as approximate values.

OPEN TEST SITE

General. - Figure E-5 and E-6 present three of the Open Test Site test facility. This test facility consisted of a large, parabolic-shaped, dirt-reinforced, steel blast director with the round and film cassette located near the focus. Two X-ray pulsers, Field Emission Model 233, were located behind protective aluminum plates outside the vertex of the parabolic wall. The X-ray pulsers were mounted in a support stand so that one pulser was located directly above the other pulser. The gun stood vertically on a piece of thin cardboard that was secured to a wooden stand. A blast-proof film cassette was positioned approximately 6-inches from the gun central axis.

A twisted pair of wires was placed in direct contact with the explosive filler and shorted when the gun was detonated. These wires were attached to two delay amplifiers, Field Emission Corporation, Model 154, by means of a trigger circuit. When the wires shorted, the delay amplifiers were started. These delay amplifiers triggered the discharge of the X-ray pulsers, at predetermined times, through pulser triggering step-up transformers.

A single trace oscilloscope, Tektronix Model 545, with a

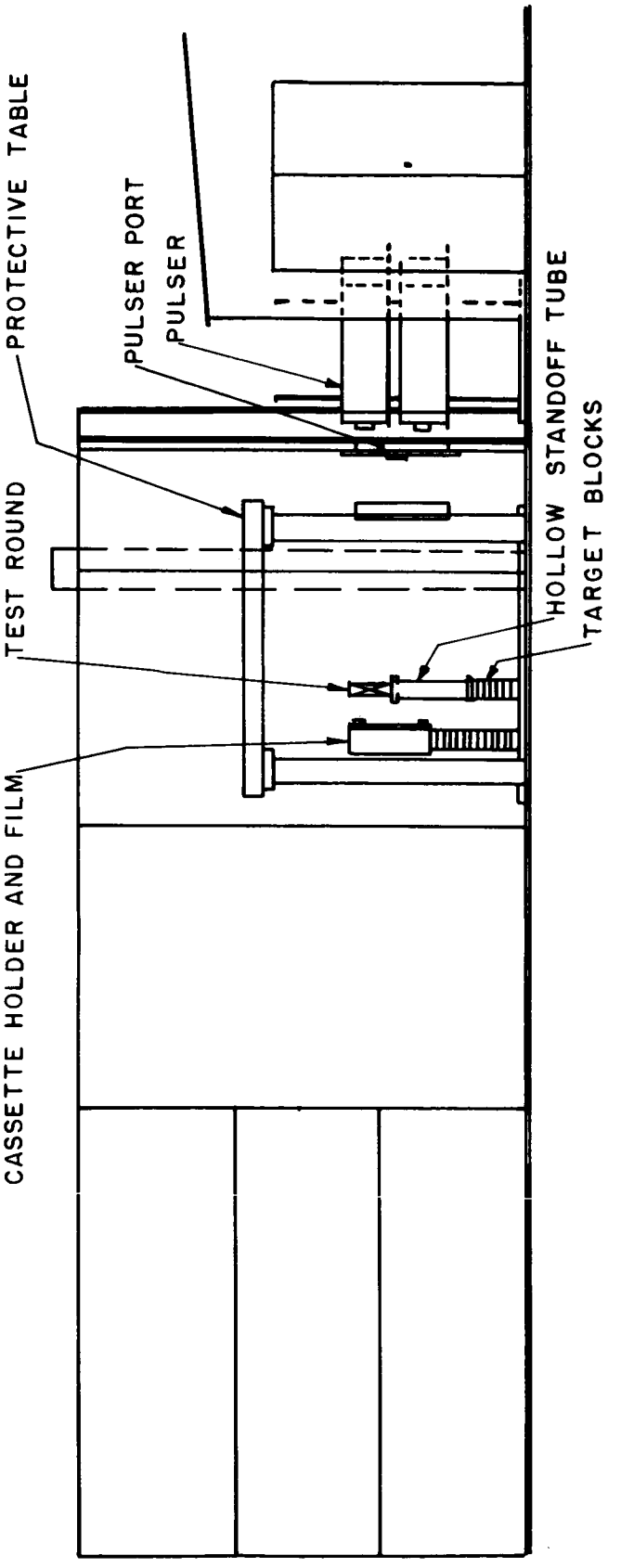

Fig. E-5. Schematic Side View of Open Test Site.

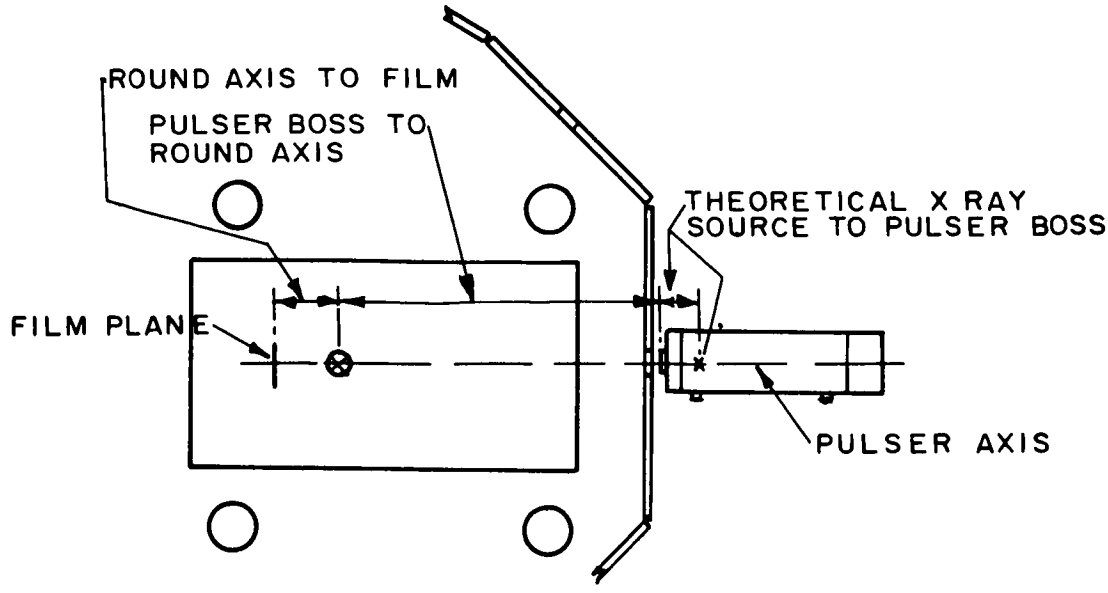

TOP VIEW

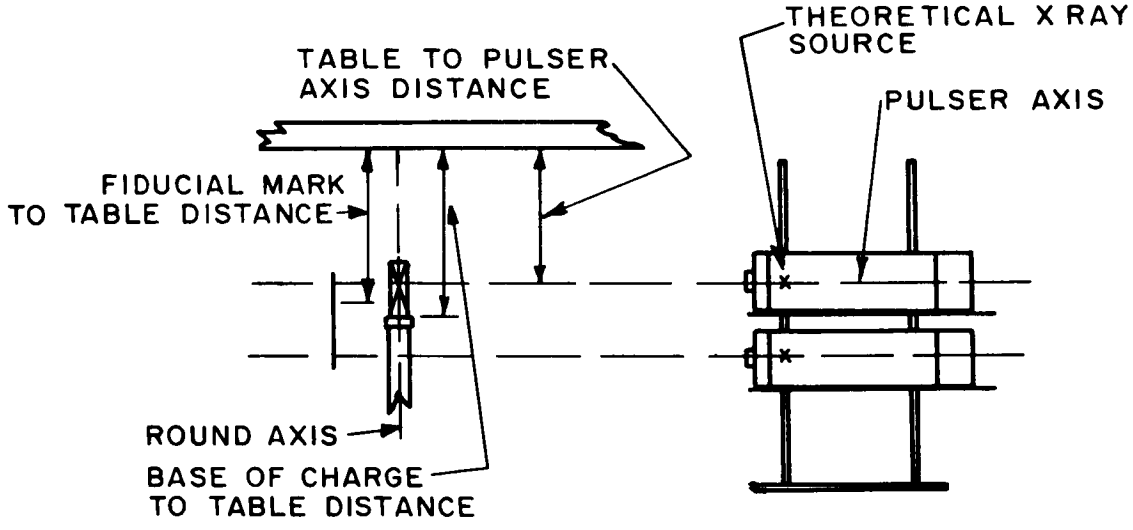

SIDE VIEW

Fig. E-6. Schematic Top and Side Views of Open Test Site.

Polaroid camera attached was attached to the triggering transformers so that the oscilloscope displayed the discharge of the X-ray pulsers. The oscilloscope sweep was started by the shorting of the twisted pair of wires at the gun.

Eastman Kodak "Royal Blue Medical Film" was used with DuPont Industrial Intensifying Screens in the blast-proof cassette. The upper window of the cassette was positioned so that the liner end of the gun would be radiographed with the pellet a few inches from the base of the liner. The second window of the cassette was located so that the pellet could be radiographed at a distance of about 10 inches from the base of the liner.

Measurement procedure. - Since this facility did not afford two simultaneous views of the pellet, but instead, two independent views, the pellet could not be analyzed three-dimensionally. The pellet flight path was assumed to be down the center of the X-ray system. Measurements of locations of fiducial marks were made with reference to the underside of the 6-inch thick steel platform standing above the gun and cassette. Information required for the alignment of the systems included: pulser to film relationship, pulser to round central axis relationship, pulser to platform distance, film to platform distance, and the distance from the X-ray source to the film. Additonal information needed for computing the pellet velocity included: the vertical distance between X-ray pulsers, the time interval between X-ray pulser discharges, and the vertical distance from the pellet image to the fiducial mark on the film.

System alignment measurements were made using a tape measure and plumb line. Time intervals between X-ray pulser discharges were measured with oscilloscope and counters as at the NASA Test Site. The film measuring procedures used for this facility were identical to those used for the NASA Test Site. The mass and velocity data obtained from the Open Test Site testing did not include the three-dimensional corrections used for the NASA Test Site; therefore, the mass and velocity values obtained for Open Test Site tests should be considered as approximate values.

Appendix F

SPATIAL DATA REDUCTION

The purpose of this section is to define a method of data reduction by which the spatial properties of a shaped charge pellet can be easily determined. These properties are length, orientation, and linear and angular velocity. It is also desirable to know the ratio of pellet size to image size for each of the X-ray shadowgraphs.

Figure F-1 is a simple sketch of the NASA Test Site at the Ravenna Army Ammunition Plant, Ravenna, Ohio. The sketch suggests a natural coordinate system. The Z axis is the line formed by the intersection of the planes of the films. The X axis is a line perpendicular to the Z axis in the plane of films 2 and 4 through the point P. The Y axis is the line, in the plane of films 1 and 3, perpendicular to the X and Z axes at point P. Fiducial lines are located on each film along the X (or Y) axis and at a given distance from the Z axis as shown in Fig. F-2.

In the ideal case the coordinates of the pellet tip can be found by locating the intersection of lines P_1 P_2 and P_4 P_5 as shown in Fig. F-3. Likewise the pellet tail is at the intersection of lines P_1 P_3 and P_4 P_6. However, due to errors in measurement, timing, and positioning, these lines do not intersect but come very close. Thus a method must be found to determine a "best" fit.

If Q_1, (X_1, Y_1, Z_1) and Q_2 (X_2, Y_2, Z_2) are points in Euclidean three space, then the line passing through these two points is given by the parametric equation;

$$L1 : \frac{X-X_1}{X_2-X_1} = \frac{Y-Y_1}{Y_2-Y_1} = \frac{Z-Z_1}{Z_2-Z_1} = t \qquad (1)$$

Let Q_1' (X_1', Y_1', Z_1') and Q_2' (X_2', Y_2', Z_2') be two other points in three space. Then a line between these two points is given by

$$L2 : \frac{X'-X_1'}{X_2'-X_1'} = \frac{Y'-Y_1'}{Y_2'-Y_1'} = \frac{Z'-Z_1'}{Z_2'-Z_1'} = s \qquad (2)$$

Appendix F

If Q is a point on L1 and Q' is a point on L2, then the distance between Q and Q' is given by

$$d = ((X-X')^2 + (Y-Y')^2 + (Z-Z')^2)^{1/2} \tag{3}$$

and

$$d^2 = (t\,(X_2-X_1) - s\,(X_2'-X_1') - (X_1-X_1'))^2 + (t\,(Y_2-Y_1) - s\,(Y_2'-Y_1') - (Y_1-Y_1'))^2 + (t\,(Z_2-Z_1) - s\,(Z_2'-Z_1') - (Z_1-Z_1'))^2 \tag{4}$$

The shortest distance between point Q and line L2 can be found by solving the equation,

$$\frac{\partial d}{\partial s} = 0 \tag{5}$$

for s and substituting into equation (4).

In a similar manner the shortest distance, between Q' and L1 can be found by solving,

$$\frac{\partial d}{\partial t} = 0 \tag{6}$$

If (5) and (6) are solved simultaneously we can determine the shortest distance between lines L1 and L2. Thus,

$$-2d\frac{\partial d}{\partial s} = 2\,(t\,(X_2-X_1) - s\,(X_2'-X_1') - (X_1'-X_1'))(X_2'-X_1') + 2\,(t\,(Y_2-Y_1) - s\,(Y_2'-Y_1') - (Y_1'-Y_1))(Y_2'-Y_1') \tag{5a}$$

$$+ 2\,(t\,(Z_2-Z_1) - s\,(Z_2'-Z_1') - (Z_1'-Z_1))(Z_2'-Z_1) = 0$$

and

$$2d\frac{\partial d}{\partial t} = 2(t\,(X_2-X_1) - s\,(X_2'-X_1') - (X_1'-X_1))(X_2-X_1) +$$

$$2(t\,(Y_2-Y_1) - s\,(Y_2'-Y_1') - (Y_1'-Y_1))(Y_2-Y_1) + \qquad (6a)$$

$$2(t\,(Z_2-Z_1) - s\,(Z_2'-Z_1') - (Z_1'-Z_1))(Z_2-Z_1) = 0$$

By use of the vectors,

$$\vec{a} = (X_2-X_1,\ Y_2-Y_1,\ Z_2-Z_1) \qquad (7)$$

$$\vec{a}' = (X_2'-X_1',\ Y_2'-Y_1',\ Z_1'-Z_1') \qquad (8)$$

$$\vec{X} = (X_1'-X_1,\ Y_1'-Y_1,\ Z_1'-Z_1) \qquad (9)$$

We can change (5a) and (6a) into the equivalent vector forms

$$0 = t\,(\vec{a}\cdot\vec{a}) - s\,(\vec{a}\cdot\vec{a}') - \vec{X}\cdot\vec{a} \qquad (10)$$

$$0 = t\,(\vec{a}\cdot\vec{a}') - s\,(\vec{a}\cdot\vec{a}') - \vec{X}\cdot\vec{a}' \qquad (11)$$

Solving for s, we get,

$$s = \frac{(\vec{a}\cdot\vec{a})(\vec{X}\cdot\vec{a}') + (\vec{a}\cdot\vec{a}')(\vec{X}\cdot\vec{a})}{(\vec{a}\cdot\vec{a}')^2 - (\vec{a}\cdot\vec{a})(\vec{a}'\cdot\vec{a}')}$$

and t can be found by substituting s into (10) or (11).

Appendix F

Since the shortest distance between two points in Euclidean three space is a straight line, then the line given by $P_\alpha(X_\alpha, Y_\alpha, Z_\alpha)$ $P_\beta(X_\beta, Y_\beta, Z_\beta)$ where

$$X_\alpha = t\,(X_2-X_1) + X_1 \tag{12}$$

$$X_\beta = s\,(X_2'-X_1') + X_1' \tag{13}$$

$$Y = t\,(Y_2-Y_1) + Y_1 \tag{14}$$

$$Y = s\,(Y_2-Y_1) + Y_1 \tag{15}$$

$$Z_\alpha = t\,(Z_2-Z_1) + Z_1 \tag{16}$$

$$Z_\beta = s\,(Z_2'-Z_1') + Z_1' \tag{17}$$

If we let

$$Q_1 = P_1 \tag{18}$$

$$Q_2 = P_3 \tag{19}$$

$$Q_1' = P_4 \tag{20}$$

$$Q_2 = P_6 \tag{21}$$

in Fig. F-3, then the midpoint of the line segment represents the "best" fit for the pellet tip P_7 by the least squares method. The length of Q Q' is then a measurement of the error in our determination of point P_7.

Likewise if we let

$$Q_1 = P_1 \tag{22}$$

$$Q_2 = P_2 \tag{23}$$

$$Q_1' = P_4 \tag{24}$$

$$Q_2' = P_5 \tag{25}$$

then the midpoint of the line segment represents the "best" fit for the pellet tail P_8 and the length $Q\,Q'$ is then a measurement of the error in our determination of point P_8.

If the coordinates of P_7 and P_8 are known, then the pellet length can be computed by

$$L = ((X_7-X_8)^2 + (X_7-Y_8)^2 + (Z_7-Z_8)^2)^{1/2} \tag{26}$$

Since,

$$(\tan^2\alpha) + 1 = \frac{1}{\cos^2\alpha} \tag{27}$$

then

$$\alpha = \tan^{-1}\sqrt{\frac{1 - \cos^2\alpha}{\cos^2\alpha}} \tag{28}$$

The angle γ in Fig. F-4 can then be computed from the relation

$$\cos\gamma = \frac{Z_7-Z_8}{L} \tag{29}$$

and the angle θ can be computed by

$$\theta = \tan^{-1}\frac{Y_7-Y_8}{X_7-X_8} \tag{30}$$

Appendix F

The coordinates of the pellet midpoint are calculated from

$$\bar{X} = \frac{X_7+X_8}{2.0} \tag{31}$$

$$\bar{Y} = \frac{Y_7+Y_8}{2.0} \tag{32}$$

$$\bar{Z} = \frac{Z_7+Z_8}{2.0} \tag{33}$$

The reduction factors are defined to be the ratio of the object size to the image size. We can see from Fig.F-5 that

$$\frac{X_P}{i} = \frac{\bar{X}}{o} \tag{34}$$

or

$$R_f = \frac{o}{i} = \frac{\bar{X}}{X_P} \tag{35}$$

For films 2 and 4 the reduction factors are given by

$$R_f = \frac{X_4-Y}{Y_4} \tag{37}$$

and for films 1 and 3 the reduction factors are

$$R_f = \frac{X_1-X}{X_1} \tag{38}$$

Now assume that we have a second view of the pellet at a time Δt later. Assume also that the pellet position is recorded in a second coordinate frame which has been displaced from the first by a distance F along the Z axis. Then the velocity is given by

$$v = ((\bar{X}_2 - X_1)^2 + (\bar{Y}_2 - \bar{Y}_1)^2 + (F + \bar{Z}_2 - Z_1)^2)^{1/2} / \Delta t \tag{39}$$

We know that for any two vectors, $\vec{a}$ and $\vec{b}$

$$\vec{a} \cdot \vec{b} = |\vec{a}||\vec{b}| \cos \alpha \tag{40}$$

$$\cos \alpha = \frac{\vec{a} \cdot \vec{b}}{|\vec{a}||\vec{b}|} \tag{41}$$

$$\vec{a} \cdot \vec{b} = p = (x_{(7,1)} - x_{(8,1)})(x_{(7,2)} - x_{(8,2)}) + (Y_{(7,1)} - Y_{(8,1)}) \tag{42}$$

$$(y_{(7,2)} - y_{(8,2)}) + (z_{(7,1)} - z_{(8,1)})(z_{(7,2)} - z_{(8,2)})$$

$$|\vec{a}| = L_1 \quad \text{(length at position 1)} \tag{43}$$

$$|\vec{b}| = L_2 \quad \text{(length at position 2)} \tag{44}$$

then

$$\cos \alpha = \frac{P}{L_1 L_2} \tag{45}$$

or from equation (29)

$$\alpha = \tan^{-1}\sqrt{\frac{L_1^2 L_2^2 - P^2}{P^2}} \tag{46}$$

and the angular velocity can be calculated from

$$\omega = \frac{\alpha}{\Delta t} \tag{47}$$

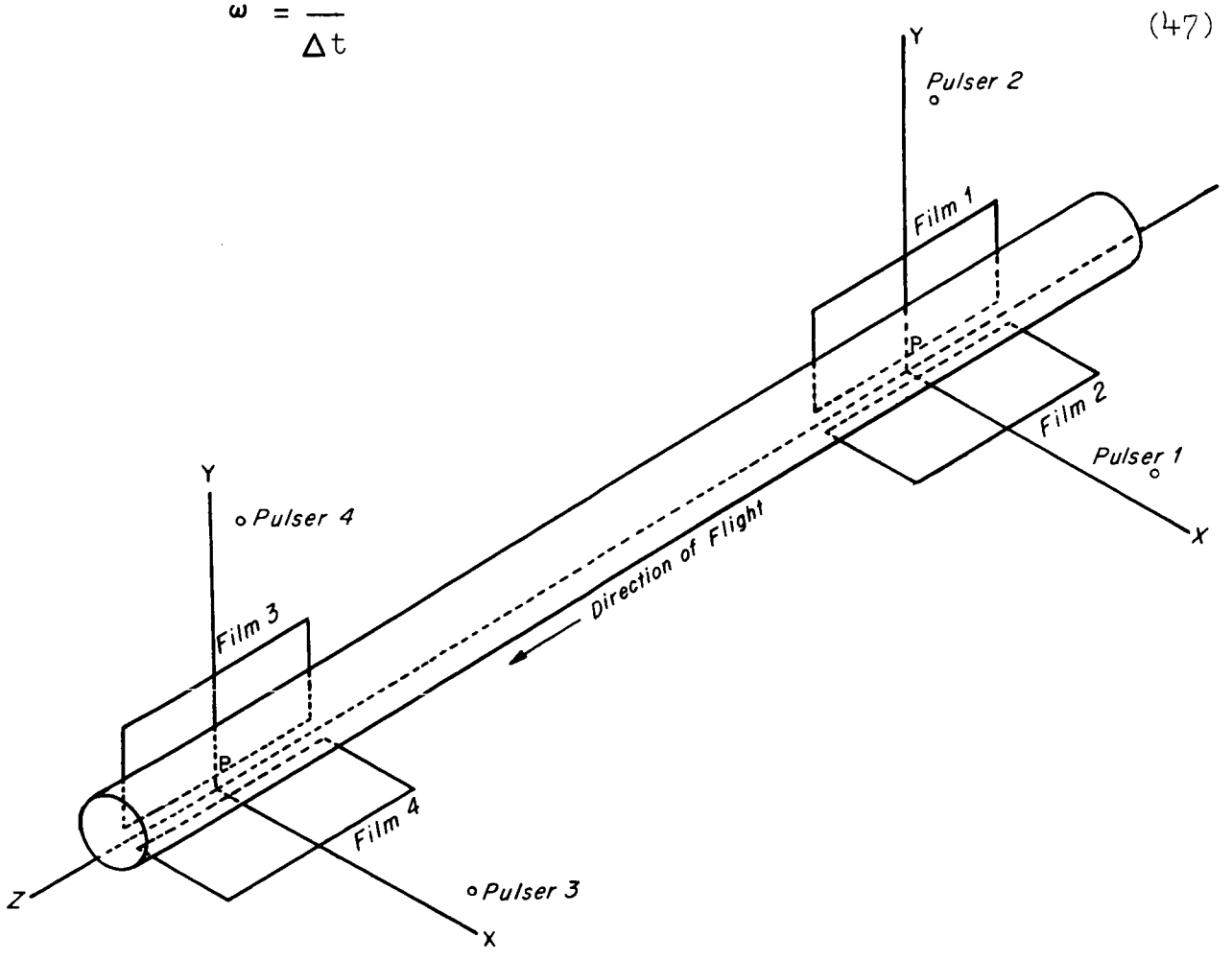

Fig. F-1. Sketch of NASA Test Site Vacuum Tube and Film Geometry.

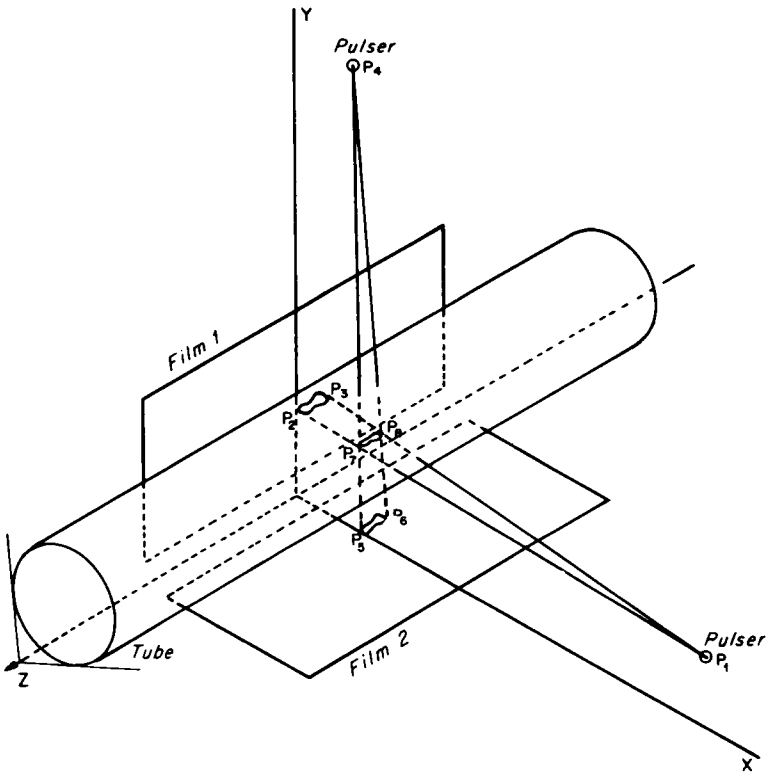

Fig. F-3. Sketch of NASA Test Site Pellet, Film Images, and X-ray Sources at One Station.

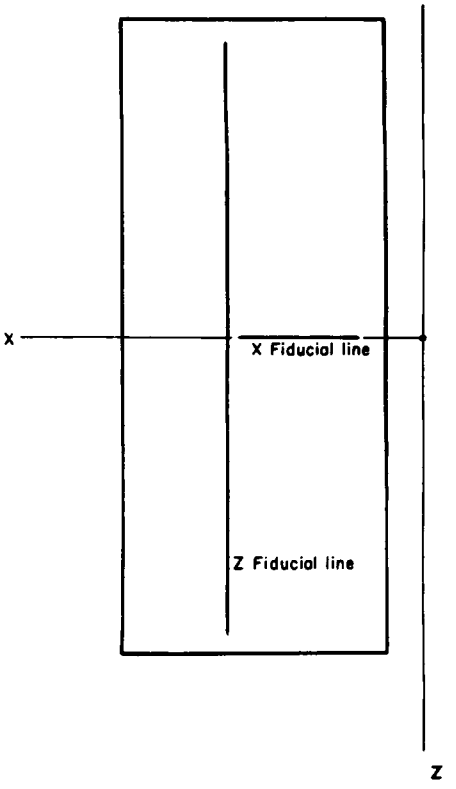

Fig. F-2. Sketch of NASA Test Site Film and Fiducial Line Geometry.

Appendix F

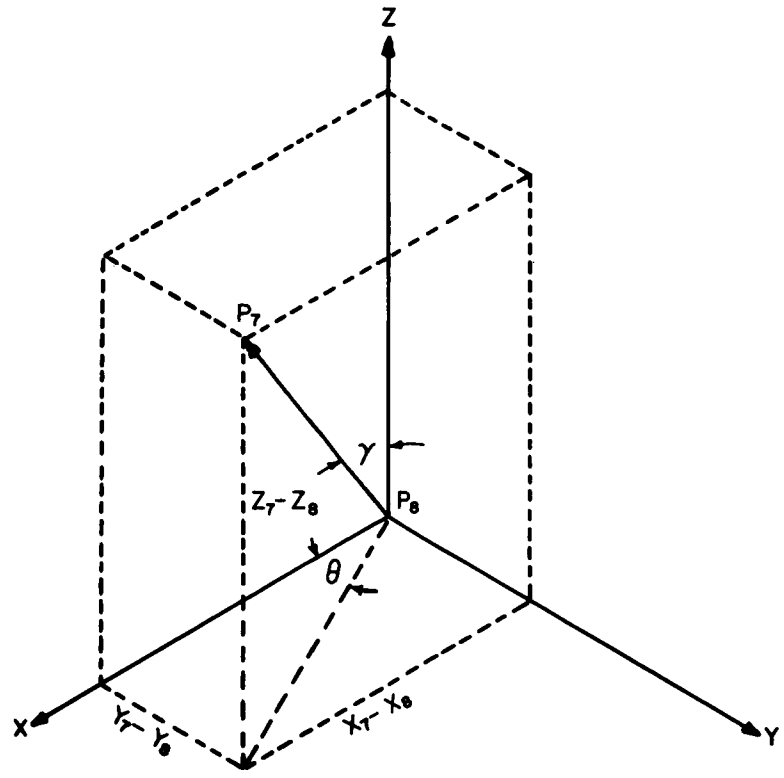

Fig. F-4. Sketch of Spherical Coordinate System Used for the NASA Test Site Pellet Orientation Calculations.

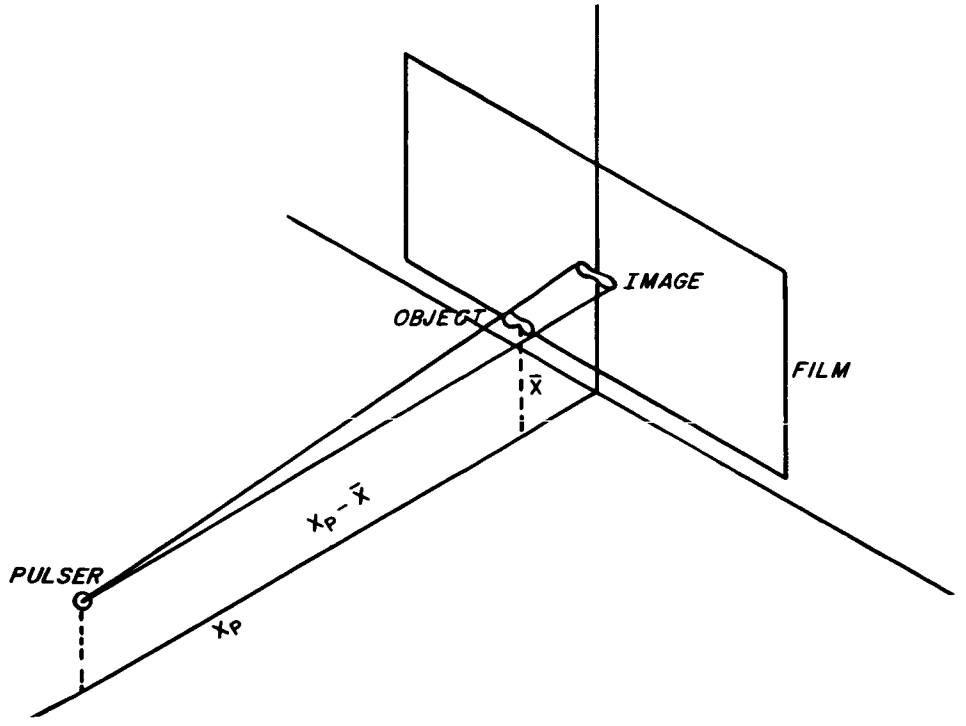

Fig. F-5. Sketch of NASA Test Site Pellet, Film Image, and X-ray Source At One Station.

Appendix F

```
C PELLET SIZE AND VELOCITY
C DRD-31, AUGUST 22, 1966
      DIMENSION X7(2), Y7(2), Z7(2), X8(2), Y8(2), Z8(2)
      DIMENSION PLEN(2), RF(4), XB(2), YB(2), ZB(2), ERROR(4)
      COMMON X1, Y1, Z1, X4, Y4, Z4, I, ERR, PLEN
      COMMON X7, Y7, Z7, X8, Y8, Z8, GAMMA, THETA
      X2 = 0.0
      X3 = 0.0
      Z1 = 0.0
      Y5 = 0.0
      Y6 = 0.0
      Z4 = 0.0
      READ 1000, FX, FY, FDIS, PROG
      PRINT 1010, PROG
    5 I = 0
   10 I = I + 1
      READ 1020, Y2, Z2, Y3, Z3, X1, Y1, SER
      READ 1030, X5, Z5, X6, Z6, X4, Y4, T
      IF (I - 2) 20, 30, 30
   20 PRINT 1040
   30 Y2 = FY - Y2
      Y3 = FY - Y3
      X5 = FX - X5
      X6 = FX - X6
      CALL POINT(X3, Y3, Z3, X6, Y6, Z6, X7, Y7, Z7)
      ERROR(2*I) = ERR
      CALL POINT(X2, Y2, Z2, X5, Y5, Z5, X8, Y8, Z8)
      ERROR(2*I-1) = ERR
   50 XL = X7(I) - X8(I)
      YL = Y7(I) - Y8(I)
      ZL = Z7(I) - Z8(I)
      PLEN(I) = SQRTF(XL*XL + YL*YL + ZL*ZL)
      CALL ANGLE
   59 XB(I) = (X7(I) + X8(I))/2.0
      YB(I) = (Y7(I) + Y8(I))/2.0
      ZB(I) = (Z7(I) + Z8(I))/2.0
      RF(2*I-1) = 1.0 - XB(I)/X1
      RF(2*I) = 1.0 - YB(I)/Y4
      GAMMA = GAMMA*57.295
      THETA = THETA*57.295
      PRINT 1050, SER, PLEN(I), GAMMA, THETA
      PUNCH 1090, PLEN(I), RF(2*I-1), SER
      PUNCH 1090, PLEN(I), RF(2*I), SER
      IF (I-2) 10, 60, 60
```

Appendix F

```
 60 XL = XB(2) - XB(1)
    YL = YB(2) - YB(1)
    ZL = ZB(2) - ZB(1) + FDIS
    VEL = SQRTF(XL*XL + YL*YL + ZL*ZL)*25.4/T
    XL = (X7(1) - X8(1))*(X7(2) - X8(2))
    YL = (Y7(1) - Y8(1))*(Y7(2) - Y8(2))
    ZL = (Z7(1) - Z8(1))*(Z7(2) - Z8(2))
    XL = XL + YL + ZL
    COSG = XL/(PLEN(1)*PLEN(2))
    SING = SQRTF(1.0 - COSG*COSG)
    OMEGA = ATANF(SING/COSG)
    IF (COSG) 70, 80, 80
 70 OMEGA = OMEGA + 3.1415927
 80 OMEGA = OMEGA*159154.94/T
    PRINT 1060, VEL, OMEGA
    PRINT 1070, RF(1), RF(2), RF(3), RF(4)
    PRINT 1080, ERROR(1), ERROR(2), ERROR(3), ERROR(4)
    GO TO 5
1000 FORMAT(3F10.4, A4)
1010 FORMAT(1H1, 10X, 7HPROGRAM, 2X, A4)
1020 FORMAT(6F10.4,A4)
1030 FORMAT(6F10.4,F5.1)
1040 FORMAT(1HO, 10X, 5HROUND, 7X, 13HPELLET LENGTH, 8X,
   C       5HGAMMA, 7X, 5HTHETA)
1050 FORMAT(1HO, 10X, A4, F17.3, F17.2, F12.2)
1060 FORMAT(1HO, 10X, 10HVELOCITY =, F6.2, 2X, 6HKM/SEC, 7X,
   C       18HANGULAR VELOCITY =, F8.1, 1X, 7HREV/SEC)
1070 FORMAT(1HO, 10X, 17HREDUCTION FACTORS, F7.3, 2X, 3H(1), F7.3,
   C       1X, 3H(2), F7.3, 1X, 3H(3), F7.3, 1X, 3H(4))
1080 FORMAT(1HO, 10X, 13HERROR FACTORS, F7.3, 2X, 6HTAIL 1, F7.3,
   C       2X, 5HTIP 1, F7.3, 2X, 6HTAIL 2, F7.3, 2X, 5HTIP 2, //)
1090 FORMAT(10X, 2F9.3, 1X, A4)
     END
```

```
      SUBROUTINE ANGLE
      DIMENSION X7(2), Y7(2), Z7(2), X8(2), Y8(2), Z8(2), PLEN(2)
      COMMON X1, Y1, Z1, X4, Y4, Z4, I, ERR, PLEN
      COMMON X7, Y7, Z7, X8, Y8, Z8, GAMMA, THETA
      COSG = (Z7(I) - Z8(I))/PLEN(I)
      SING = SQRTF(1.0 - COSG*COSG)
      GAMMA = ATANF(SING/COSG)
      IF (COSG) 52, 54, 54
   52 GAMMA = GAMMA + 3.1415927
   54 THETA = ATANF((Y7(I) - Y8(I))/(X7(I) - X8(I)))
      IF (X7(I) - X8(I)) 55, 59, 59
   55 IF (Y7(I) - Y8(I)) 57, 56, 56
   56 THETA = THETA + 3.1415927
      GO TO 59
   57 THETA = THETA - 3.1415927
   59 RETURN
      END

SUBROUTINE POINT(XR, YR, ZR, XS, YS, ZS, XA, YA, ZA)
DIMENSION XA(2), YA(2), ZA(2)
DIMENSION X7(2), Y7(2), Z7(2), X8(2), Y8(2), Z8(2), PLEN(2)
COMMON X1, Y1, Z1, X4, Y4, Z4, I, ERR, PLEN
COMMON X7, Y7, Z7, X8, Y8, Z8, GAMMA, THETA
CR = -X1
DR = YR - Y1
CS = XS - X4
DS = -Y4
CC = X4 - X1
DC = Y4 - Y1
R1 = CR*CR + DR*DR + ZR*ZR
R2 = CS*CS + DS*DS + ZS*ZS
R3 = CR*CS + DR*DS + ZR*ZS
R4 = CC*CR + DC*DR
R5 = CC*CS + DC*DS
S = (R1*R5 - R3*R4)/(R3*R3 - R1*R2)
T = (S*R3 + R4)/R1
R1 = T*CR + X1
R2 = T*DR + Y1
R3 = T*ZR
R4 = S*CS + X4
R5 = S*DS + Y4
R6 = S*ZS
XA(I) = (R1 + R4)/2.0
YA(I) = (R2 + R5)/2.0
ZA(I) = (R3 + R6)/2.0
R1 = R1 - R4
R2 = R2 - R5
R3 = R3 - R6
ERR = SQRTF(R1*R1 + R2*R2 + R3*R3)
RETURN
END
```

Appendix F

PROGRAM 839

ROUND	PELLET LENGTH	GAMMA	THETA
1.1	.486	27.21	-101.70
1.2	.488	53.20	-115.17

VELOCITY = 9.46 KM/SEC ANGULAR VELOCITY = 448.0 REV/SEC

REDUCTION FACTORS .844 (1) .822 (2) .816 (3) .764 (4)

ERROR FACTORS .029 TAIL 1 .030 TIP 1 .036 TAIL 2 .079 TIP 2

ROUND	PELLET LENGTH	GAMMA	THETA
2.1	.396	43.61	-41.61
2.2	.349	84.64	25.99

VELOCITY = 9.34 KM/SEC ANGULAR VELOCITY = 1162.0 REV/SEC

REDUCTION FACTORS .867 (1) .825 (2) .881 (3) .770 (4)

ERROR FACTORS .040 TAIL 1 .039 TIP 1 .035 TAIL 2 .039 TIP 2

ROUND	PELLET LENGTH	GAMMA	THETA
4.1	.352	26.25	86.48
4.2	.326	14.33	-70.08

VELOCITY = 9.47 KM/SEC ANGULAR VELOCITY = 644.8 REV/SEC

REDUCTION FACTORS .864 (1) .878 (2) .861 (3) .916 (4)

ERROR FACTORS .005 TAIL 1 .006 TIP 1 .048 TAIL 2 .029 TIP 2

ROUND	PELLET LENGTH	GAMMA	THETA
7.1	.370	39.64	-159.22
7.2	.369	126.36	-147.03

VELOCITY = 9.53 KM/SEC ANGULAR VELOCITY = 1445.7 REV/SEC

REDUCTION FACTORS .834 (1) .828 (2) .780 (3) .781 (4)

ERROR FACTORS .017 TAIL 1 .021 TIP 1 .055 TAIL 2 .046 TIP 2

Appendix G

MASS DATA REDUCTION

The purpose of this section is to describe a method of data reduction by which the mass of a shaped charge pellet can be determined. Figure G-1 below, presents a sketch of a typical pellet, X-ray pulser source, and film situation in the NASA Test Site orthogonal X-ray system.

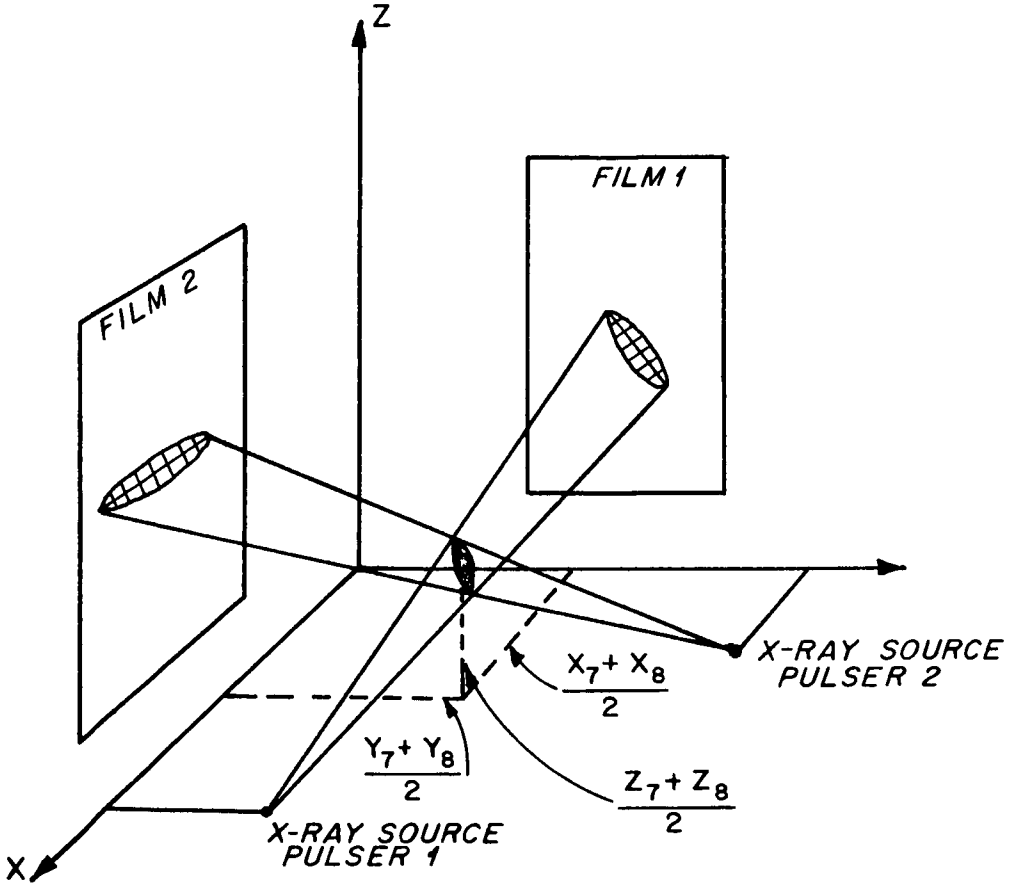

Fig. G-1. Sketch of NASA Test Site Pellet, X-ray Source, and Film Geometry.

Appendix G

In Fig.G-1the projected pellet shadow is shown in the Y-Z plane, representing film 1, and in the X-Z plane, representing film 2. Each shadow was divided into a number of increments of equal length. Each increment was assumed to have a circular cross-section and possibly with a tapered lateral surface. Therefore, the increments were assumed to be of the form of a circular conic frustum. When the diameters at both ends of an increment were equal, the form reduced to a right circular cylinder.

A sketch of a typical film image of a pellet in the orthogonal system is shown below, Fig. G-2

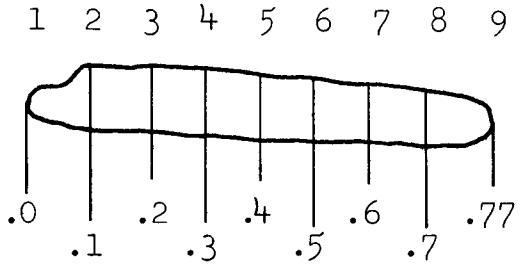

Figure G-2.Sketch of Typical Film Image of Pellet.

The pellet image above has been divided into seven uniform increments of 0.1 inch and one increment of length .07 inch. The expression for the volume of one circular conic frustum increment can be written as:

$$V = \frac{\pi h}{12}\left[D_1^2 + D_1 D_2^2 + D_2^2\right] \qquad (48)$$

where, h is the length of the increment and D_1 and D_2 represent the diameter of the frustum ends.

Appendix G

The total volume of the pellet can be computed by using the following equation:

$$V = \frac{\pi h}{12}\left[(d_1^2 + d_1d_2 + d_2^2) + (d_2^2 + d_2d_3 + d_3^2) + (d_3^2 + d_2d_3 + d_3^2) + (d_3^2 + d_3d_4 + d_4^2) + \ldots.\right] + \frac{\pi (\Delta h)}{12}\left[d_8^2 + d_8d_9 + d_9^2\right] \quad (49)$$

where h = height of increment = 0.1 inch

(Δh) = height of partial increment = .07 inch

d_j = diameter measurement

By changing the mode of expression to that of a summation and using the notation used in the computer program at the end of this section:

$$V = \frac{\pi h}{12}\sum_{J=1}^{K}\left[DIAM.^2(J) + DIAM.(J) \times DIAM.(J+1) + DIAM.^2(J+1)\right] + \frac{\pi(\Delta h)}{12}\left[DIAM.^2(K+1) + DIAM.(K+1) \times DIAM.(K+2) + DIAM.^2(K+2)\right] \quad (50)$$

where K = number of complete increments

$DIAM.(J) = d_J$ = diameter measurement

and other notation is defined in the same way.

In computing the pellet volume in the above manner, each of the three dimensions of measurement were increased by a magnification factor, M, from the pellet to the film image. Therefore, the dimensions of the pellet measured on the film must be decreased by a factor of 1/M. Applying $(1/M)^3$, or the volume reduction factor, $(REFAC)^3$, through the pellet's midpoint for the appropriate film, the corrected volume was found to be:

$$V_c = (REFAC)^3 V \qquad (51)$$

But, most pellets were found to be oriented such that the film image was foreshortened, with respect to the full profile pellet image, and therefore the pellet length was greater than it appeared to be. Figure G-3 presents a sketch of a case of pellet image foreshortening.

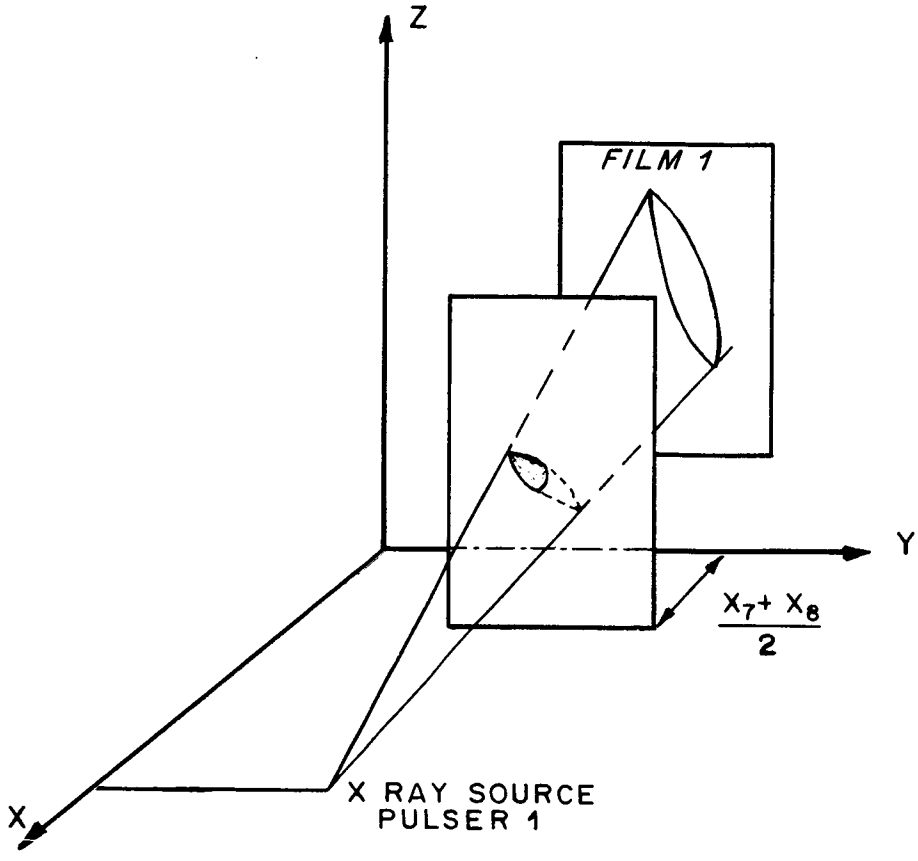

Figure G-3 Sketch of Pellet Image Foreshortening Situation.

Assume that an image of the pellet exists in the plane parallel to the Y-Z plane at the distance of [(X7+X8)/2] from the Y-Z plane. The reduced length of the image in the new plane would be:

$$(RLEN) = (REFAC)(FLEN) \qquad (52)$$

where, REFAC = Reduction factor

FLEN = Length of pellet image on film
RLEN = Reduced length in the new plane

Since the new plane was made parallel to the Y-Z plane and intersected the pellet's center, the ratio of the true pellet length, as determined by the distance equation (53) shown below, to the reduced pellet length, as determined in equation (52) yielded the correction factor for the pellet's actual volume.

$$d = PLEN = ((X_7-X_8)^2 + (Y_7-Y_8)^2 + (Z_7-Z_8)^2)^{1/2} \quad (53)$$

Where, $d = PLEN$ = pellet length
(X_7, Y_7, Z_7) = pellet tip coordinate

(X_8, Y_8, Z_8) = pellet tail coordinate

Therefore:

$$(RATIO) = \frac{PLEN}{RLEN} \quad \text{where, RATIO} \geq 1. \quad (54)$$

By multiplying the pellet volume, as computed from film measurements with magnification correction applied, by the pellet material density, the uncorrected value for the mass was written:

$$PMASS = V_c \rho. \quad (55)$$

Multiplying by the foreshortening correction ratio, the corrected mass was:

$$CMASS = (PMASS)(RATIO). \quad (56)$$

This computation procedure was used for each of the films at station 1 and station 2, i.e., films 1 and 2, and films 3 and 4 respectively. Then the two mass values obtained at each station were averaged and the resulting mass was taken to be the measured mass of that station. Program DRD-19, written in Fortran II-D language, was used to compute pellet masses in the manner just outlined. The calculations were performed on an IBM 1620 computer.

Appendix G

```
      DRD-19, PELLET MASS
      K S HOVAN MAY 27, 1966
      DIMENSION DIAM(14),SER(4)
      DIMENSION PMASS(4),CMASS(4)
      CON=12.0
      PI=3.14159265
      READ 1000,DEN,STEP,NUM
      PRINT 2000,NUM
    6 M=0
    7 DO 22 L=1,4
      SIGMA=0.0
      READ 1001,FLEN,PLEN,REFAC,SER(L)
      READ 1002,(DIAM(J),J=1,14)
      K=FLEN/STEP
      DO 14 J=1,K
      VIN=STEP*(DIAM(J)*DIAM(J)+DIAM(J)*DIAM(J+1)+DIAM(J+1)*DIAM(J+1))
   14 SIGMA=SIGMA+VIN
      AK=K
      DELTA=FLEN-(0.1*AK)
      DEVOL=DELTA*(DIAM(J+1)*DIAM(J+1)+DIAM(J+1)*DIAM(J+2)+DIAM(J+2)*DIA
     1M(J+2))
      TOVOL=SIGMA+DEVOL
      PROD=((((PI*DEN)*REFAC)*REFAC)*REFAC)/CON
      PMASS(L)=TOVOL*PROD
   22 CMASS(L)=PMASS(L)*(PLEN/(REFAC*FLEN))
      AMAS1=(PMASS(1)+PMASS(2))/2.0
      AMAS2=(PMASS(3)+PMASS(4))/2.0
      CMAS1=(CMASS(1)+CMASS(2))/2.0
      CMAS2=(CMASS(3)+CMASS(4))/2.0
      PRINT 2001
      PRINT 2002
      PRINT 2003,SER(1),PMASS(1),PMASS(2),AMAS1
      PRINT 2006,CMASS(1),CMASS(2),CMAS1
      PRINT 2004,SER(3),PMASS(3),PMASS(4),AMAS2
      PRINT 2007,CMASS(3),CMASS(4),CMAS2
      M=M+1
      IF (M-4) 7,26,26
   26 PRINT 2005
      GO TO 6
 1000 FORMAT (2F10.4,I4)
 1001 FORMAT (3F10.4,A4)
 1002 FORMAT (14F5.3)
 2000 FORMAT (1H1,10X7HPROGRAM,2XI4)
 2001 FORMAT (1H0,10X5HROUND,10X4HMASS,11X4HMASS,11X12HAVERAGE MASS)
 2002 FORMAT (1H ,25X4H(GM),11X4H(GM),15X4H(GM))
 2003 FORMAT (1H0,10XA4,F15.2,1X3H(1),F11.2,1X3H(2),F15.2)
 2004 FORMAT (1H0,10XA4,F15.2,1X3H(3),F11.2,1X3H(4),F15.2)
 2005 FORMAT (1H0,10X1H*,2X45HMASS VALUES ADJUSTED FOR IMAGE FORESHORTEN
     1ING/1H1)
 2006 FORMAT (1H0,12X1H*,F16.2,1X3H(1),F11.2,1X3H(2),F15.2)
 2007 FORMAT (1H0,12X1H*,F16.2,1X3H(3),F11.2,1X3H(4),F15.2,/)
      END
```

Appendix G

PROGRAM 8390			
ROUND	MASS (GM)	MASS (GM)	AVERAGE MASS (GM)
1.1	.87 (1)	.97 (2)	.92
*	.86 (1)	1.14 (2)	1.00
1.2	.89 (3)	.79 (4)	.84
*	.98 (3)	1.23 (4)	1.10
ROUND	MASS (GM)	MASS (GM)	AVERAGE MASS (GM)
2.1	.62 (1)	.86 (2)	.74
*	.74 (1)	.98 (2)	.86
2.2	.61 (3)	.71 (4)	.66
*	.78 (3)	.77 (4)	.78
ROUND	MASS (GM)	MASS (GM)	AVERAGE MASS (GM)
4.1	.77 (1)	.62 (2)	.69
*	.77 (1)	.69 (2)	.73
4.2	.61 (3)	.73 (4)	.67
*	.60 (3)	.75 (4)	.67
ROUND	MASS (GM)	MASS (GM)	AVERAGE MASS (GM)
7.1	.75 (1)	.80 (2)	.78
*	.84 (1)	.82 (2)	.83
7.2	.74 (3)	.73 (4)	.74
*	.90 (3)	.73 (4)	.82
* MASS VALUES ADJUSTED FOR IMAGE FORESHORTENING			

Appendix H

ANALYSIS OF FILM MEASUREMENT ERROR

Introduction

The purpose of this experiment was to experimentally determine the accuracy to which the properties of length, diameter, and mass could be determined for a shaped charge pellet by the methods described in Appendixes F and G.

A three inch rod of nickel 200 was cut into four lengths. Three of the units were flattened at one end and notched at the other end so that they roughly resembled a two gram nickel pellet. Using a micrometer the lengths and diameters were measured and recorded. The "pellets" were weighed on a balance calibrated to 0.01 gram and the masses were also recorded. They were then placed in blocks of Styrofoam which measured 1.0-inch by 5.75-inches by 12.0-inches. Each block was placed in the aluminum tube of the NASA Test Facility, shown in Fig. 14A, so that the pellet was nearly centered at station two. Then X-ray radiographs were taken. The positions, lengths, and diameters of the pellet film image were independently measured by two observers. A 6 power reticle was used to measure the film pellet images.

Table H-I. Comparison of Lengths

Data and Results

Actual Length	Observer 1	Error	Percent Error	Observer 2	Error	Percent Error
.493	.499	+.006	1.22	.487	-.006	1.22
.672	.621	-.051	7.59	.627	-.045	6.70
.567	.560	-.007	1.23	.570	+.003	0.53
.776	.682	-.094	12.11	.687	-.089	11.47
Avg.			5.54			4.98

The pellet lengths measured by the two observers are presented and compared in Table H-I. The data indicate a strong tendency to underestimate the pellet length. Of eight readings, only two were overestimates of pellet length, each by a small percentage. Only two of the eight calculated lengths were in error by more than 10% and four were in error by less than 2%.

Appendix H

Table H-2. Comparison of diameters.

Actual	Observer 1	Error	Percent Error	Observer 2	Error	Percent Error
.169	.167	-.022	1.18	.163	-.006	3.59
.167	.172	+.005	2.99	.163	-.004	2.45
.156	.156	-.000	0.00	.152	-.004	2.63
.186	.174	-.012	6.90	.170	-.016	8.60
Avg.			2.77			4.32

The measured diameters are presented and compared above. The tendency to underestimate the diameter appears to be even stronger than the tendency to underestimate the length. Seven of the eight readings were underestimates. The discrepency averages about 3% which is an error of one division on the reticle used for these measurements.

Table H-3. Comparison of masses.

Actual	Observer 1	Error	Percent Error	Observer 2	Error	Percent Error
1.45	1.70	+0.25	17.24	1.54	+0.09	5.84
2.20	2.05	-0.15	6.82	1.88	-0.32	17.02
1.52	1.45	-0.07	4.61	1.38	-0.14	10.14
2.71	2.50	-0.21	7.75	2.49	-0.22	8.84
Avg.			9.11			10.46

The masses, as shown in Table H-3 , also tend to be underestimates of their true value. Of the eight calculated masses only two exceeded the true value. Both overestimates were made on the same pellet. The other six calculated masses averaged 0.2 gram less than the true mass.

Conclusions

Though the amount of data is insufficient to state a definite conclusion, it does indicate that there might have been a tendency to underestimate the pellet mass by about 6%. It should be noted also that the data readings in this experiment were taken only once by each observer, and no attempt was made to refine the data as was done with the actual pellets of the Calibration Study.

APPENDIX I

PELLET DEBRIS ANALYSIS

Introduction

The purpose of this analysis was to study several characteristics of the debris surrounding the 40 degree Hyperbolic nickel pellets in this calibration study. The debris characteristics studied were: numbers of particles, velocity, effective center of mass, and total mass. All radiographs discussed in this appendix were taken at the NASA Test Site.

Analysis Methods

The particles are generally quite small and numerous. Many of the particle images have no definite areas which can be labeled particle or boundary. For large, solid particles, the boundary, or penumbra, is a semi-gray area about 0.005 inch wide surrounding the particle image. It is darker than the image but lighter than the background. For small particles, the penumbra may appear to constitute the entire image. Since the penumbra constitutes a significant portion of the image, any information taken from the films must be considered in the light of penumbra effects to be meaningful.

To better understand the penumbra, two sizes of steel ball-bearings were mounted on a sheet of cardboard. The cardboard was placed at station 2 in the tube of the NASA Test Site test facility at the Ravenna Army Ammunition Plant, Ravenna, Ohio, and radiographed. The image size was calculated for small bearings assuming a point X-ray source. The diameters for the small and large bearing images were measured to the discernible outer edges of the penumbra. For each bearing size, the penumbra was consistently measured to be 0.007 inch greater than the calculated image diameter. This result indicated that the penumbra diameter and the point source image diameter differed by a constant which was identical for all image diameters and that the eye was able to judge film intensity with good consistency. This judgement was later found to vary over a period of several days. Since about one day is required to measure all the debris recorded on a radiograph, the measurements should be calibrated daily by measuring known images before and after viewing the debris. In this way the appropriate penumbra effect correction factor could be determined.

The debris particles appearing on the radiograph are evenly distributed if one only considers a small area. If the particle placement is random or nearly random with respect to mass also, as appears to be the case, then the total mass of the particles may be treated as though it were at the centroid of the area.

Thus, if the radiograph is divided into coordinate squares one inch on each side, only a small amount of error will be introduced by treating the particles as though they were at the squares' centers, greatly simplifying measurements and calculations.

Most of the particles generally appeared to be prolate spheroids as shown in Fig. I-1. Therefore, the assumption was made that all of the particle volume could be calculated from a volume formula for a prolate spherical. This relation is:

$$V = \frac{4}{3} \pi ab^2$$

where "a" is the long axis of the configuration. For any orientation of a given particle the dimension b is always measurable because of symmetry. However, the dimension "a" which is measured from the film depends on an angle α which it makes with the plane of the film. Since there is no practical way of determining this angle for each particle it was assumed that all values of α between 0 and $\pi/2$ are equally probable. An average value for cos α was then used to correct the measured lengths of "a" which were obtained from these radiographs.

The center of mass of the particles were estimated for each radiograph, then, when two sequential radiographs of the same debris pattern were analysed, it was possible to determine the debris velocity.

If the center of mass of the debris which is seen on the film, has a value $\bar{X}$ relative to some reference line on the film, one can calculate a value.

$$\bar{X}_r = \frac{\sum_{i=1}^{n} m_i \left|(\bar{X} - x_i)\right|}{\sum_{i=1}^{n} m_i}$$

where m_i is the mass of the individual particle and x_i is its distance from $\bar{X}$. The quantity $\bar{X}_r$ might be termed a polar center of mass. This value was determined for each film in order to obtain an idea of how rapidly the debris was spreading radially. A radial velocity was calculated when two successive values of $\bar{X}_r$ were determined. This radial velocity is reported in Table however, it should be noted that the $\bar{X}_r$ value is strongly affected by a few large particles which tend to stay near the jet pellet. Consequently the radial velocities determined from a value of $\bar{X}_r$ are low. Actually there are a large number of small particles which are traveling much faster than the values listed in Table

Appendix I

Discussion of Data and Results

The debris seen on 9 radiographs of pellets were measured. These radiographs represented 5 pellets of the calibration study. The following program round numbers and corresponding film numbers were measured: 839-1, films 2 and 4; 847-4, films 1, 2, and 4; 847-6, film 3; 847-12, film 4; 851-2, films 2 and 4. A tenth radiograph was measured, 866-5, film 3. The tenth radiograph was used for calibration of the measuring technique used. Stationary artificial debris was used to simulate the debris observed in the actual test shots. The total mass of this test debris was 1.33 grams.

During the debris measurement, several characteristics were noted which could not be included in the data reduction. For many of the particle images, an extremely wide penumbra was observed. Since a similar effect was observed with the artificial debris when smaller particles adhered to the surface of a larger one, it was concluded that the extra width was due to diffusion of the X-rays through fine particles. In such a case, an attempt was made to determine where the edge of the penumbra would have normally been and measurements were made to that point. Some of the debris images appeared to be much fainter than others of similar size. It was assumed that these particles were farther from the film.

Table I-I presents the results of the debris analysis. There seemed to be some differences between the Modified Flight Test and Full Flight Test debris. There appeared to be less debris accompanying the Full Flight Test pellet than the Modified Flight Test pellets. The average mass of the Modified Flight Test debris observed at station 1 was 1.12 gram while the mass of the one Full Flight Test debris observed was 0.33 gram. Therefore, the mass of the Full Flight Test debris observed was about 58% less than the mass of the Modified Flight Test debris observed at both station 1 and station 2. Examination of the radiographs of other calibration rounds, that were not included in this analysis, tended to confirm the difference between the Full Flight Test pellet debris and the Modified Flight Test pellet debris.

Since much of the large debris was probably generated by pellet fragmentation, the difference in debris mass of the Full Flight Test pellets and the Modified Flight Test pellets would imply a pellet mass difference of about 0.5 gram. The mass of the Full Flight Test pellet observed was 0.41 gram larger than the Modified Flight Test pellets observed average mass at station 1 and 0.27 gram larger at station 2. Although the differences in pellet mass do not exactly account for the computed debris mass differences, they do confirm the trend. Therefore, the debris data tends to confirm the hypothesis that the difference between the Full Flight pellet mass and the Modified Flight Test pellet

mass was caused by a difference in extent of pellet fragementation, i.e., the Full Flight Test pellet did not fragment as much as the Modified Flight Test pellet.

In the determination of the mass of the artificial debris of 866-5, the calculated mass was found to be 0.28 gram too low. About 0.10 gram was probably caused by the fact that the very small debris could not be seen on the film and therefore was immeasureable. A small portion of the error could have been caused by the fact that the artificial debris were small pieces of wire and therefore cylindrical instead of spherical in form. The main error was probably caused by measurement and judgement error.

Conclusions

The debris analysis indicated that the bulk of the debris that was found to surround the 40 Degree Hyperbolic nickel pellets was probably caused by the breaking up or fragmenting of the rear of the pellets. The computed mass of the debris, combined with the correction for errors in measurement and observation, confirms that the difference in pellet mass of the Full Flight Test pellets and the Modified Flight Test pellets was due to the extent of fragmentation of the pellet.

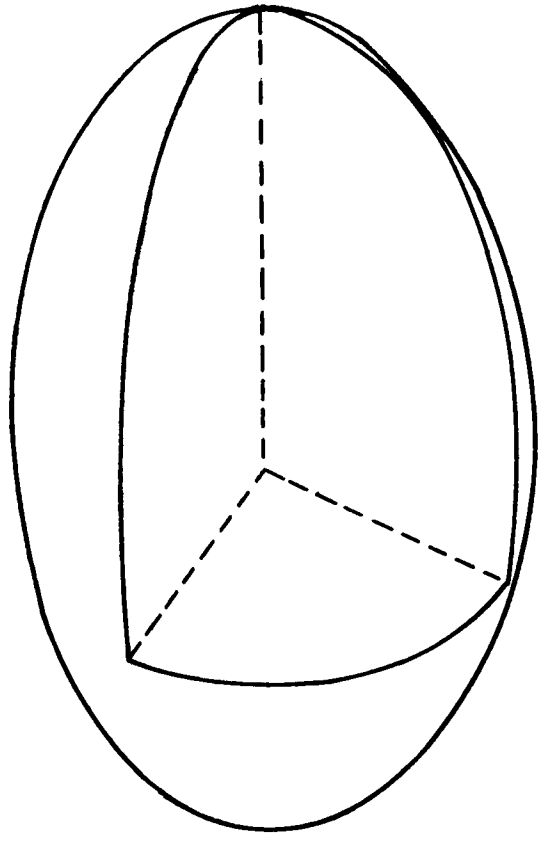

Fig. I-1. Prolate Spheroid.

Table I-I
DEBRIS ANALYSIS RESULTS

LINE	Program Round Number	Film Number	DEBRIS							PELLET				LINE
			Number of Particles	Velocity (km/sec)	Radial Velocity (m/sec)	Polar Center of Mass (in)	Center of Mass In Film Coordinates (inches)		Mass (grams)	Velocity (km/sec)	Location In Film Coordinates (inches)		Mass (grams)	
							X	Y			X	Y		
1	839-1	2	260	9.75	6.44	1.395	2.70	1.88	0.98	9.46	2.73	1.66	1.14	1
2	839-1	4	197	9.75	6.44	1.438	2.83	5.81	0.49	9.46	3.63	4.50	1.23	2
3	847-4	1	442	9.41	29.73	1.556	1.97	3.23	1.06	9.50	1.77	2.66	0.73	3
4	847-4	2	454	9.41	29.73	1.461	2.73	3.30	1.17	9.50	2.27	2.81	0.76	4
5	847-4	4	175	9.41	29.73	1.263	2.40	3.64	0.77	9.50	2.33	4.58	0.78	5
6	847-6	3	247	--	--	1.669	3.03	3.29	0.97	9.50	3.97	4.24	0.76	6
7	847-12	4	193	--	--	1.368	2.64	2.36	0.63	9.56	1.85	3.18	1.05	7
8	851-2	2	421	9.59	2.42	1.341	2.59	6.42	0.46	9.63	2.72	6.65	1.15	8
9	851-2	4	200	9.59	2.42	1.357	2.68	5.73	0.33	9.63	2.35	6.43	1.30	9
10	866-5*	3	183	--	--	1.151	2.26	2.76	1.05	--	--	--	--	10

* Artificial debris - known mass = 1.33 grams.

REFERENCES

1. Statement of Work L-4318; Mar. 24, 1964. NASA, Langley Research Center.

2. Jervell, W.O., and Wineman, A.R.: Preliminary Analysis of a Simulated Meteor Re-entry 9.8 Kilometers per Second. NASA TN D-2268.

TABLE IA

TEST PLAN

40 Degree Hyperbolic Nickel Liner

65/35 Octol Explosive Filler

Type of Test	Program Number	Ambient Pressure	No. of firings
1. Body Confinement	839	30-60 microns	5
2. Modified Flight Test	847	30-60 microns	12
3. Spin Test (25rps)	850	Atmospheric	5
4. Full Flight Test	851	30-60 microns	3
5. Initial Pellet Mass Test	856	Atmospheric	2
6. Flight Test by NASA	---	----------	3

TABLE IB

TEST PLAN

30 Degree Conic Ingot Iron Liner

Composition B Explosive Filler

Type of Test	Program Number	Ambient Pressure	No. of firings
1. Modified Flight Test	853	30-60 microns	12
2. Spin Test (25rps)	858	Atmospheric	5
3. Full Flight Test	859	30-60 microns	3
4. Flight Test by NASA	---	----------	3

TABLE II.

ITEMIZED WEIGHT OF THE FLIGHT ASSEMBLY

Assembly - 40 Degree Hyperbolic Nickel Liner

(ASSEMBLY DRAWING DRC-23-2062-2)

Description	Drawing Number	Wt. gms.	Wt. lbs.
Adapter-Base Plug	DRB-23-2305-4	77.5	.171
Tetryl Booster	None	16.2	.036
16 Blind Rivets	Huck CKL-P4E	3.6	.008
Felt Pad	1/16 x 2-1/8 Dia.	1.3	.003
Body	DRB-23-2306	167.1	.368
Octol Charge	From Loading Fixture DRC-11-2040	562.5	1.240
200 Nickel Liner	DRB-23-2295	59.0	.130
Retainer Ring	DRB-23-2299	10.3	.023
Adapter Plate	DRB-23-2300	38.9	.086
	Total Assembly Weight	936.4	2.065

Note: All weights shown were experimentally determined by using average weights of several pieces.

TABLE III.

ITEMIZED WEIGHT OF THE SHORT FLIGHT ASSEMBLY

Assembly - 30 Degree Conic Ingot Iron Liner

(ASSEMBLY DRAWING DRC-N-58)

Description	Drawing Number	Wt. gms.	Wt. lbs.
Adapter - Base Plug	DRB-N-62	88.5	.195
Tetryl Booster	None	16.2	.036
24 Blind Rivets	Huck CKL-P4E	5.4	.012
Felt Pad	1/16 x 2-61/64 Dia.	2.5	.005
Fiberglass Body	DRB-N-63	162.8	.359
Composition B Charge	From Loading Fixture DRB-N-57	898.1	1.980
Ingot Iron Liner	DRB-N-54	339.0	.747
Ingot Iron Liner Cap	.005 x .531 Dia.	.2	.001
Lucite Inhibitor	DRB-N-56	136.9	.302
Retainer	DRB-N-55	23.3	.051
Total Assembly Weight Less Adhesives		1672.9	3.688

Note: All weights shown were experimentally determined by using average weights of several pieces

TABLE IV.

ITEMIZED WEIGHT OF THE LONG FLIGHT ASSEMBLY

Assembly - 30° Conic Ingot Iron Liner

(ASSEMBLY DRAWING DRC-N-57)

Description	Drawing Number	Wt. gms.	Wt. lbs.
Adapter-Base Plug		90.5	.200
Tetryl Booster	None	16.2	.036
24 Blind Rivets	Huck CKL-P4E	5.4	.012
Felt Pad	1/16 x 2-61/64 Dia.	2.5	.005
Fiberglass Body	DRB-N-61	157.3	.347
Composition B Charge	From Loading Fixture DRB-N-57	898.1	1.980
Ingot Iron Liner	DRB-N-54	339.0	.747
Ingot Iron Liner Cap	.005 x .531 Dia.	.2	.001
Lucite Inhibitor	DRB-N-56	136.9	.302
Retainer	DRB-N-55	23.3	.051
Total Assembly Weight Less Adhesives		1669.4	3.681

Note: All weights shown were experimentally determined by using average weights of several pieces.

Table V
PELLET MASS AND DIMENSION DATA
40 Degree Nickel Hyperbolic Liner

LINE	Type of Test	Program Round Number	Ambient Pressure (microns) (Note 1)	Station 1 Length (in.)	Station 1 Ave. Diam. (in.)	Station 1 Mass (grams)	Station 2 Length (in.)	Station 2 Ave. Diam. (in.)	Station 2 Mass (grams)	Combined Station Data Ave. Length (in.)	Combined Station Data Ave. Diam. (in.)	Combined Station Data Ave. Mass (grams)
1	Body Confinement Test	839-1	49	.486	.140	1.00	.488	.148	1.10	.487	.144	1.05
2	"	839-2	140	.396	.149	.86	.349	.140	.78	.372	.144	.82
3	"	839-4	50 [1]	.352	.148	.73	.326	.149	.67	.339	.148	.70
4	"	839-7	60 [1]	.370	.150	.83	.369	.153	.82	.370	.152	.82
5	"	839-8	59 [1]	.406	.149	.85	.375	.153	.80	.390	.151	.82
6	Modified Flight Test	847-1	55 [1]	.385	.144	.75	.358	.141	.69	.372	.142	.72
7	"	847-3	60 [1]	.351	.147	.67	.381	.145	.83	.366	.146	.75
8	"	847-4	45 [1]	.361	.150	.74	.324	.152	.65	.342	.151	.70
9	"	847-5	49 [1]	.372	.144	.74	.342	.147	.62	.357	.146	.68
10	"	847-6	35 [2]	.351	.141	.69	.244	.153	.62	.298	.147	.66
11	"	847-7	30 [2]	.391	.164	.96	.381	.169	.97	.386	.166	.96
12	"	847-8	30 [2]	.359	.154	.79	.385	.141	.91	.372	.148	.85
13	"	847-9	31 [2]	.514	.146	1.05	.521	.148	1.11	.518	.147	1.08
14	"	847-10	28 [2]	.511	.155	1.18	——	——	——	——	——	——
15	"	847-11	28 [2]	.552	.139	.95	.463	.152	1.05	.508	.146	1.00
16	"	847-12	24 [2]	.452	.150	.95	.474	.148	1.00	.463	.149	.98
17	Full Flight Test	851-2	27 [2]	.506	.149	1.11	.504	.159	1.32	.505	.154	1.22
18	"	851-3	26 [2]	.443	.161	1.06	.408	.156	.91	.426	.158	.98
19	"	851-4	24 [2]	.474	.157	1.09	.453	.158	1.06	.464	.158	1.08
20	Spin Test (-25 rps)	850-9	Atm.	.60	.143	1.34	——	——	——	——	——	——
21	"	850-10	Atm.	.57	.150	1.33	——	——	——	——	——	——
22	"	850-11	Atm.	.56	.143	1.37	——	——	——	——	——	——
23	"	850-13	Atm.	.42	.172	1.14	——	——	——	——	——	——
24	"	850-14	Atm.	.55	.156	1.42	——	——	——	——	——	——
25	Initial Pellet Mass Test	856-1	Atm.	—	—	—	——	——	——	——	——	——
26	"	856-2	Atm.	.83	.136	1.68	——	——	——	——	——	——

Note: 1. All pressure readings with superscript 1 were measured at the pump gauge location. All other pressure readings were measured at the tank gauge location. The pump gauge typically indicated the pressure to be about 20 microns lower than the tank gauge.
All pressure readings with superscript 2 were corrected for ambient temperature according to the gauge manufacturers instruction.

Table VI
PELLET VELOCITY AND ORIENTATION DATA
40 Degree Nickel Hyperbolic Liner

LINE	Type of Test	Program Round Number	Ambient Pressure (microns) (Note 1)	Station 1		Station 2		Tumbling Rate (rps.) (Note 3)	Velocity (Km/sec)
				Theta (deg.)	Gamma (deg.)	Theta (deg.)	Gamma (deg.)		
1	Body Confinement Test	839-1	49	-101.70	27.21	-115.17	53.20	448.0	9.46
2	"	839-2	140	-41.61	43.61	25.99	84.64	1162.0	9.34
3	"	839-4	50 [1]	86.48	26.25	-70.08	14.33	644.8	9.47
4	"	839-7	60 [1]	-159.22	39.64	-147.03	126.36	1445.7	9.53
5	"	839-8	59 [1]	81.80	50.59	74.72	108.14	958.3	9.52
6	Modified Flight Test	847-1	55 [1]	-108.81	56.22	-125.46	141.24	1419.6	9.39
7	"	847-3	60 [1]	-85.95	48.72	-148.71	150.73	1864.3	9.43
8	"	847-4	45 [1]	-141.08	30.18	-148.96	66.67	606.2	9.50
9	"	847-5	49 [1]	162.44	24.36	176.50	60.08	606.7	9.49
11	"	847-6	35 [2]	0.05	9.29	0.51	33.34	396.2	9.50
12	"	847-7	30 [2]	-169.91	16.32	-164.65	53.48	623.3	9.55
13	"	847-8	30 [2]	11.01	39.77	13.91	115.73	1246.9	9.62
14	"	847-9	31 [2]	-119.27	7.83	-110.62	35.59	458.5	9.60
15	"	847-10	28 [2]	-17.83	34.40	-135.00	126.10	2215.6	9.66
16	"	847-11	28 [2]	164.10	74.86	-42.24	158.83	2074.7	9.60
17	"	847-12	24 [2]	-63.00	17.30	-56.06	36.38	316.0	9.56
18	Full Flight Test	851-2	27 [2]	-36.13	24.49	-40.82	61.68	617.9	9.63
19	"	851-3	26 [2]	28.68	4.16	29.25	32.29	469.9	9.66
20	"	851-4	24 [2]	-129.37	41.40	-131.76	112.99	1207.1	9.68
21	Spin Test (-25 rps)	850-9	Atm.	--	--	--	--	--	9.39
22	"	850-10	Atm.	--	--	--	--	--	9.45
23	"	850-11	Atm.	--	--	--	--	--	9.38
24	"	850-13	Atm.	--	--	--	--	--	9.62
25	"	850-14	Atm.	--	--	--	--	--	9.61
26	Initial Pellet Mass Test	856-1	Atm.	--	--	--	--	--	--
27	"	856-2	Atm.	--	--	--	--	--	--

Notes:
1. All pressure readings with superscript 1 were measured at the pump gauge location. All other pressure readings were measured at the tank gauge location. The pump gauge typically indicated the pressure to be about 20 microns lower than the tank gauge. All pressure readings with superscript 2 were corrected for ambient temperature according to the gauge manufacturers instructions.
2. Spherical coordinates were used. Gamma here is the same as phi commonly used in spherical coordinates. The pellet was traveling in the +Z direction.
3. The value shown was calculated by assuming that the pellet did not tumble more than 1/2 revolution from Station 1 to Station 2. Since only two radiographic stations were available, the direction of tumble could not be determined. The pellet could have tumbled several revolutions between radiographic stations and not have been observed. Therefore, the 1/2 revolution restriction was necessary.

Table VII
PELLET MASS AND DIMENSION DATA
30 Degree Ingot Iron Conic Liner

LINE	TYPE OF TEST	PROGRAM ROUND NUMBER	AMBIENT PRESSURE (MICRONS) (NOTEL)	STATION 1			STATION 2			COMBINED STATION DATA		
				LENGTH (IN.)	AVE. DIAM. (IN.)	MASS. (GRAMS)	LENGTH (IN.)	AVE. DIAM. (IN.)	MASS (GRAMS)	AVE. LENGTH (IN.)	AVE. DIAM. (IN.)	AVE. MASS (GRAMS)
1	Modified Flight Test	853-1	54	.653	.103	.84	.634	.106	.80	.644	.104	.82
2	"	853-2	50	.668	.105	.79	.685	.104	.82	.676	.104	.80
3	"	853-3	45	.587	.102	.69	.600	.104	.69	.594	.103	.69
4	"	853-4	50	.629	.107	.77	.617	.107	.74	.623	.107	.76
5	"	853-5	34	.726	.108	.86	.738	.102	.92	.732	.105	.89
6	"	853-6	50	.741	.102	.81	.733	.103	.81	.737	.102	.81
7	"	853-7	40	.590	.104	.66	.595	.113	.74	.592	.108	.70
8	"	853-8	49	.612	.106	.70	.595	.110	.68	.604	.108	.69
9	"	853-10	56	.639	.108	.78	.652	.111	.80	.646	.110	.79
10	"	853-11	54	.625	.108	.80	.660	.112	.87	.642	.110	.84
11	"	853-12	40	.532	.114	.68	.544	.115	.73	.538	.114	.70
12	Full Flight Test	859-1	43	.684	.112	.92	.701	.110	.94	.692	.111	.93
13	"	859-2	40	.754	.110	.93	.730	.110	.91	.742	.110	.92
14	"	859-3	42	.741	.111	1.01	.775	.117	1.01	.758	.114	1.01
15	Spin Test (-25 rps)	858-17	Atm.	.40	.098	.44	----	----	----	----	----	----
16	"	858-22	Atm.	.51	.098	.62	----	----	----	----	----	----
17	"	858-23	Atm.	.61	.080	.54	----	----	----	----	----	----
18	"	858-24	Atm.	.61	.082	.56	----	----	----	----	----	----
19	"	858-25	Atm.	.38	.081	.27	----	----	----	----	----	----

Note 1. All pressures were measured at the tank gauge location and corrected for amtient temperature according to the gauge manufacturers instructions.

Table VIII
PELLET VELOCITY AND ORIENTATION DATA
30 Degree Ingot Iron Conic Liner

LINE	Type of Test	Program Round Number	Ambient Pressure (microns) (Note 1)	Pellet Orientation (Note 2) Station 1 Theta (deg.)	Station 1 Gamma (deg.)	Station 2 Theta (deg.)	Station 2 Gamma (deg.)	Tumbling Rate (rps)	Velocity (Km/sec)
1	Modified Flight Test	853-1	54	-125.84	24.09	-169.86	47.32	484.5	8.56
2	"	853-2	50	70.04	6.42	73.51	25.18	275.4	8.57
3	"	853-3	45	-42.54	11.37	-20.19	44.88	508.8	8.55
4	"	853-4	50	-57.60	2.68	12.74	8.74	118.8	8.57
5	"	853-5	34	-107.31	16.77	-116.72	35.53	280.9	8.57
6	"	853-6	50	-24.46	6.51	-45.16	15.92	146.0	8.58
7	"	853-7	40	-103.40	13.95	-107.20	58.33	644.6	8.53
8	"	853-8	49	156.52	8.40	-176.37	16.21	138.0	8.58
9	"	853-10	56	63.34	5.17	41.08	10.08	81.8	8.55
10	"	853-11	54	-139.05	13.59	-123.19	39.67	388.9	8.54
11	"	853-12	40	12.26	20.12	17.96	43.90	349.2	8.57
12	Full Flight Test	859-1	43	117.83	19.65	112.02	47.91	413.4	8.55
13	"	859-2	40	45.82	15.37	49.27	41.29	381.0	8.60
14	"	859-3	42	60.86	7.31	55.49	20.29	192.5	8.59
15	Spin Test (-rps)	858-17	Atm.	——	——	——	——	——	8.32
16	"	858-22	Atm.	——	——	——	——	——	8.49
17		858-23	Atm.	——	——	——	——	——	8.33
18	"	858-24	Atm.	——	——	——	——	——	8.35
19	"	858-25	Atm.	——	——	——	——	——	8.44

Notes:
1. All pressures were measured at the tank gauge location and corrected for ambient temperature according to the gauge manufacturers instructions.
2. Spherical coordinates were used. Gamma here is the same as Phi commonly used in spherical coordinates. The pellet was traveling in the +Z direction.
3. The value shown was calculated by assuming that the pellet did not tumble more than 1/2 revolution from Station 1 to Station 2. Since only two radiographic stations were available, the direction of tumble could not be determined. The pellet could have tumbled several revolutions between radiographic stations and not have been observed. Therefore, the 1/2 revolution restriction was necessary.

Table IX
PELLET VELOCITY DATA SUMMARY

LINE	Type of test	Program Number	Liner type	Sample Size	Mean Ambient Pressure	Pellet Velocity (Km/sec)					
						Sample Mean		Maximum Spread of Sample	Standard Deviation		
						Mean Value	95% Confidence Interval (Note 1)		Sample Standard Deviation	95% Confidence Interval (Note 2)	
										Upper	Lower
1	Body Confinement Test	839	40° Nickel Hyperbolic	5	71.6	9.464	0.0940	0.19	0.0757	0.1943	0.0423
2	Modified Flight Test	847		11	37.7	9.536	0.0557	0.27	0.0829	0.1397	0.0562
3	Full Flight Test	851		3	25.7	9.657	0.0625	0.05	0.0252	0.1223	0.0115
4	Spin Test (-25rps)	850		5	Atm.	9.490	0.1456	0.24	0.1173	0.3010	0.0655
5											
6	Modified Flight Test	853	30° Ingot Iron Conic	11	47.5	8.562	0.0103	0.05	0.0154	0.0260	0.0104
7	Full Flight Test	859		3	41.7	8.580	0.0657	0.05	0.0265	0.1286	0.0121
8	Spin Test (-25rps)	858		5	Atm.	8.386	0.0932	0.17	0.0750	0.1926	0.0419

Note: 1. The 95% Confidence Interval must be added to and subtracted from the Mean Value to obtain the limits.
2. The values shown are the actual limits predicted for the standard deviation of the population.

Table X
PELLET MASS AND DIMENSIONS DATA SUMMARY

LINE	Type of test	Program Number	Liner Type	Station Number	Sample Size	Ambient Pressure (microns)	Pellet Dimensions		Pellet Mass (grams)					
							Mean Diameter (in.)	Mean Length (in.)	Sample Mean		Maximum Spread of Sample	Standard Deviation		
									Mean Value	95% Confidence Interval (Note 1)		Sample Std. Dev.	95% Confidence Interval (Note 2)	
													Upper	Lower
1	Body Confinement Test	839	40° Nickel Hyperbolic	1	5	71.6	0.147	0.402	0.854	0.1199	0.27	0.0966	0.2479	0.0540
2				2	5	71.6	0.149	0.381	0.834	0.1982	0.43	0.1596	0.4098	0.0892
3				1+2	5	71.6	0.148	0.392	0.842	0.1581	0.35	0.1274	0.3269	0.0712
4	Modified Flight Test	847		1	11	37.7	0.148	0.418	0.861	0.1115	0.51	0.1660	0.2798	0.1126
5				2	10	37.7	0.150	0.387	0.845	0.1348	0.49	0.1885	0.3290	0.1255
6				1+2	10	37.7	0.149	0.398	0.838	0.1112	0.42	0.1554	0.2713	0.1035
7	Full Flight Test	851		1	3	25.7	0.156	0.474	1.087	0.0625	0.05	0.0252	0.1223	0.0115
8				2	3	25.7	0.158	0.455	1.097	0.5154	0.41	0.2074	1.0080	0.0950
9				1+2	3	25.7	0.157	0.465	1.093	0.2995	0.24	0.1206	0.5858	0.0552
10	Spin Test (-25rps)	850		1	5	Atm.	0.153	0.54	1.32	0.1323	0.28	0.1065	0.2735	0.0596
11														
12	Modified Flight Test	853	30° Ingot Iron Conic	1	11	47.5	0.106	0.637	0.762	0.0459	0.20	0.0684	0.1153	0.0464
13				2	11	47.5	0.108	0.641	0.782	0.0497	0.24	0.0740	0.1248	0.0502
14				1+2	11	47.5	0.107	0.639	0.772	0.0462	0.20	0.0688	0.1160	0.0467
15	Full Flight Test	859		1	3	41.7	0.111	0.726	0.953	0.1225	0.09	0.0493	0.2397	0.0226
16				2	3	41.7	0.112	0.735	0.953	0.1275	0.10	0.0513	0.2493	0.0235
17				1+2	3	41.7	0.112	0.731	0.953	0.1225	0.09	0.0493	0.2397	0.0226
18	Spin Test (-25rps)	858		1	5	Atm.	0.088	0.502	0.486	0.1701	0.35	0.1370	0.3518	0.0766

Note: 1. The 95% Confidence Interval must be added to and subtracted from the Mean Value to obtain the limits.
2. The values shown are the actual limits predicted for the standard deviation of the population.

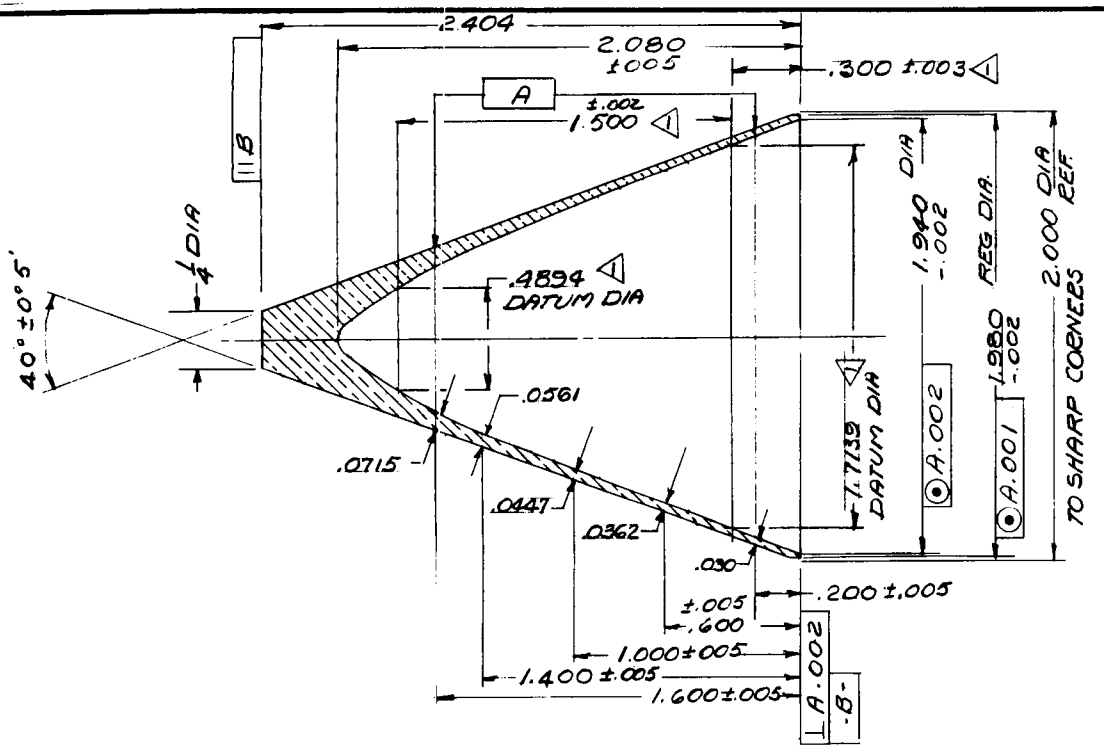

REVISIONS			
SYM	DESCRIPTION	DATE	APPROVAL
1	DATUM DIAS & RELATED DIMS ADDED	8/9/65	

NOTE
1. WALL THICKNESS MEASURED PERPENDICULAR TO OUTSIDE SURFACE OF LINER SHALL NOT VARY MORE THAN ±.002
2. IN ANY GIVEN PLANE PERPENDICULAR TO ℄ OF PART, WALL THICKNESS SHALL NOT VARY MORE THAN .002 IN 360°
3. FINISH 63
4. FOR INSIDE CONTOUR USE TRACER TEMPLATE DRB-10-2074

PHYSICAL PROPERTIES					
YP					
TS					
EL-2					
BA					
BN					
BN		NEXT ASSY.	USED ON	NEXT ASSY.	FINAL ASSY.
		APPLICATION		QTY. REQD.	

UNLESS OTHERWISE SPECIFIED DIMENSIONS ARE IN INCHES
TOLERANCES ON DECIMALS ±.010
ANGLES ±1/2° FRACTIONS ±1/64
MATERIAL TO BE SPECIFIED ON ORDER.
HEAT TREATMENT
FINAL PROTECTIVE FINISH

DRAWN	Lasaly	3/29/65
CHECKED		
SUBMITTED		
APPROVED		
APPROVED		DATE
E.R. Dayton		4-13-65

LINER,
40° HYPERBOLIC

DEFENSE RESEARCH DIVISION
THE FIRESTONE TIRE & RUBBER CO.
AKRON, OHIO

DWG. NO. DRB-23-2073-1

SCALE 2:1 | SPEC | CODE | SHEET 6F

Fig. 1. Liner, 40° Hyperbolic. DRB-23-2073-1

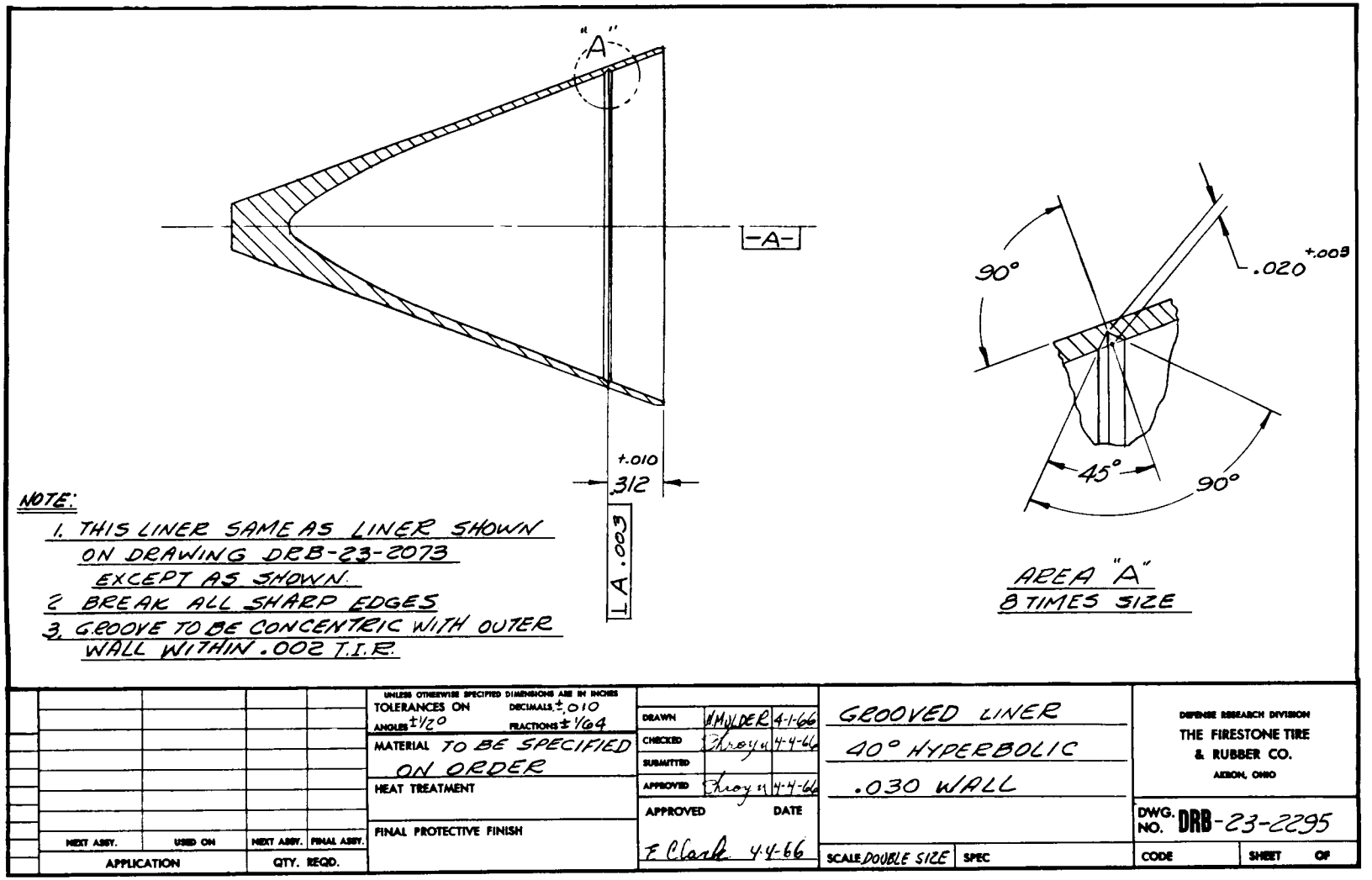

Fig. 2. Grooved Liner, 40° Hyperbolic, .030 Wall. DRB-23-2295

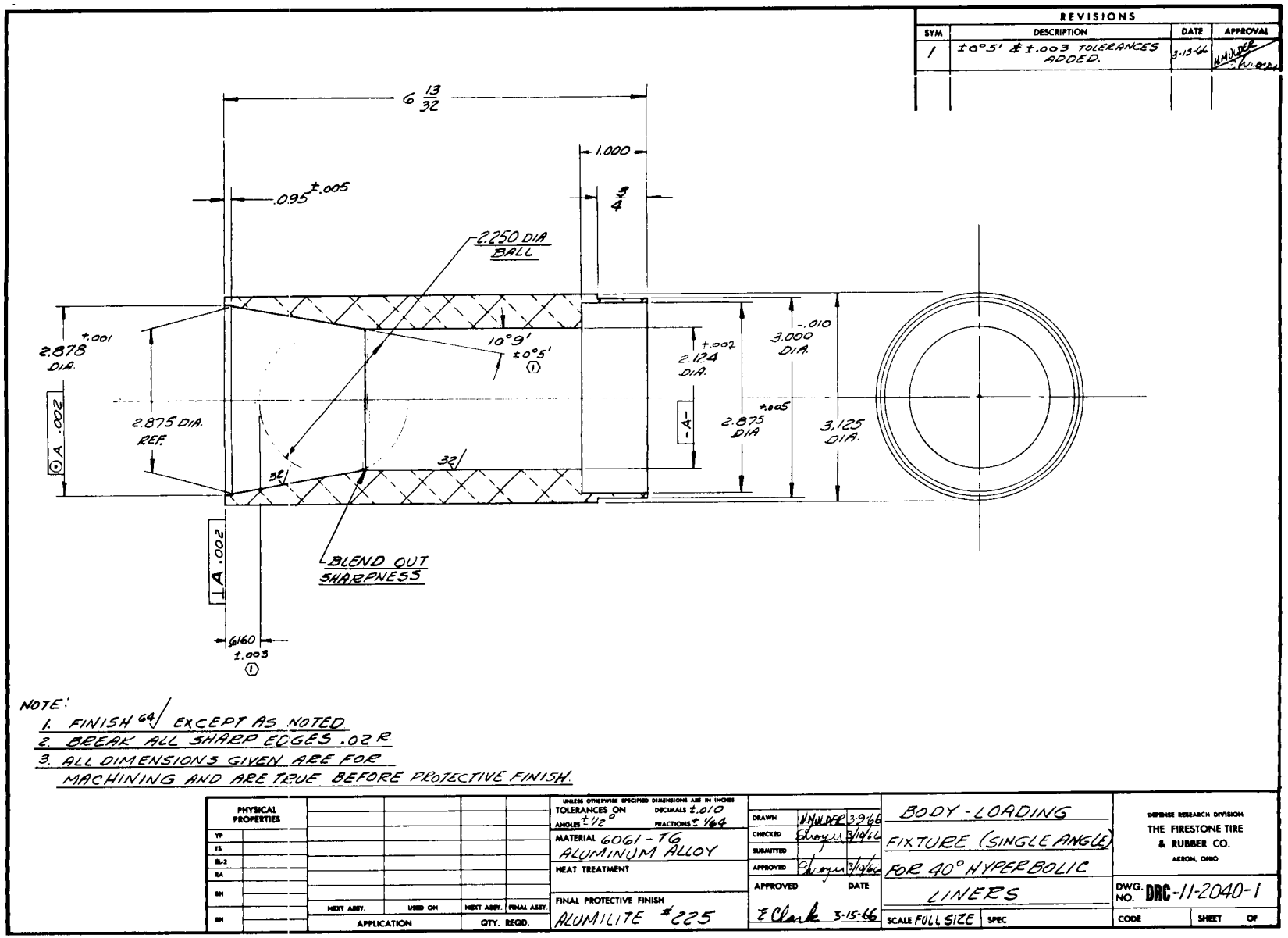

Fig. 3. Body, Loading Fixture, For 40° Hyperbolic Liners. DRC-11-2040-1

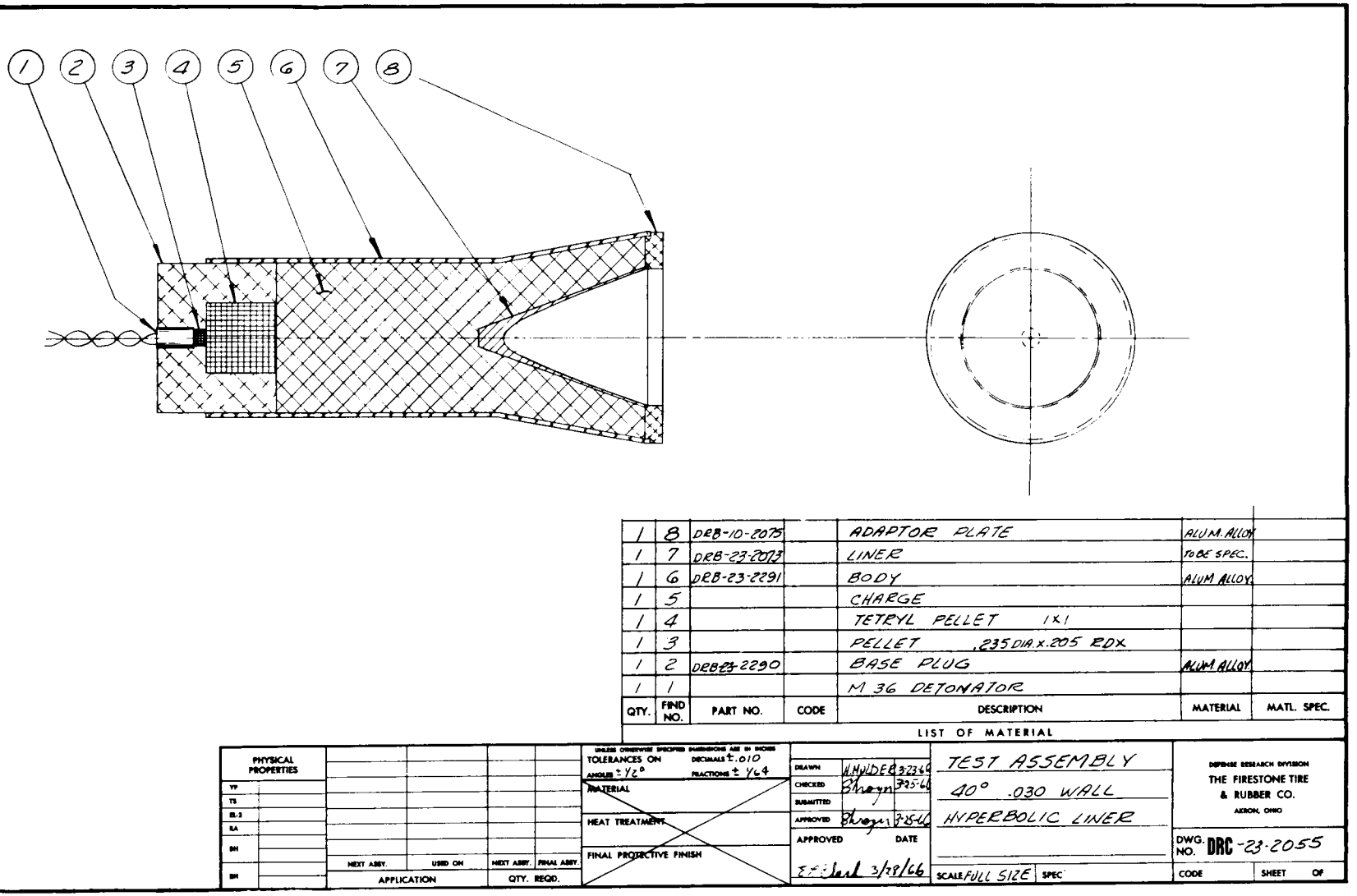

QTY.	FIND NO.	PART NO.	CODE	DESCRIPTION	MATERIAL	MATL. SPEC.
1	8	DRB-10-2075		ADAPTOR PLATE	ALUM. ALLOY	
1	7	DRB-23-2073		LINER	TO BE SPEC.	
1	6	DRB-23-2291		BODY	ALUM ALLOY	
1	5			CHARGE		
1	4			TETRYL PELLET 1X1		
1	3			PELLET .235 DIA x .205 EDX		
1	2	DRB-23-2290		BASE PLUG	ALUM ALLOY	
1	1			M 36 DETONATOR		

LIST OF MATERIAL

PHYSICAL PROPERTIES: YP, TS, EL-2, RA, BH, BH

APPLICATION: NEXT ASSY. | USED ON | NEXT ASSY. | FINAL ASSY.

QTY. REQD.

UNLESS OTHERWISE SPECIFIED DIMENSIONS ARE IN INCHES
TOLERANCES ON DECIMALS ± .010
ANGLES ± ½° FRACTIONS ± 1/64
MATERIAL
HEAT TREATMENT
FINAL PROTECTIVE FINISH

DRAWN	H.HOLDER	3-23-66
CHECKED	[illegible]	3-25-66
SUBMITTED		
APPROVED	[illegible]	3-28-66
APPROVED	DATE	
[illegible]	3/28/66	

TEST ASSEMBLY
40° .030 WALL
HYPERBOLIC LINER

SCALE FULL SIZE | SPEC

DEFENSE RESEARCH DIVISION
THE FIRESTONE TIRE & RUBBER CO.
AKRON, OHIO

DWG. NO. DRC-23-2055

CODE | SHEET OF

Fig. 4. Test Assembly, 40° Hyperbolic Liners, .030 Wall. DRC-23-2055

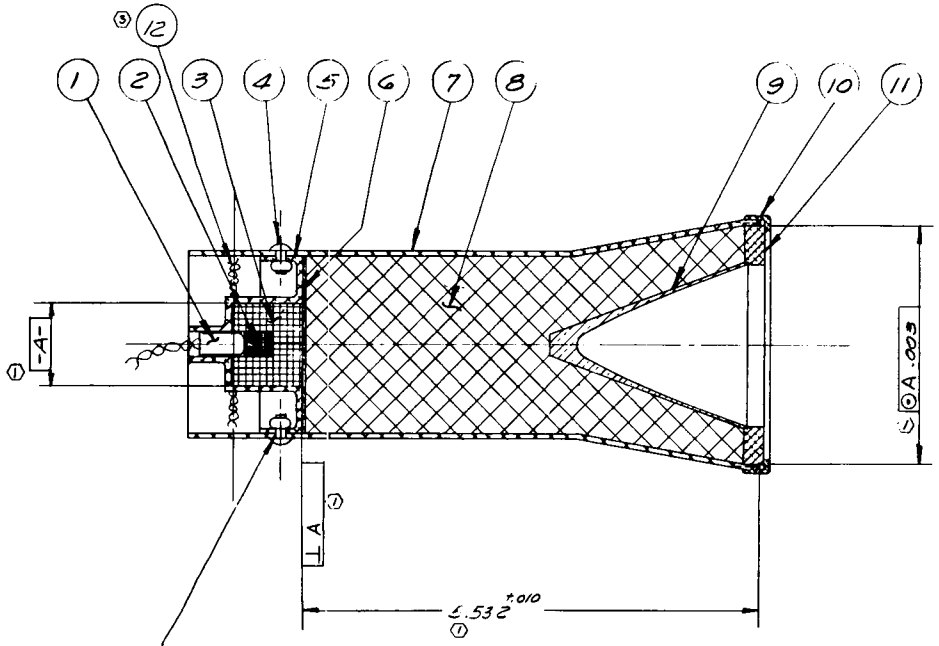

REVISIONS			
SYM	DESCRIPTION	DATE	APPROVAL
1	CONTROL SYMS., 5.532 +.010 DIM. & RIVET ASSEMBLY NOTE ADDED	4-28-66 LL	
2	RIVET CKL-P4E WAS - P4C	5-18-66	
3	ITEM #12 ADDED	8-29-66	

	QTY.	FIND NO.	PART NO.	CODE	DESCRIPTION	MATERIAL	MATL. SPEC.
③	1	12			TWISTED PAIR OF WIRES TO SENSOR	STD	
	1	11	DRB-23-2300		ADAPTER PLATE	ALUM. ALLOY	
	1	10	DRB-23-2299		RETAINER	ALUM ALLOY	
	1	9	DRB-23-2073		LINER	TO BE SPEC.	
	1	8			CHARGE		
	1	7	DRB-23-2309		BODY	ALUM ALLOY	
	1	6			FELT PAD	FELT	
	1	5	DRB-23-2308		BASE PLUG	ALUM. ALLOY	
②	8	4			CKL-P4E HUCK BLIND RIVET OR EQUIV.	STD.	
	1	3			TETRYL PELLET		
	1	2			M18 STAB DETONATOR .291 DIA X .342		
	1	1			M36A1 DETONATOR		

LIST OF MATERIAL

PHYSICAL PROPERTIES					
YP					
TS					
EL-2					
RA					
BH					
BH					
	NEXT ASSY.	USED ON	NEXT ASSY.	FINAL ASSY.	
	APPLICATION		QTY. REQD.		

UNLESS OTHERWISE SPECIFIED DIMENSIONS ARE IN INCHES
TOLERANCES ON DECIMALS
ANGLES FRACTIONS
MATERIAL
HEAT TREATMENT
FINAL PROTECTIVE FINISH

DRAWN	J.M. DEC 4-21-66
CHECKED	Shoyer 4-25-66
SUBMITTED	
APPROVED	Shoyer 4-25-66
APPROVED DATE	E. Pierce 4-26-66

TEST ASSEMBLY
40° HYPERBOLIC
LINER

DEFENSE RESEARCH DIVISION
THE FIRESTONE TIRE & RUBBER CO.
AKRON, OHIO

DWG. NO. DRC-23-2063-3

SCALE FULL SIZE | SPEC | CODE | SHEET OF

Fig. 5. Test Assembly, 40° Hyperbolic Liner. DRC-23-2063-3

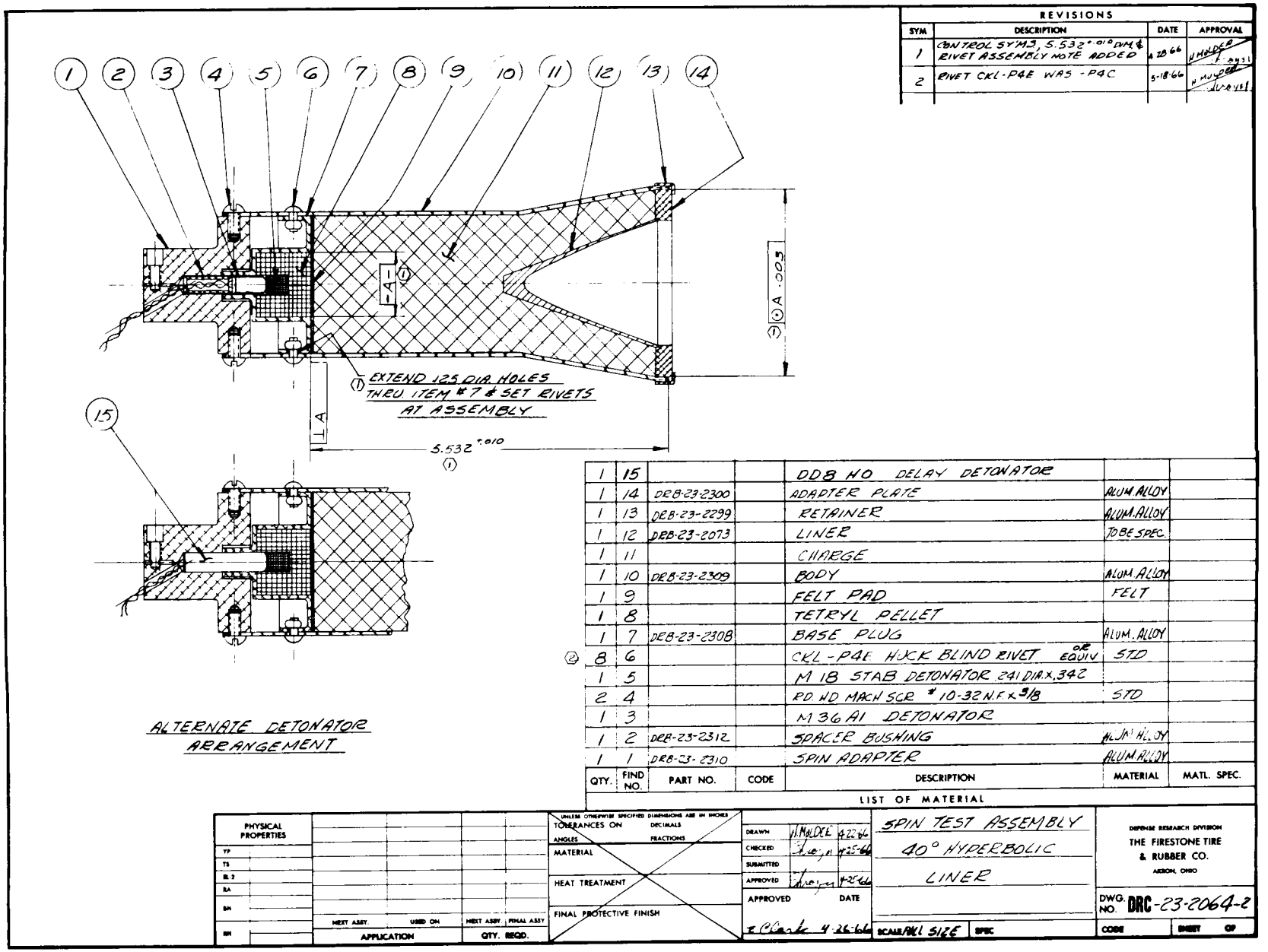

REVISIONS			
SYM	DESCRIPTION	DATE	APPROVAL
1	CONTROL SYMB, S.532 +.010 DIM & RIVET ASSEMBLY NOTE ADDED	4-28-66	H MOLDE
2	RIVET CKL-P4E WAS -P4C	5-18-66	H MOLDE

QTY.	FIND NO.	PART NO.	CODE	DESCRIPTION	MATERIAL	MATL. SPEC.
1	15			DDB HO DELAY DETONATOR		
1	14	DRB-23-2300		ADAPTER PLATE	ALUM. ALLOY	
1	13	DRB-23-2299		RETAINER	ALUM. ALLOY	
1	12	DRB-23-2073		LINER	TO BE SPEC.	
1	11			CHARGE		
1	10	DRB-23-2309		BODY	ALUM. ALLOY	
1	9			FELT PAD	FELT	
1	8			TETRYL PELLET		
1	7	DRB-23-2308		BASE PLUG	ALUM. ALLOY	
(2) 8	6			CKL-P4E HUCK BLIND RIVET OR EQUIV	STD	
1	5			M 18 STAB DETONATOR .241 DIA. X .342		
2	4			RD HD MACH SCR # 10-32 N.F. x 3/8	STD	
1	3			M 36 A1 DETONATOR		
1	2	DRB-23-2312		SPACER BUSHING	ALUM. ALLOY	
1	1	DRB-23-2310		SPIN ADAPTER	ALUM. ALLOY	

LIST OF MATERIAL

PHYSICAL PROPERTIES			
YP			
TS			
EL 2			
RA			
BH			
BH			

NEXT ASSY. USED ON — APPLICATION

NEXT ASSY | FINAL ASSY — QTY. REQD.

UNLESS OTHERWISE SPECIFIED DIMENSIONS ARE IN INCHES
TOLERANCES ON DECIMALS
ANGLES FRACTIONS
MATERIAL
HEAT TREATMENT
FINAL PROTECTIVE FINISH

DRAWN	H MOLDE	4-22-66
CHECKED	[illegible]	4-25-66
SUBMITTED		
APPROVED	[illegible]	4-25-66

APPROVED DATE
E Clark 4-26-66

SPIN TEST ASSEMBLY
40° HYPERBOLIC
LINER

SCALE/ALL SIZE | SPEC

DEFENSE RESEARCH DIVISION
THE FIRESTONE TIRE & RUBBER CO.
AKRON, OHIO

DWG. NO. DRC-23-2064-2

CODE | SHEET OF

Fig. 6. Spin Test Assembly, 40° Hyperbolic Liner. DRC-23-2064-2

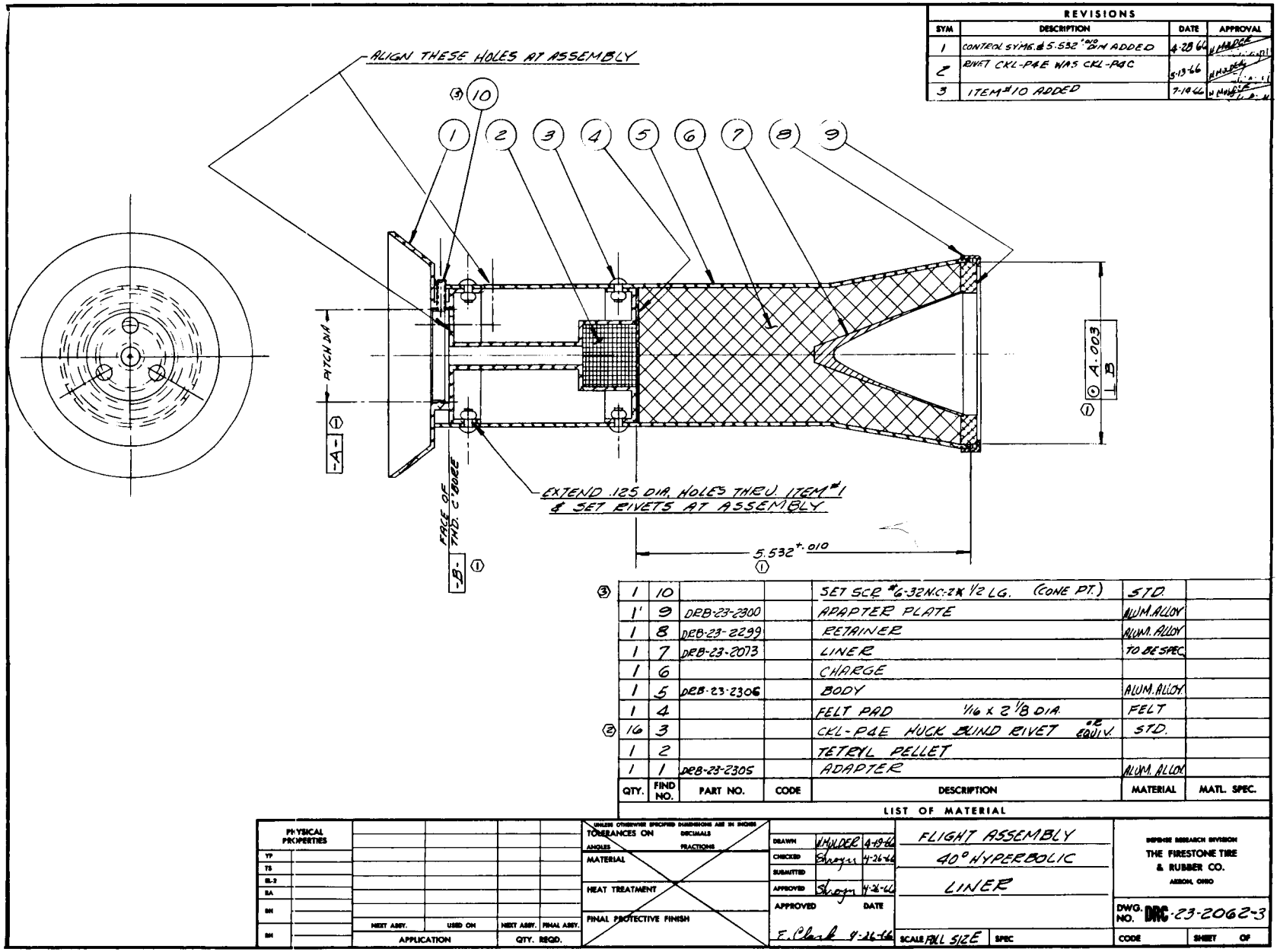

Fig. 7. Flight Assembly, 40° Hyperbolic Liner. DRC-23-2062-3

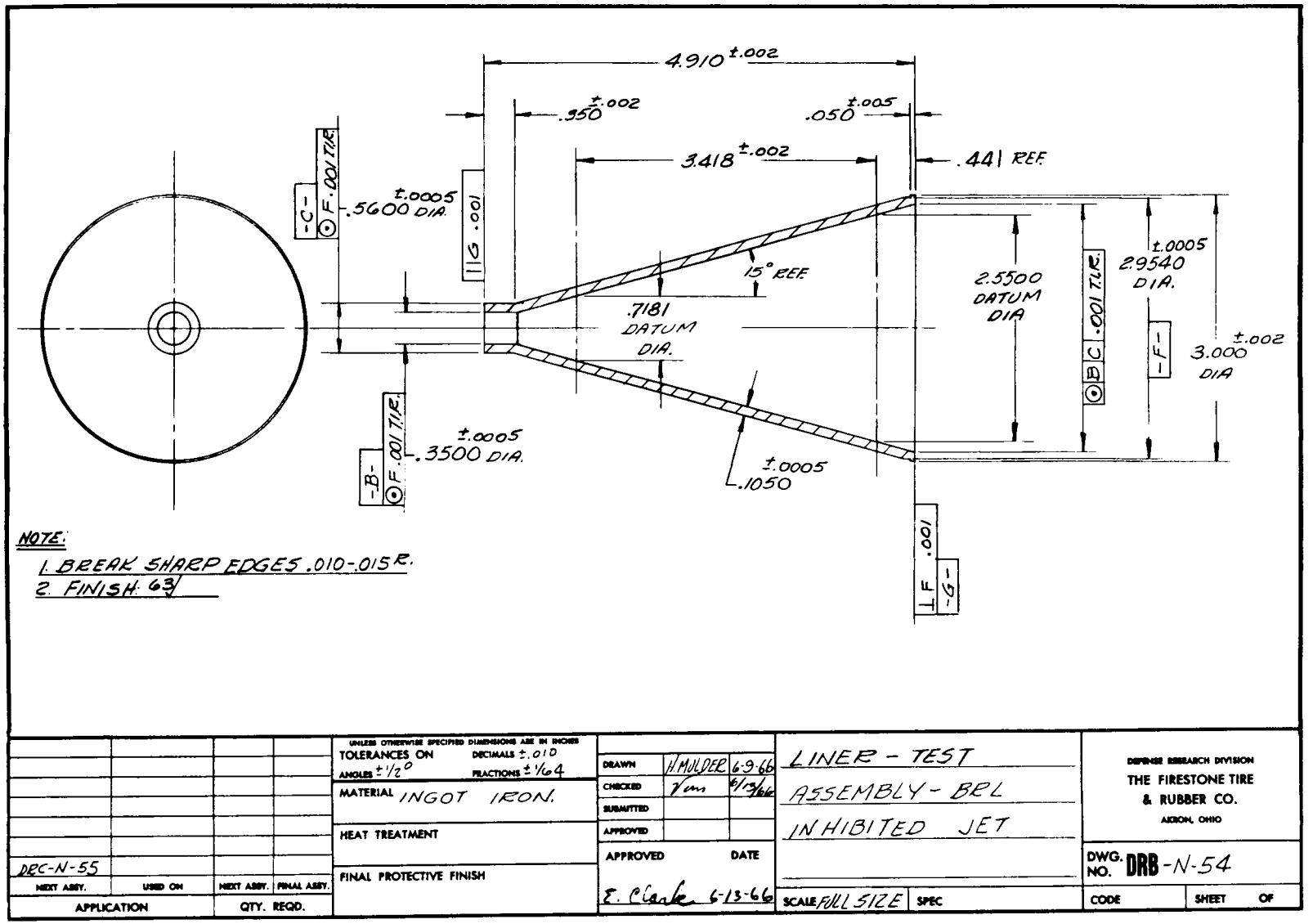

Fig. 8. Liner - BRL Inhibited Jet. DRB-N-54

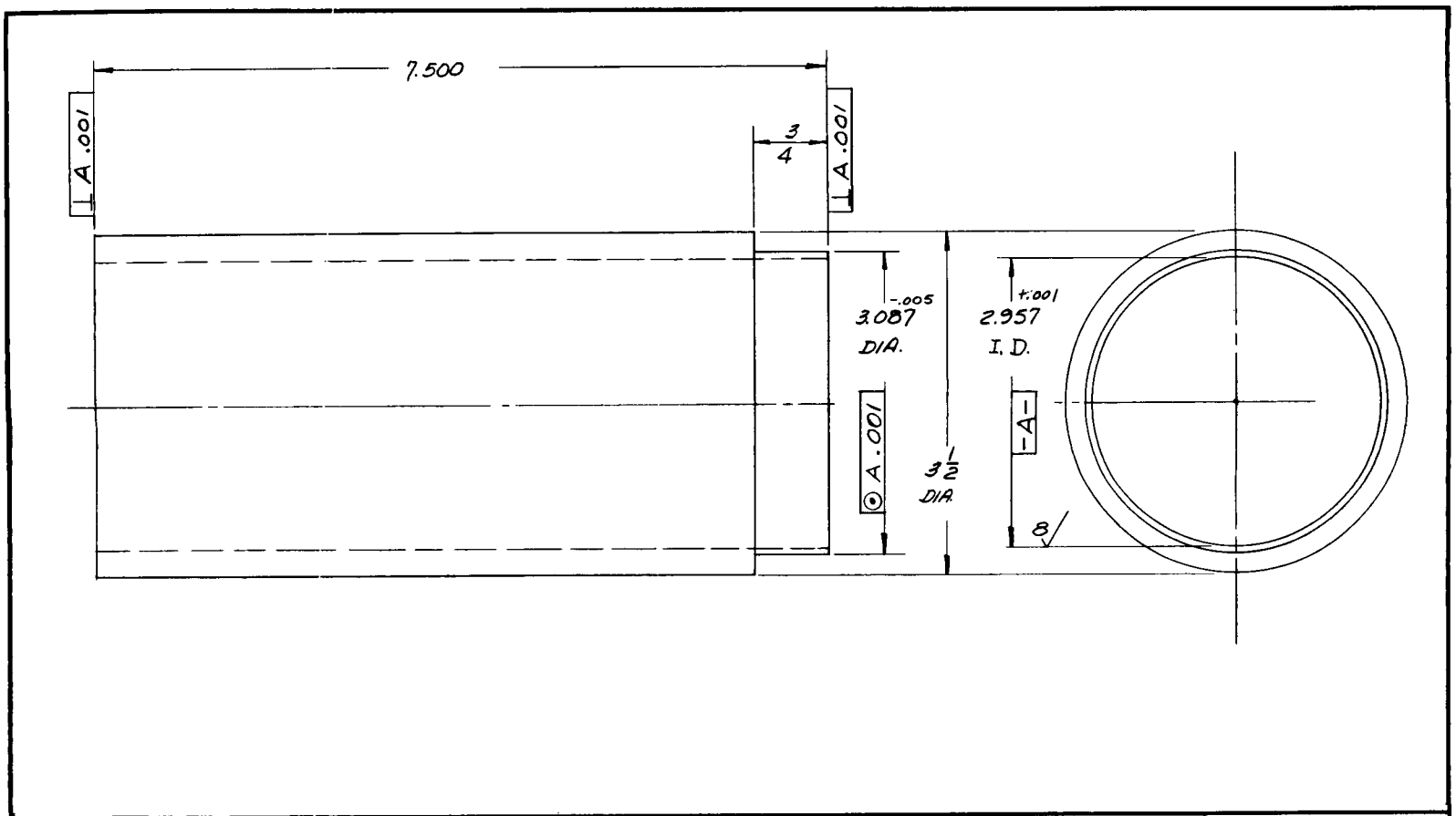

Fig. 9. Body, Casting Fixture. 30° NASA Liner. DRB-N-57

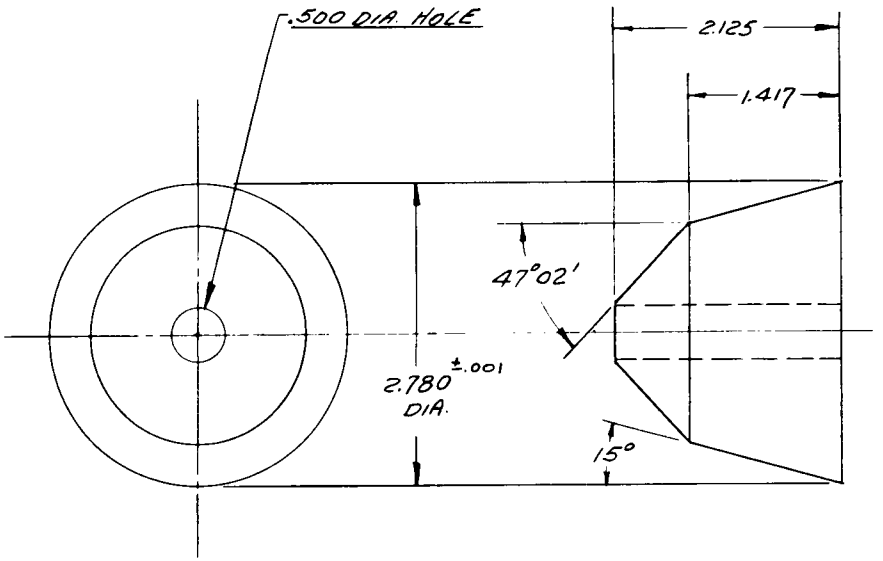

NOTE:
1. BREAK SHARP EDGES .010-.015 R.
2. FINISH 125

				UNLESS OTHERWISE SPECIFIED DIMENSIONS ARE IN INCHES					
				TOLERANCES ON DECIMALS ±.010	DRAWN	H. MULDER	6-9-66	INHIBITOR - TEST	DEFENSE RESEARCH DIVISION
				ANGLES ±½° FRACTIONS ±1/64	CHECKED		6/13/66	ASSEMBLY - BRL	THE FIRESTONE TIRE & RUBBER CO.
				MATERIAL LUCITE PLASTIC	SUBMITTED			INHIBITED JET	AKRON, OHIO
				HEAT TREATMENT	APPROVED				DWG. NO. DRB-N-56
DRC-N-55				FINAL PROTECTIVE FINISH	APPROVED	DATE			
NEXT ASSY.	USED ON	NEXT ASSY.	FINAL ASSY.		E. Clarke	6-13-66	SCALE FULL SIZE	SPEC	CODE / SHEET OF
APPLICATION		QTY. REQD.							

Fig. 10. Inhibitor, BRL Inhibited Jet. DRB-N-56

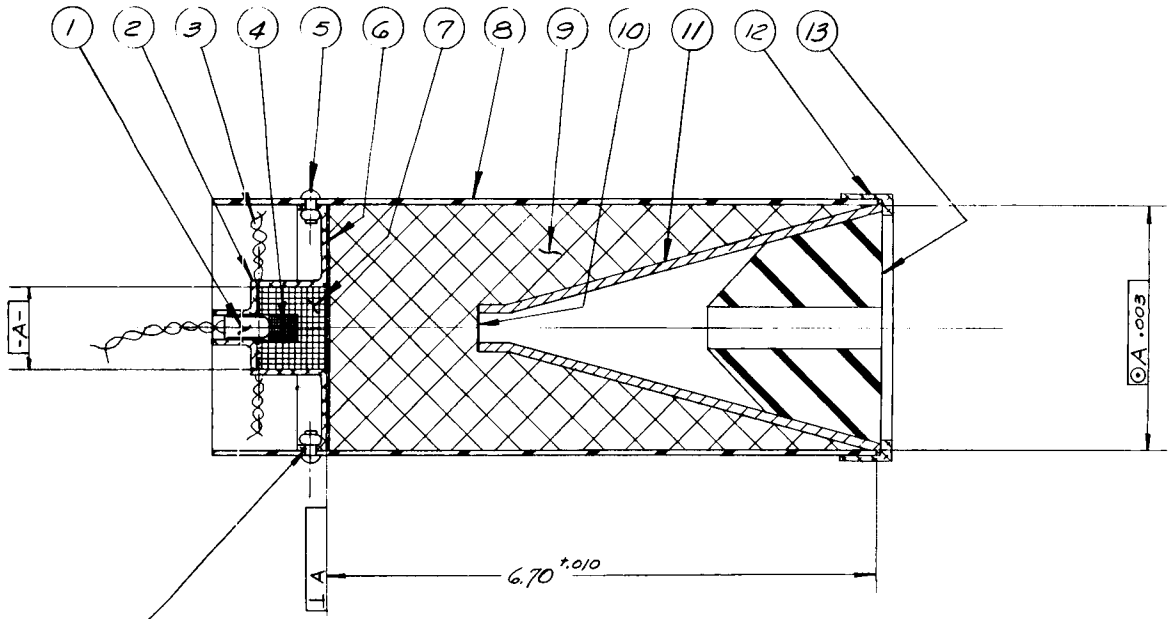

ASSEMBLY NOTES:

NOTE 1: COAT THE CHARGE WITH THE FOLLOWING LAMINAC MIXTURE JUST PRIOR TO INSERTING INTO THE BODY:
RESIN - LAMINAC 4116 ---------- 99% (NOTE 2)
CATALYST - LUPERSOL DDM ------- 1% (NOTE 3)
PERCENTAGES ARE BY WEIGHT
IMMEDIATELY BEFORE USE, MIX RESIN AND CATALYST THOROUGHLY IN A STEEL OR ALUMINUM CONTAINER.
POT LIFE OF MIXTURE - 2 HOURS. MAINTAIN PROPER VENTILATION.

NOTE 2: APPROVED SOURCE - AMERICAN CYANAMIDE CO., NEW YORK, NEW YORK.

NOTE 3: APPROVED SOURCE - LUCIDOL DIVISION OF NOVADEL-AGENE CORPORATION, BUFFALO, NEW YORK.

NOTE 4: APPLY A 1/4-INCH WIDE BAND OF EPOXY CEMENT (NOTE 6) TO THE INSIDE OF THE MOUTH OF THE LINER BEFORE INSERTING THE LUCITE INHIBITOR.

NOTE 5: CEMENT THE RETAINER TO THE BODY AND INHIBITOR WITH EPOXY CEMENT (NOTE 6).

NOTE 6: USE GARLOCK 201 ADHESIVE COMPONENTS A AND B, MIXING ONE PART BY WEIGHT OF EACH COMPONENT (GARLOCK INC., 1276 WEST THIRD STREET, CLEVELAND, OHIO 44113).

NOTE 7: AFTER APPLYING THE CEMENTS AND ASSEMBLING, STAND THE ASSEMBLY ON END WITH THE BASE PLUG END DOWN, WITH A 10-POUND WEIGHT RESTING ON THE RETAINER. ALLOW THE ASSEMBLY TO STAND FOR 24 HOURS AT APPROXIMATELY 70°F TO ALLOW THE CEMENT TO HARDEN.

QTY.	FIND NO.	PART NO.	CODE	DESCRIPTION	MATERIAL
1	13	DRB-N-56		INHIBITOR	LUCITE PLASTIC
1	12	DRB-N-55		RETAINER	ALUM. ALLOY
1	11	DRB-N-54		LINER	INGOT IRON
1	10			METAL CAP .005 THICKNESS	INGOT IRON
1	9			CHARGE (CAST IN DRB-N-57)	
1	8	DRB-N-53		BODY	FIBRE GLASS
1	7			TETRYL PELLET .388 DIA x .848 LG WITH .298 DIA x .500 DP HOLE	
1	6			FELT PAD 1/16 X 2 6/64 DIA	FELT
12	5			CKL-P4E HUCK BLIND RIVET OR EQUIV.	STD
1	4			M18 STAB DETONATOR .241 DIA. X .342	
1	3			TWISTED PAIR OF WIRES TO SENSOR	STD
1	2	DRB-N-52		BASE PLUG	ALUM ALLOY
1	1			M36 A1 DETONATOR	

LIST OF MATERIAL

PHYSICAL PROPERTIES					
YP					
TS					
EL-2					
RA					
BH					
BH					
	NEXT ASSY.	USED ON	NEXT ASSY.	FINAL ASSY.	
	APPLICATION		QTY. REQD.		

UNLESS OTHERWISE SPECIFIED DIMENSIONS ARE IN INCHES
TOLERANCES ON DECIMALS ANGLES FRACTIONS
MATERIAL
HEAT TREATMENT
FINAL PROTECTIVE FINISH

DRAWN	A. MULDER	6-7-66
CHECKED	[illegible]	6/13/66
SUBMITTED		
APPROVED		
APPROVED		DATE
E Clark		6-13-66

TEST ASSEMBLY
BRL. INHIBITED JET

DEFENSE RESEARCH DIVISION
THE FIRESTONE TIRE & RUBBER CO.
AKRON, OHIO

DWG. NO. DRC-N-55-1

SCALE FULL SIZE | SPEC | CODE | SHEET OF

Fig. 11. Test Assembly, BRL Inhibited Jet. DRC-N-55-1

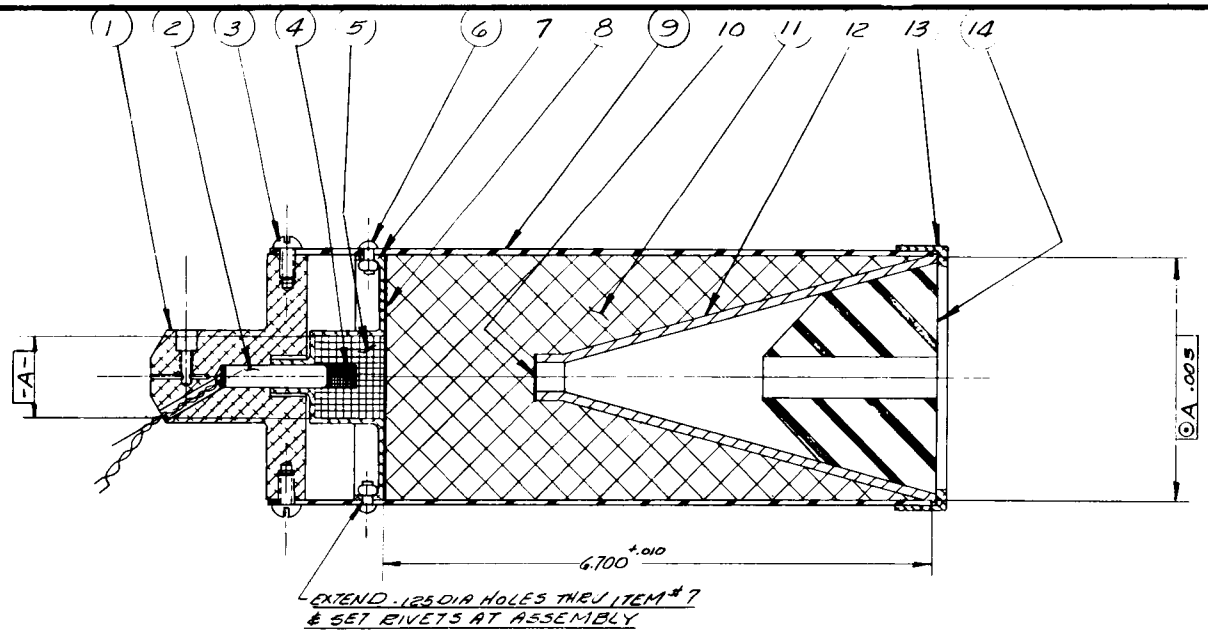

ASSEMBLY NOTES:

NOTE 1: COAT THE CHARGE WITH THE FOLLOWING LAMINAC MIXTURE JUST PRIOR TO INSERTING INTO THE BODY:
RESIN - LAMINAC 4116 ---------- 99% (NOTE 2)
CATALYST - LUPERSOL DDM -------- 1% (NOTE 3)
PERCENTAGES ARE BY WEIGHT
IMMEDIATELY BEFORE USE, MIX RESIN AND CATALYST THOROUGHLY IN A STEEL OR ALUMINUM CONTAINER.
POT LIFE OF MIXTURE - 2 HOURS. MAINTAIN PROPER VENTILATION.

NOTE 2: APPROVED SOURCE - AMERICAN CYANAMIDE CO., NEW YORK, NEW YORK.

NOTE 3: APPROVED SOURCE - LUCIDOL DIVISION OF NOVADEL-AGENE CORPORATION, BUFFALO, NEW YORK.

NOTE 4: APPLY A 1/4-INCH WIDE BAND OF EPOXY CEMENT (NOTE 6) TO THE INSIDE OF THE MOUTH OF THE LINER BEFORE INSERTING THE LUCITE INHIBITOR.

NOTE 5: CEMENT THE RETAINER TO THE BODY AND INHIBITOR WITH EPOXY CEMENT (NOTE 6).

NOTE 6: USE GARLOCK 201 ADHESIVE COMPONENTS A AND B, MIXING ONE PART BY WEIGHT OF EACH COMPONENT (GARLOCK INC., 1276 WEST THIRD STREET, CLEVELAND, OHIO 44113).

NOTE 7: AFTER APPLYING THE CEMENTS AND ASSEMBLING, STAND THE ASSEMBLY ON END WITH THE BASE PLUG END DOWN, WITH A 10-POUND WEIGHT RESTING ON THE RETAINER. ALLOW THE ASSEMBLY TO STAND FOR 24 HOURS AT APPROXIMATELY 70°F TO ALLOW THE CEMENT TO HARDEN.

QTY.	FIND NO.	PART NO.	CODE	DESCRIPTION	MATERIAL
1	14	DRB-N-56		INHIBITOR	LUCITE PLASTIC
1	13	DRB-N-55		RETAINER	ALUM. ALLOY
1	12	DRB-N-54		LINER	INGOT IRON
1	11			CHARGE (CAST IN DRB-N-57)	
1	10			METAL CAP .005 THICKNESS	INGOT IRON
1	9	DCB-N-59		BODY	FIBREGLASS
1	8			FELT PAD 1/16 X 2 6/64 DIA.	FELT
1	7	DRB-N-52		BASE PLUG	ALUM. ALLOY
12	6			CKL-P4E HUCK BLIND RIVET OREQUIV.	STD
1	5			TETRYL PELLET .988 DIA X .848 LG H.IN-.238 DIA X .500 DP. HOLE	
1	4			M18 STAB DETONATOR .241 DIA X .342	
2	3			RD HD. MACH. SCR. #10-32 N.F. X 3/8	STD
1	2			X98AA ARC FIRING DETONATOR	
1	1	DRB-N-58		SPIN ADAPTER	ALUM. ALLOY

LIST OF MATERIAL

PHYSICAL PROPERTIES					
YP					
TS					
EL-2					
BA					
BH					
BH					
	NEXT ASSY.	USED ON	NEXT ASSY.	FINAL ASSY.	
	APPLICATION		QTY. REQD.		

UNLESS OTHERWISE SPECIFIED DIMENSIONS ARE IN INCHES
TOLERANCES ON DECIMALS
ANGLES FRACTIONS
MATERIAL
HEAT TREATMENT
FINAL PROTECTIVE FINISH

DRAWN	W. HALDER	6-17-66
CHECKED	C. Strong	6-20-66
SUBMITTED		
APPROVED	C. Strong	6-20-66
APPROVED		DATE
E Clark		6-20-66

SPIN TEST ASSEMBLY -
BRL INHIBITED JET

DEFENSE RESEARCH DIVISION
THE FIRESTONE TIRE & RUBBER CO.
AKRON, OHIO

DWG. NO. DRC-N-56-1

SCALE FULL SIZE | SPEC | CODE | SHEET OF

Fig. 12. Spin Test Assembly - BRL Inhibited Jet. DRC-N-56-1

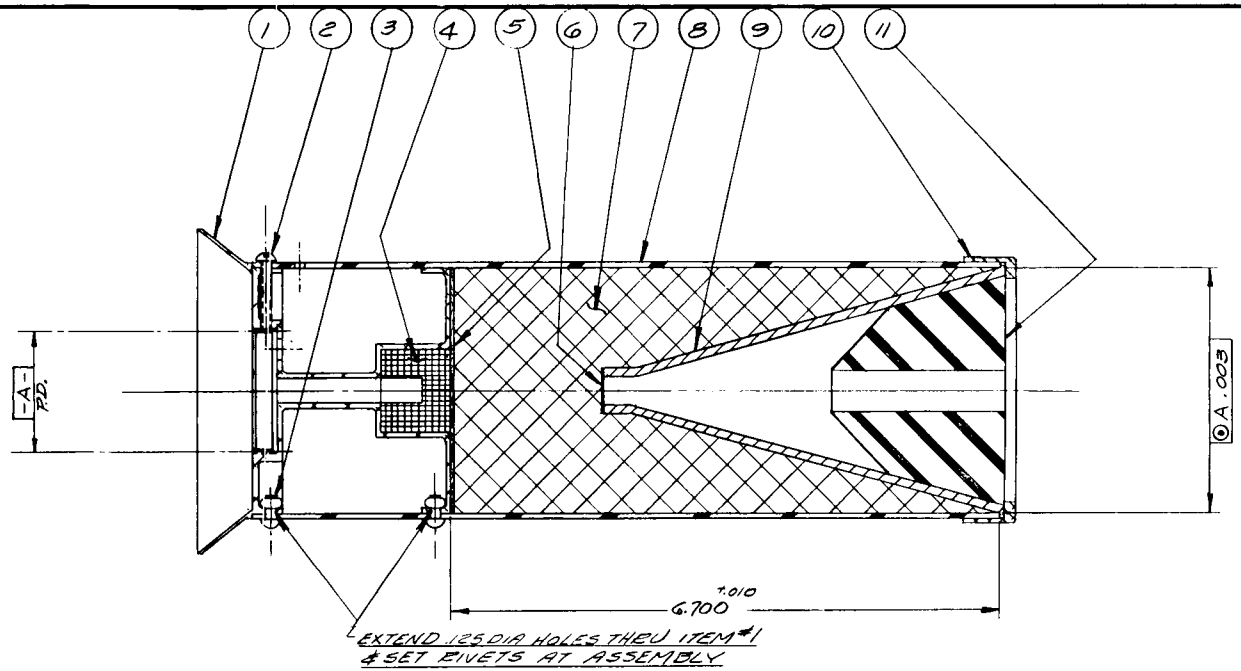

ASSEMBLY NOTES:

NOTE 1: COAT THE CHARGE WITH THE FOLLOWING LAMINAC MIXTURE MUST PRIOR TO INSERTING INTO THE BODY:
RESIN - LAMINAC 4116 ---------- 99% (NOTE 2)
CATALYST - LUPERSOL DDM -------- 1% (NOTE 3)
PERCENTAGES ARE BY WEIGHT
IMMEDIATELY BEFORE USE, MIX RESIN AND CATALYST THOROUGHLY IN A STEEL OR ALUMINUM CONTAINER.
POT LIFE OF MIXTURE - 2 HOURS. MAINTAIN PROPER VENTILATION.

NOTE 2: APPROVED SOURCE - AMERICAN CYANAMIDE CO., NEW YORK, NEW YORK.

NOTE 3: APPROVED SOURCE - LUCIDOL DIVISION OF NOVADEL-AGENE CORPORATION, BUFFALO, NEW YORK.

NOTE 4: APPLY A 1/4-INCH WIDE BAND OF EPOXY CEMENT (NOTE 6) TO THE INSIDE OF THE MOUTH OF THE LINER BEFORE INSERTING THE LUCITE INHIBITOR.

NOTE 5: CEMENT THE RETAINER TO THE BODY AND INHIBITOR WITH EPOXY CEMENT (NOTE 6).

NOTE 6; USE GARLOCK 201 ADHESIVE COMPONENTS A AND B, MIXING ONE PART BY WEIGHT OF EACH COMPONENT (GARLOCK INC., 1276 WEST THIRD STREET, CLEVELAND, OHIO 44113).

NOTE 7: AFTER APPLYING THE CEMENTS AND ASSEMBLING, STAND THE ASSEMBLY ON END WITH THE BASE PLUG END DOWN, WITH A 10-POUND WEIGHT RESTING ON THE RETAINER. ALLOW THE ASSEMBLY TO STAND FOR 24 HOURS AT APPROXIMATELY 70°F TO ALLOW THE CEMENT TO HARDEN.

QTY.	FIND NO.	PART NO.	CODE	DESCRIPTION	MATERIAL
1	11	DEB-N-56		INHIBITOR	LUCITE PLASTIC
1	10	DEB-N-55		RETAINER	ALUM ALLOY
1	9	DEB-N-54		LINER	INGOT IRON
1	8	DEB-N-63		BODY	FIBRE GLASS
1	7			CHARGE (CAST IN DEB-N-57)	
1	6			METAL CAP .005 THICKNESS	INGOT IRON
1	5			FELT PAD 1/16 X 2 6/16 DIA	FELT
1	4			TETRYL PELLET .988 DIA X .898 LG. WITH .298 DIA X .500 DP. HOLE	
24	3			CKL-P4E HUCK BLIND RIVET EQUIV. OR.	STD
1	2			RD HD. MACH SCR. #6-32 N.C. - 2 X 7/8 LG.	STD
1	1	DEB-N-62		ADAPTER	ALUM ALLOY

LIST OF MATERIAL

PHYSICAL PROPERTIES				
YP				
TS				
EL-2				
RA				
BH				
BH				
NEXT ASSY.	USED ON	NEXT ASSY.	FINAL ASSY.	
APPLICATION		QTY. REQD.		

UNLESS OTHERWISE SPECIFIED DIMENSIONS ARE IN INCHES
TOLERANCES ON DECIMALS
ANGLES FRACTIONS
MATERIAL
HEAT TREATMENT
FINAL PROTECTIVE FINISH

DRAWN	K.H.SNYDER	7-12-66
CHECKED		7-15-66
SUBMITTED		7-18-66
APPROVED		
APPROVED		DATE
E. Clark		7-18-66

FLIGHT TEST ASSEMBLY
SHORT- BRL
INHIBITED JET

DEFENSE RESEARCH DIVISION
THE FIRESTONE TIRE & RUBBER CO.
AKRON, OHIO

DWG. NO. DRC N-58

SCALE FULL 5/12E | SPEC | CODE | SHEET OF

Fig. 13. Flight Test Assembly - BRL Inhibited Jet. DRC-N-58

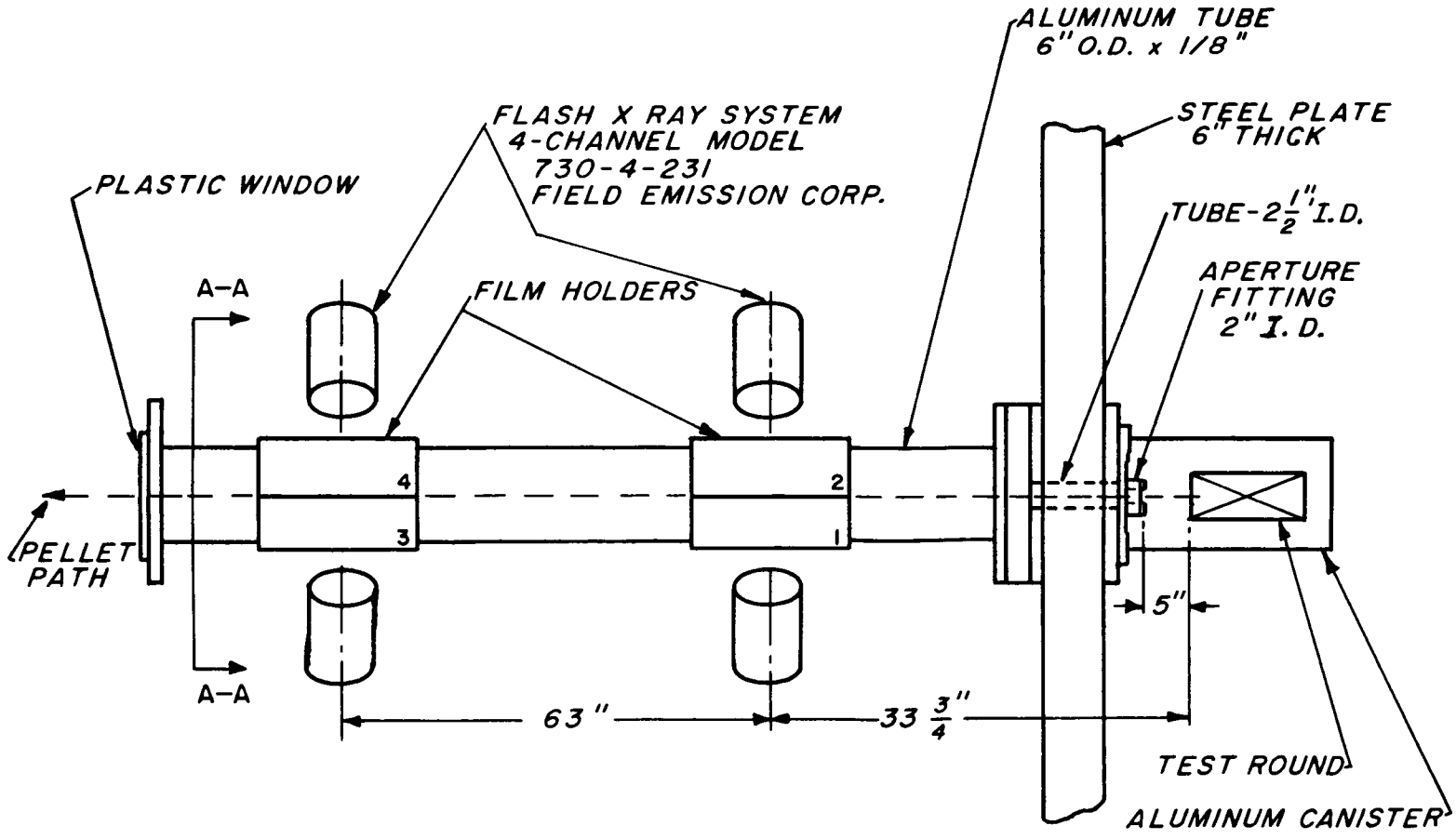

TOP VIEW ~ NOT TO SCALE

Fig. 14. A. Orthogonal Radiographic Set-up, NASA Test Site

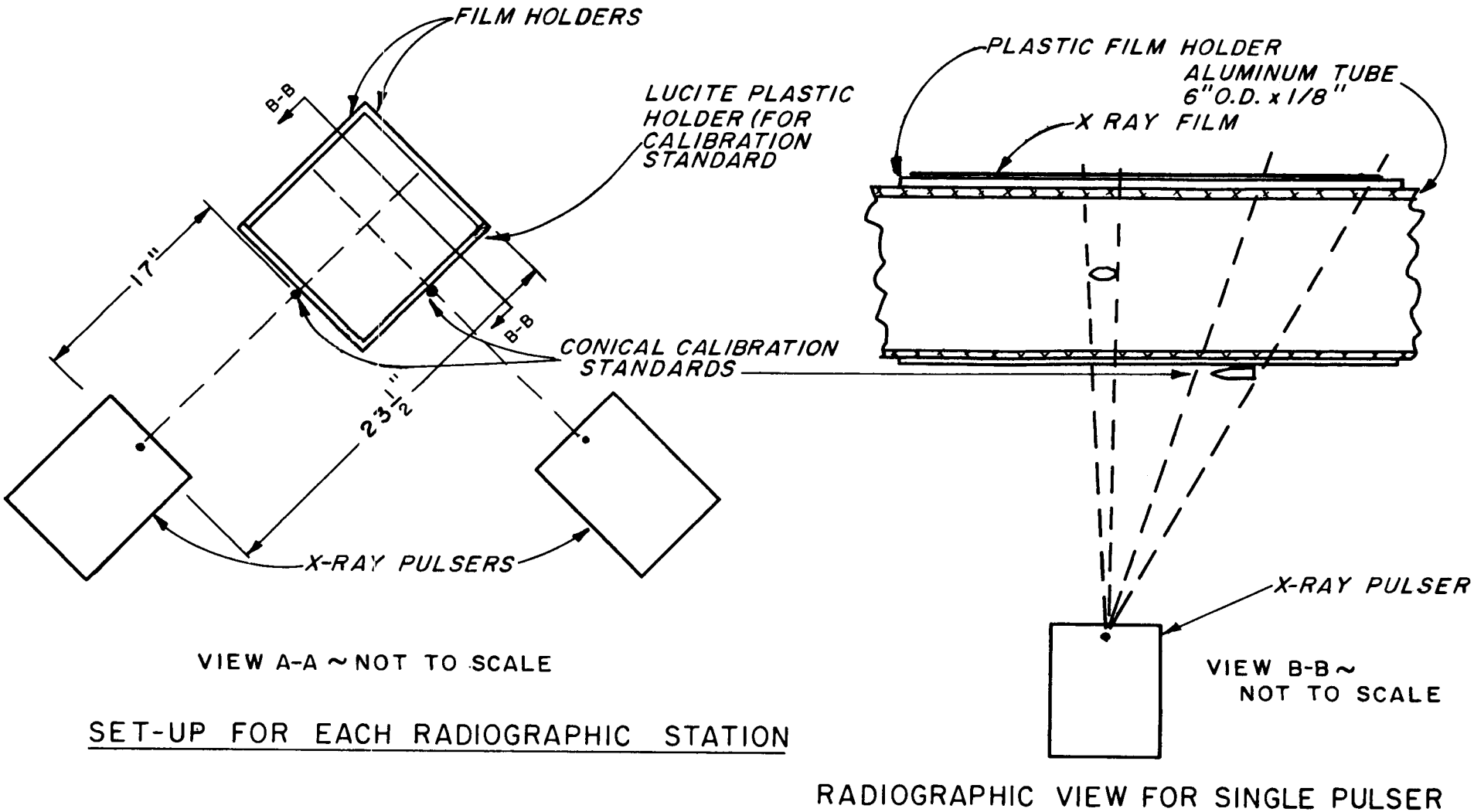

Fig. 14. B. Radiographic View For Single Station

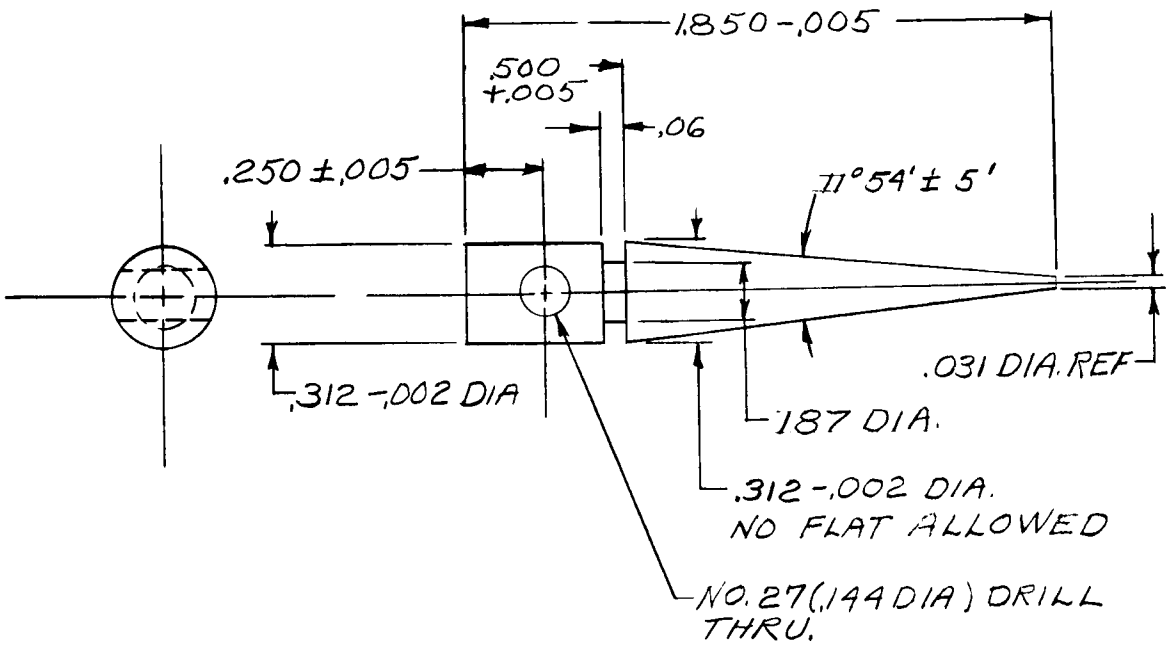

NOTE

1. FINISH 63 ALL OVER.
2. MATERIAL TO BE SPECIFIED.
3. LEAVE CORNERS SHARP.

UNLESS OTHERWISE SPECIFIED DIMENSIONS ARE IN INCHES TOLERANCES ON- DECIMALS ±.010 FRACTIONS ANGLES	DATE STARTED	TITLE STANDARD, CONIC CALIBRATION	DEFENSE RESEARCH DIVISION THE FIRESTONE TIRE & RUBBER CO. AKRON, OHIO
MATERIAL SEE NOTE 2	DATE FINISHED 9-16-66		
HEAT TREATMENT	DRAFTSMAN Stroym / CHECKER		DRA-N-25
FINAL PROTECTIVE FINISH	TRACER / CHECKER		
	ENGINEER / ENGINEER Stroym/1		
	APPROVED Roy L. Woodall Sept. 16, 1966	SCALE 2/1 UNIT WT.	SHEET OF

Fig. 15. Standard, Conic Calibration. DRA-N-25

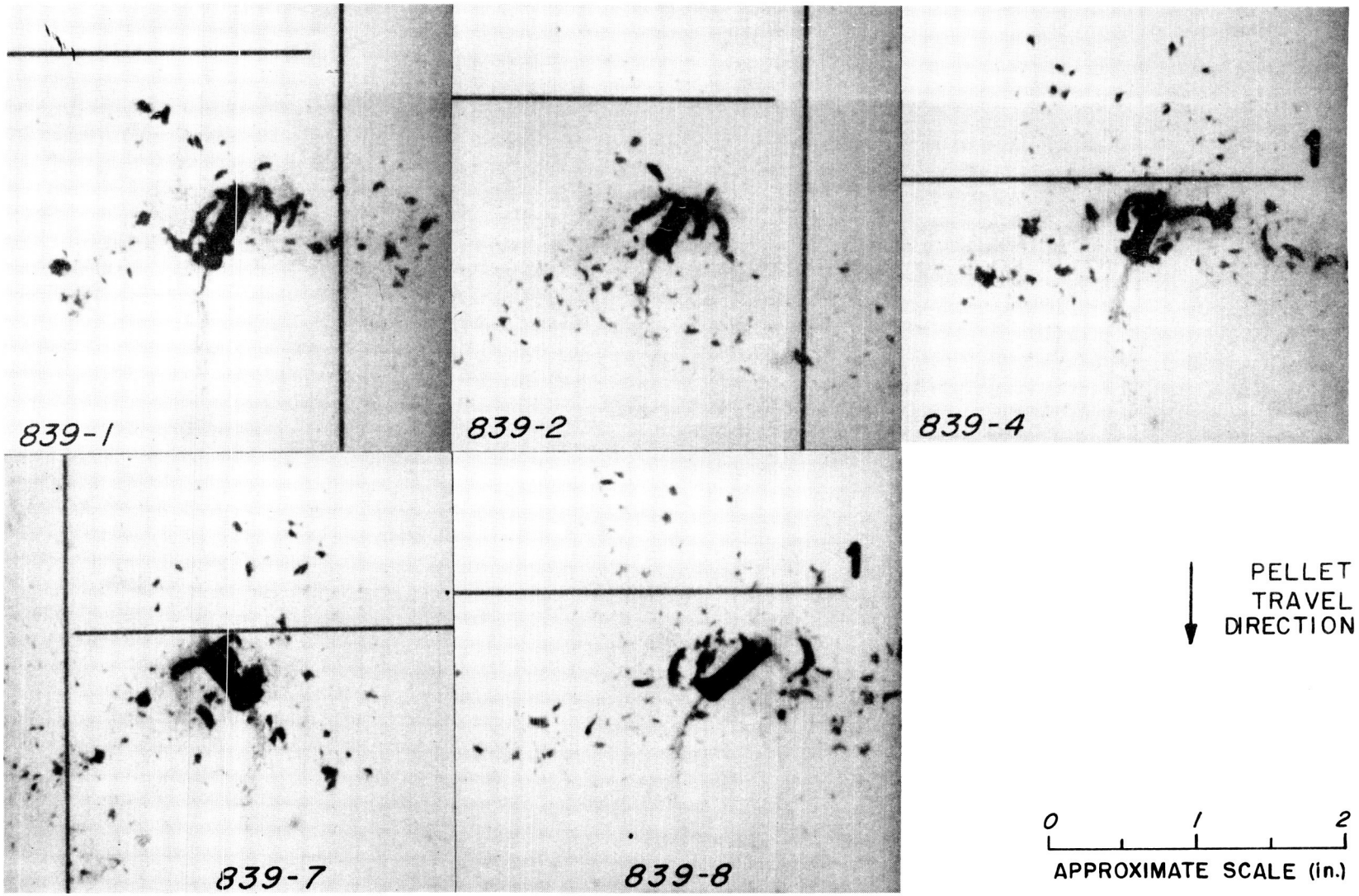

Fig. 16. Body Confinement Test - Representative Radiographs. 40° Hyperbolic Nickel Liner. (Fig. 4, Assy., NASA Test Site, Station 1, approx. 34-in. from liner base, 71.6μ avg. ambient pressure.)

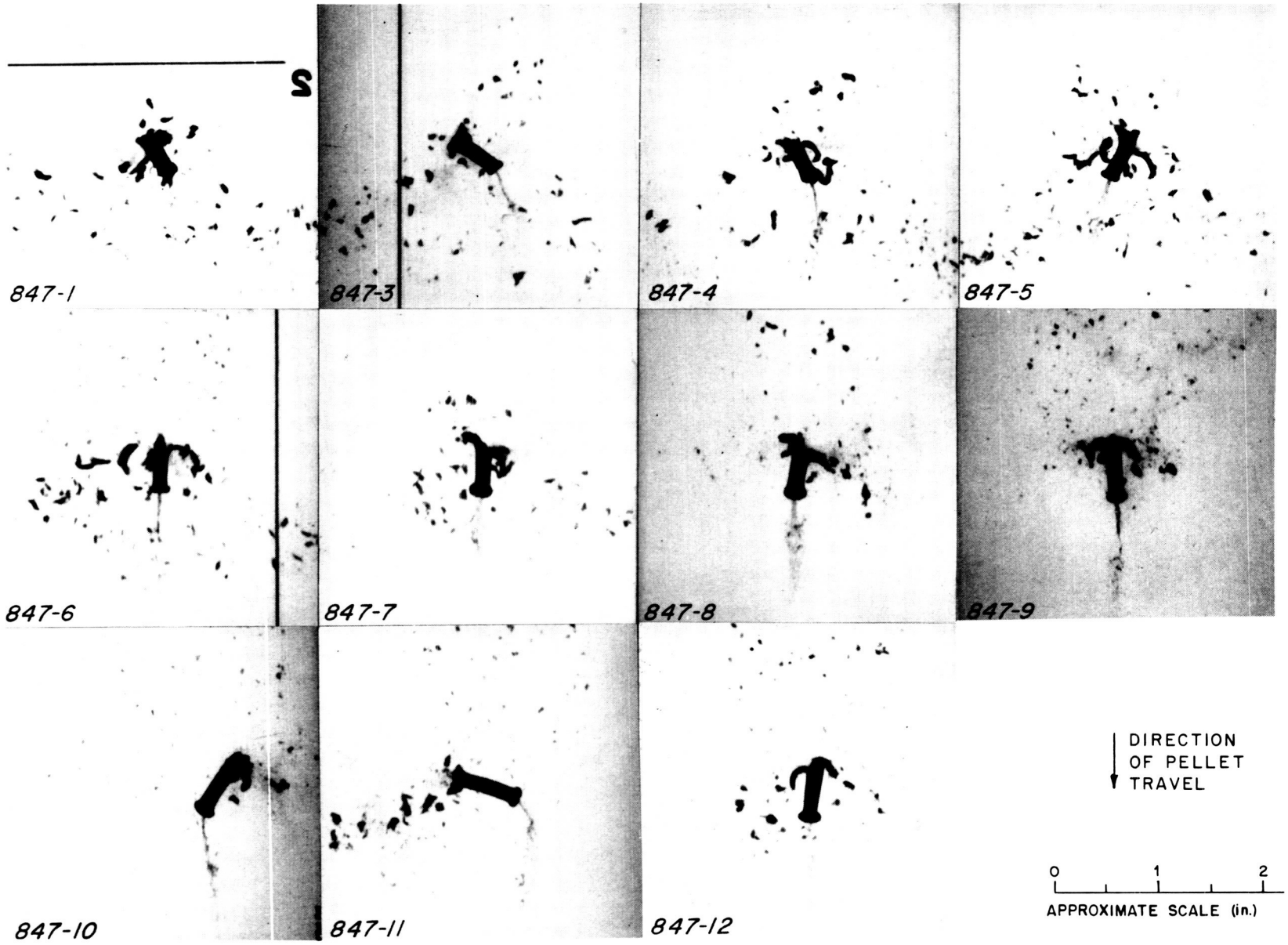

Fig. 17. Modified Flight Test - Representative Radiographs. 40° Hyperbolic Nickel Liner. (Fig. 5, Assy., NASA Test Site, Station 1, approx. 34-in. from liner base, 37.7μ avg. ambient pressure.)

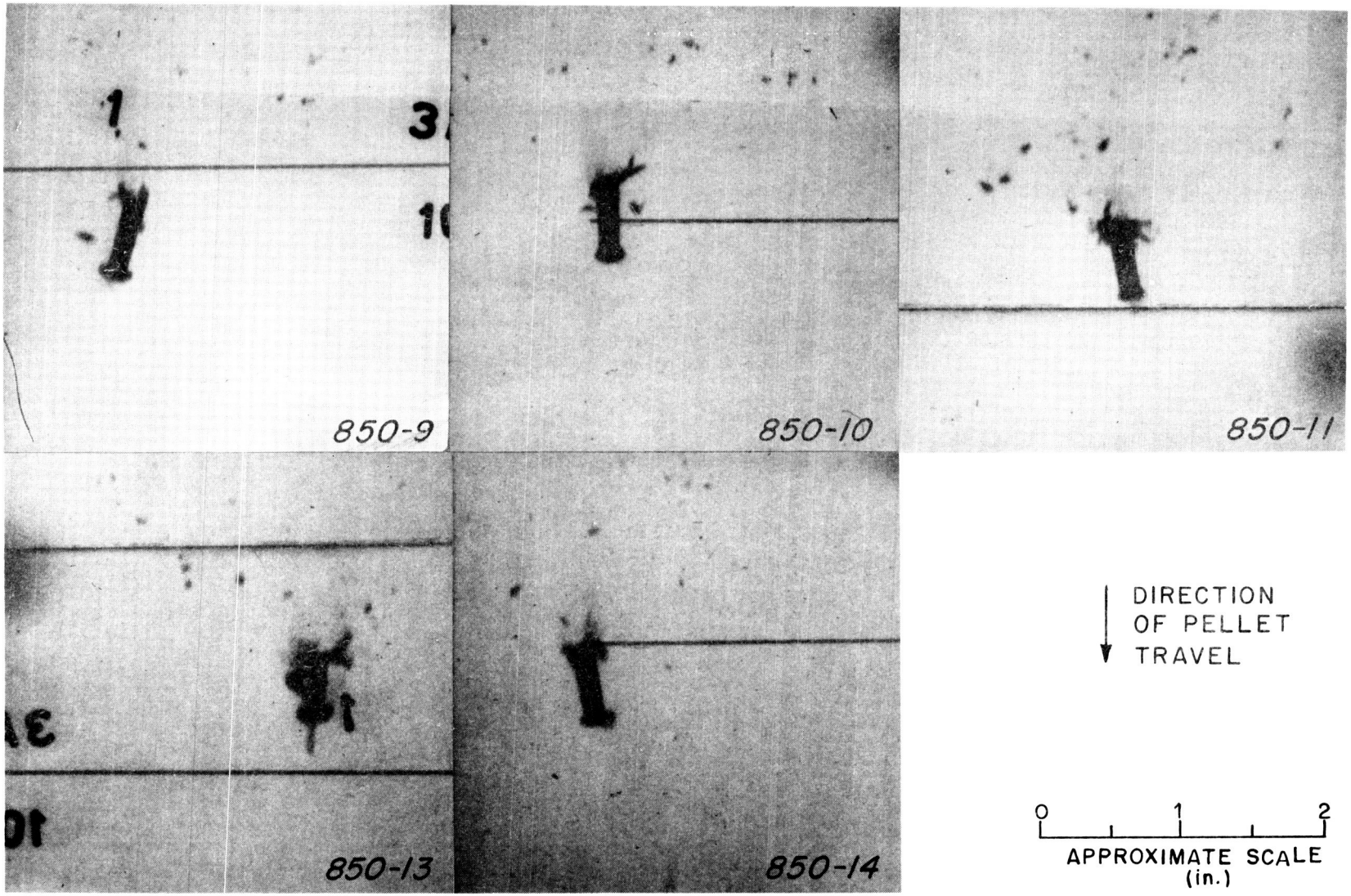

Fig. 18. Spin Test (-25rps) - Representative Radiographs. 40° Hyperbolic Nickel Liner. (Fig. 6 Assy., Large Chamber, Station 1, approx. 40-in. from liner base, atmospheric ambient pressure.)

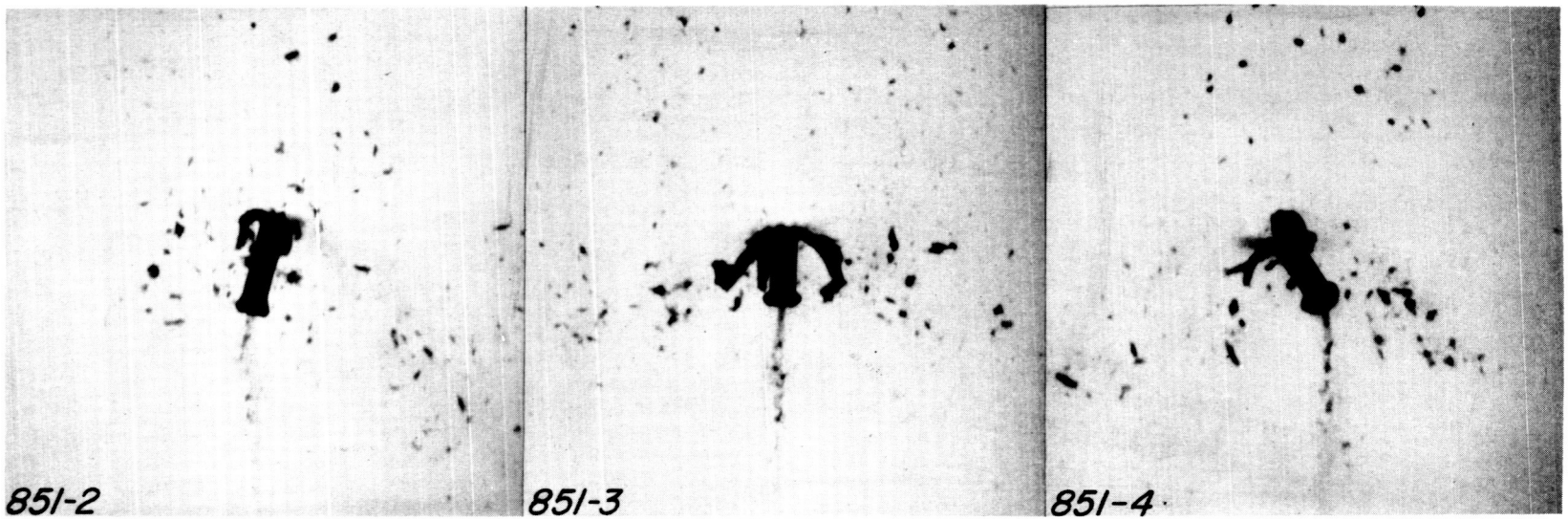

DIRECTION OF PELLET TRAVEL

0 1 2
APPROXIMATE SCALE (in.)

Fig. 19 Full Flight Test - Representative Radiographs. 40° Hyperbolic Nickel Liner. (Fig. 7 Assy., NASA Test Site, Station 1, approx. 34-in. from liner base, 25.7μ avg. ambient pressure.)

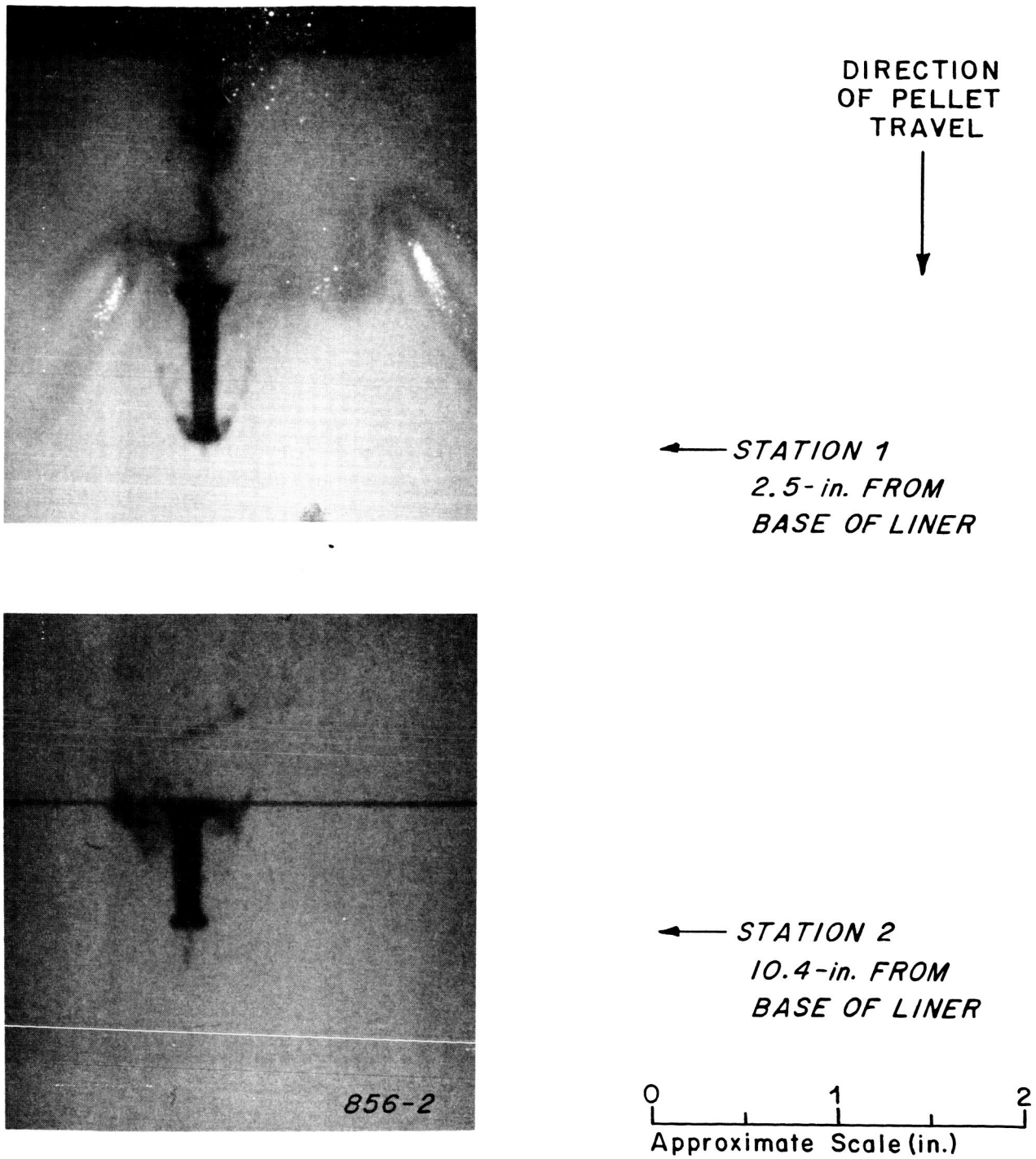

Fig. 20. Initial Pellet Mass Test- Representative Radiographs. 40° Hyperbolic nickel liner. (Fig. 4 assembly, Open Test Site, atmospheric ambient pressure.)

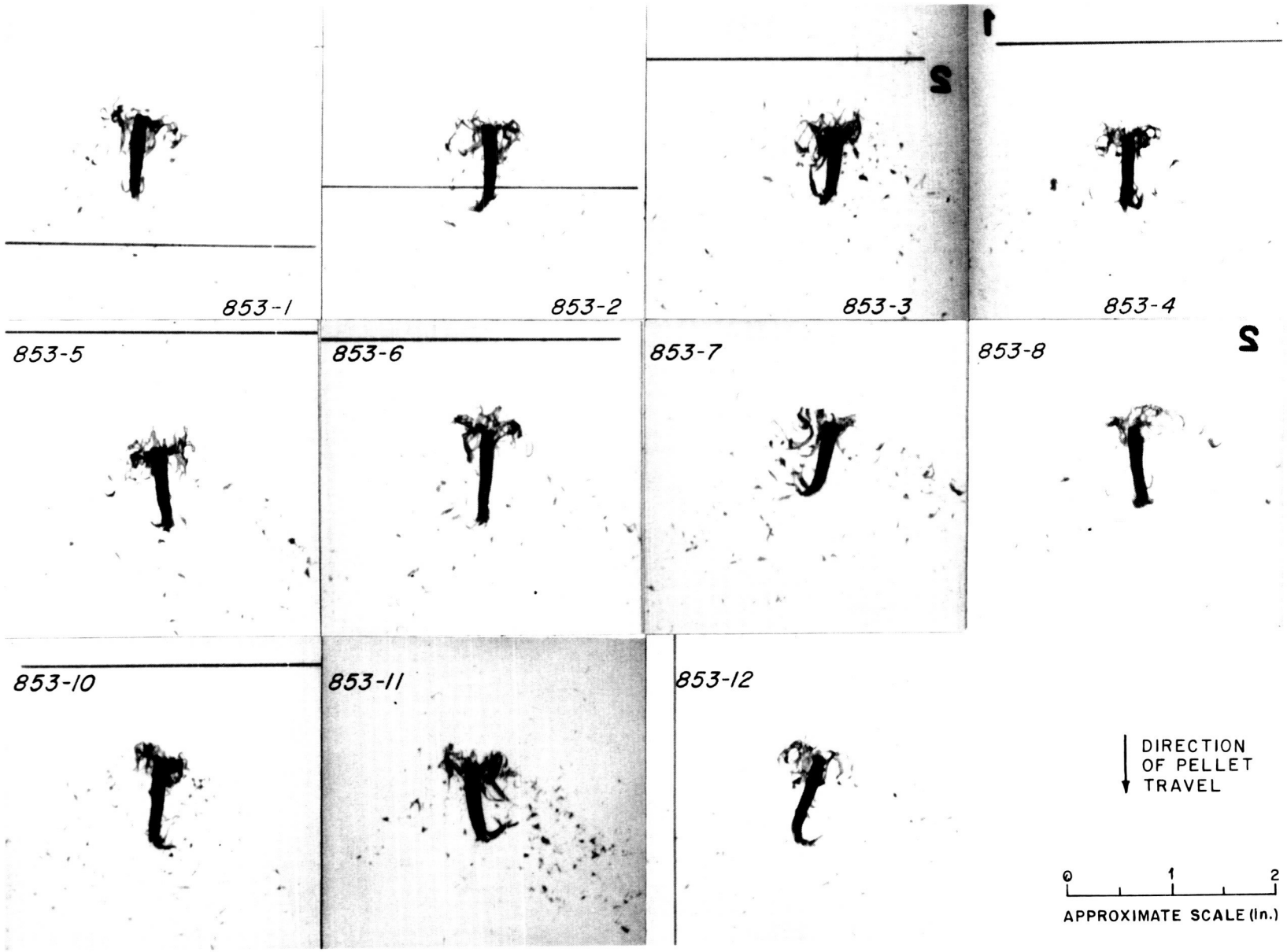

Fig. 21. Modified Flight Test - Representative Radiographs. 30° Conic Ingot Iron Liner. (Fig. 11 Assy., NASA Test Site, Station 1, approx. 34-in. from liner base, 41.7μ avg. ambient pressure.)

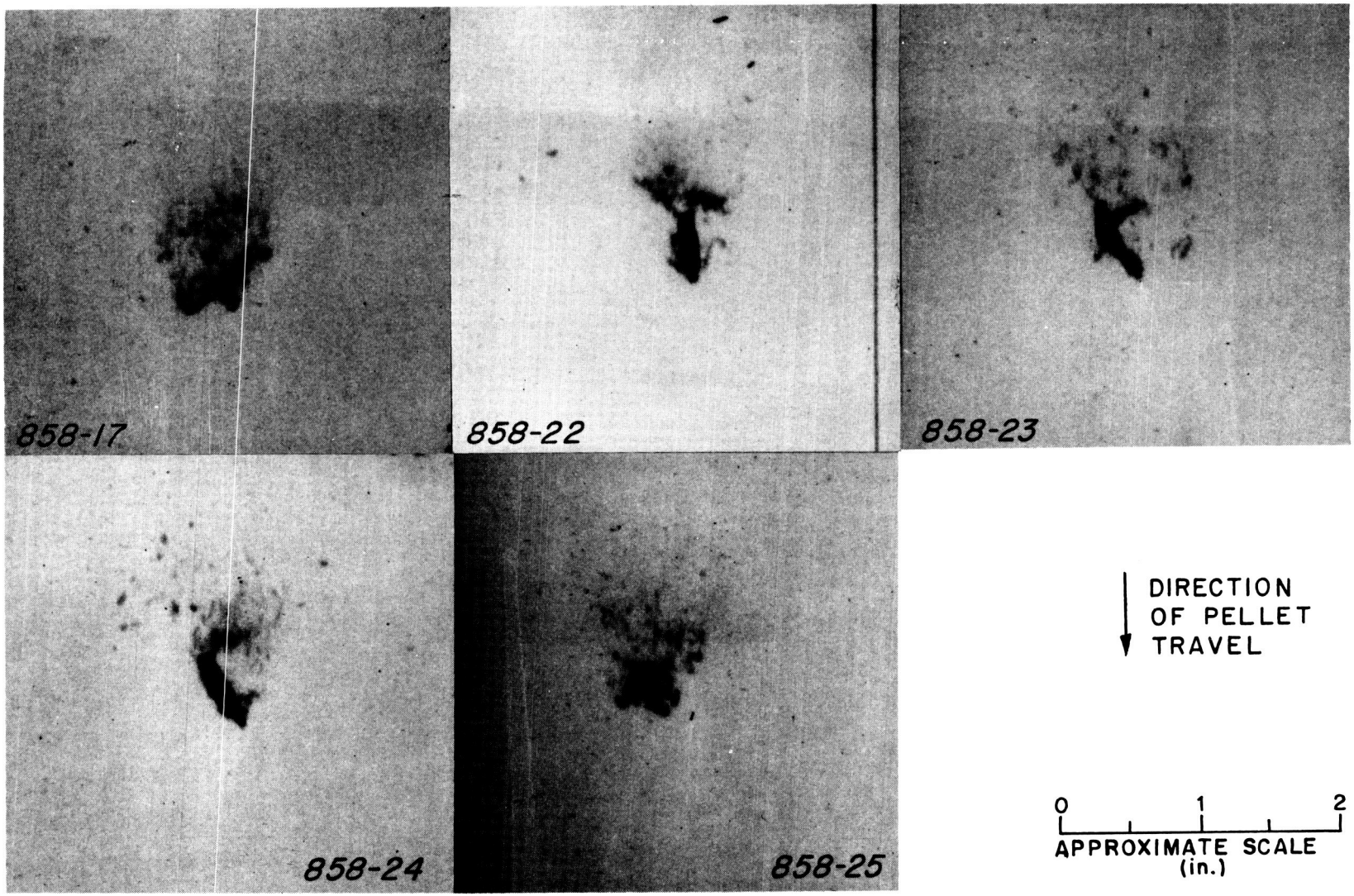

Fig. 22. Spin Test (-25rps) - Representative Radiographs. 30° Conic Ingot Iron Liner. (Fig. 12 Assy., Large Chamber, Station 1, approx. 40-in. from liner base, atmospheric ambient pressure.)

Fig. 23. Full Flight Test - Representative Radiographs. 30° Conic Ingot Iron Liner. (Fig. 13 Assy., NASA Test Site, Station 1, approx. 34-in from liner base, 41.7μ ambient pressure.)

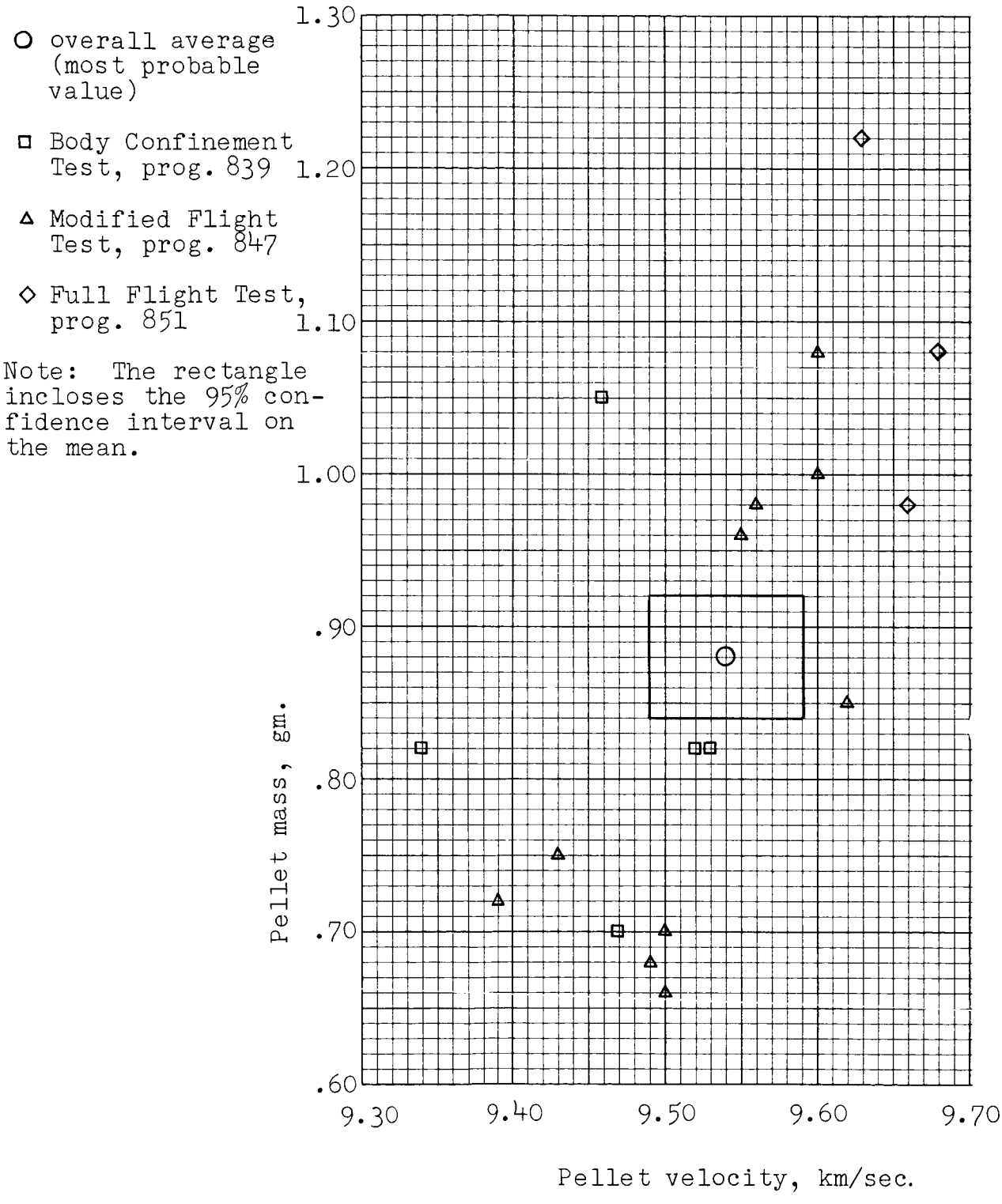

Fig. 24. Graphic presentation of pellet mass v.s. pellet velocity for low ambient pressure, 40° Hyperbolic nickel liner test programs.

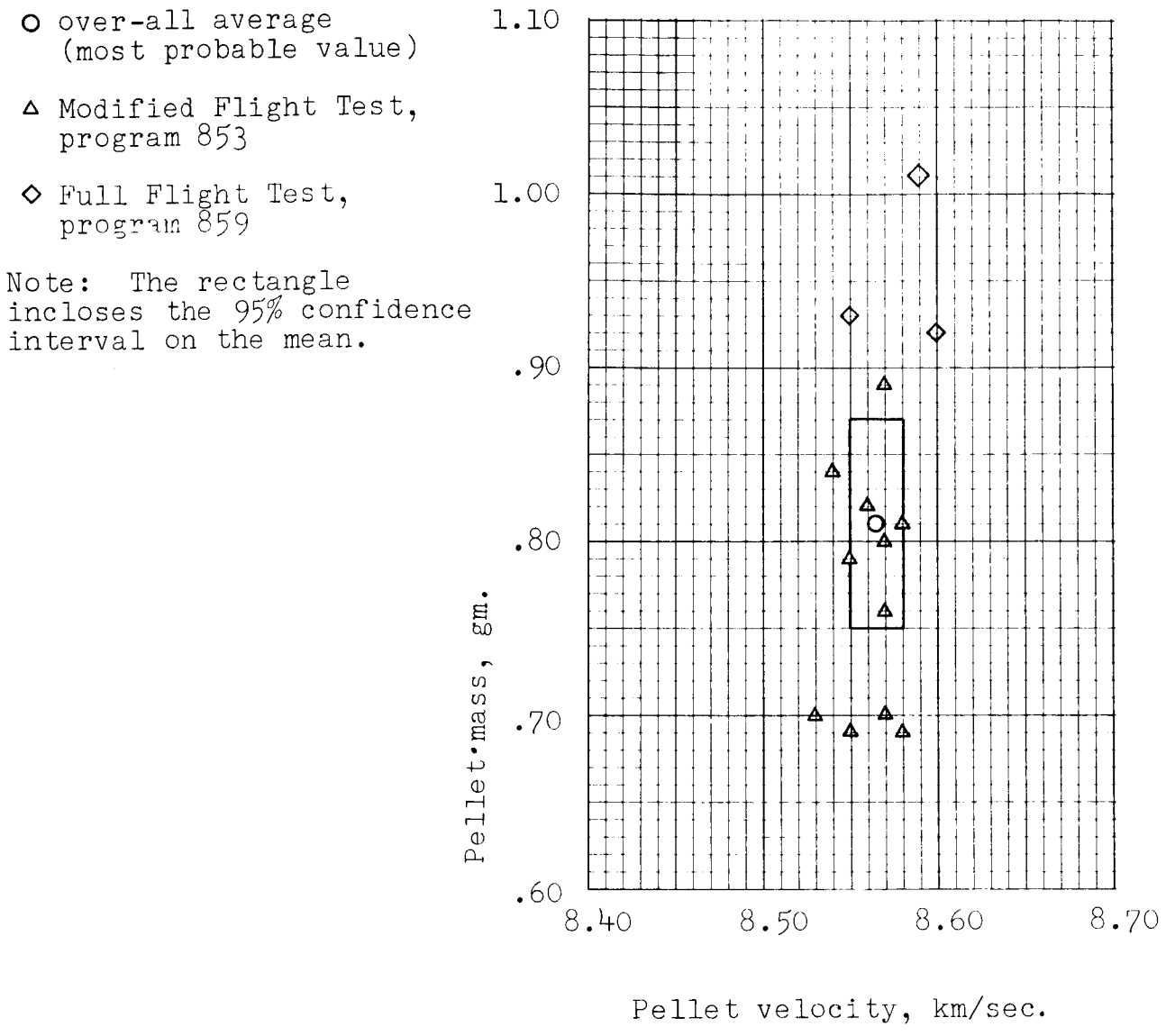

Fig. 25. Graphic presentation of pellet mass v.s. pellet velocity for low ambient pressure, 30° Conic Ingot Iron liner test programs.